

personal buildup for

# Force Motors Ltd.



MTZ worldwide 10/2010, as epaper released on 09.09.2010  
<http://www.mtz-worldwide.com>

content:

page 1: Cover. p.1

page 2: Contents. p.2

page 3: Johannes Winterhagen: Transport Agenda. p.3

page 4: Werner Bick, Markus Köhne, Ulrich Pape, Hans-Josef Schiffgens : The New Deutz Tier 4i Engines. p.4-11

page 12: Gerhard Doll, Anton Waltner, Peter Lückert, Roland Kemmler: The new 4.6 l V8 gasoline engine from Mercedes-Benz. p.12-19

page 20: Richard Bauder, Andreas Fröhlich, Danilo Rossi : The new generation of the Audi 3.0-litre V6 TDI engine Part 1: Design and Mechanics . p.20-27

page 28: Achim Koch, Hartmut Claus, Dirk Frankenstein, Roland Herfurth: Turbocharger Design for electrical Wastegate Actuation to minimize Leakage. p.28-33

page 34: Alfred Elsässer, Patric Genieser, David Gurney, Marco Warth: Systems development for future passenger car diesel engines. p.34-39

page 40: Yves Rosefort, Bernhard Lüers, Michael Wittler, Matthias Salmen, Martin Simm: Future Exhaust Emission Measurement Technology Requirements. p.40-45

page 46: Daniel Sigg, Jürgen Schneider, GAËL ANDRIEUX : New Valvetronic actuator for the Mini turbo engine. p.46-51

page 52: Research Peer Review. p.52-53

page 54: Simon Fischer, Thomas Lauer, Lukas Möltner, Stefan Schöffel, Harald Echtle, Günter Wenninger: Optimization of the Selective Catalytic Reduction by Means of Numerical Methods. p.54-59

page 60: Dominik Rether, Andreas Schmid, Michael Grill, Michael Bargende : Quasidimensional Simulation of CI-Combustion with Pilot- and Post-injections. p.60-66

**copyright**

The PDF download of contributions is a service for our subscribers. This compilation was created individually for Force Motors Ltd.. Any duplication, renting, leasing, distribution and publicreproduction of the material supplied by the publisher, as well as making it publicly available, is prohibited without his permission.

# MTZ

WORLDWIDE

10 October 2010 | Volume 71

**TURBOCHARGER** Design for  
Electrical Wastegate Actuation

**FUTURE** Exhaust Emission  
Measurement Technology  
Requirements

**OPTIMIZATION** of the Selective  
Catalytic Reduction



## EFFICIENT DRIVES FOR COMMERCIAL VEHICLES



COVER STORY

# EFFICIENT DRIVES FOR COMMERCIAL VEHICLES

4 | All manufacturers of engines for the off-road market are faced with enormous technical challenges, which can only be overcome with revised engines, extended electronic control and the use of complex exhaust gas aftertreatment. The Deutz engines with powers above 130 kW have been revised in essential parts for exhaust level Tier 4i/Stage IIIB. In the range from 130 to 520 kW, it was possible to further increase the power by up to 15 % depending on the series, while the specific fuel combustion could be reduced by up to 6 %.

personal buildup for Force Motors Ltd.

**COVER STORY**

**COMMERCIAL VEHICLE DRIVES**

- 4 The New Deutz Tier 4i Engines  
Werner Bick, Markus Köhne, Ulrich Pape,  
Hans-Josef Schiffgens [Deutz]

**INDUSTRY**

**NEW ENGINES**

- 12 The New 4.6 l V8 Gasoline Engine from Mercedes-Benz  
Gerhard Doll, Anton Waltner, Peter Lückert,  
Roland Kemmler [Daimler]
- 20 The New Generation of the Audi 3.0 l V6 TDI Engine  
Richard Bauder, Andreas Fröhlich,  
Danilo Rossi [Audi]

COVER FIGURE | FIGURE ABOVE Volvo

**TURBOCHARGING**

- 28 Turbocharger Design for Electrical Wastegate Actuation to Minimize Leakage  
Achim Koch, Hartmut Claus, Dirk Frankenstein,  
Roland Herfurth [Continental]

**EXHAUST GAS RECIRCULATION**

- 34 Systems Development for Future Passenger Car Diesel Engines  
Patric Genieser, Alfred Elsässer,  
David Gurney, Marco Warth [Mahle]

**EXHAUST GAS MEASUREMENT**

- 40 Future Exhaust Emission Measurement Technology Requirements  
Yves Rosefort, Bernhard Lüers [FEV],  
Michael Wittler, Matthias Salmen,  
Martin Simm [RWTH Aachen]

**VALVE GEAR**

- 46 New Valvetronic Actuator for the Mini Turbo Engine  
Daniel Sigg, Gaël Andrieux [Sonceboz Automotive], Jürgen Schneider [BMW]

**RESEARCH**

- 52 Peer Review

**EXHAUST GAS AFTERTREATMENT**

- 54 Optimization of the Selective Catalytic Reduction by Means of Numerical Methods  
Harald Echtle, Stefan Schöffel,  
Günter Wenninger [Daimler], Simon Fischer,  
Thomas Lauer, Lukas Möltner [TU Wien]

**COMBUSTION**

- 60 Quasidimensional Simulation of CI-Combustion with Pilot and Post Injections  
Dominik Rether, Andreas Schmid,  
Michael Grill, Michael Bargende [FKFS]

**RUBRICS | SERVICE**

- 3 Editorial
- 53 Imprint, Scientific Advisory Board

---

# TRANSPORT AGENDA

---

*Dear Reader,*

The IAA Commercial Vehicles 2010 is opening its doors at the best possible time – the start of an upturn in the economy. The transport industry, vehicle manufacturers and their suppliers, all of which were particularly hard hit by the economic crisis, can now breathe a sigh of relief. In the first half of 2010 alone, the increase in orders for heavy goods vehicles was 80 percent up on the very poor figures of the previous year. With around 1700 exhibitors, the IAA is returning to its 2006 level.

Alongside the economy, the demand for transport services is also growing, in particular in emerging nations such as China and India. However, the European truck manufacturers have a disproportionately small share of these markets, because with their high-quality and correspondingly expensive products they have nothing to offer in the face of the huge pressures on prices in these countries. As a result, four of the five largest manufacturers of heavy goods vehicles now come from China and India.

On their home markets in Europe the manufacturers are faced by political challenges. The CO<sub>2</sub> balance has to be improved, despite the fact that the volume of goods traffic is continuing to grow and the introduction of stricter exhaust emissions limits in Euro 6 will result in an increase in consumption. Finding the correct solution to these problems is even more difficult for trucks than it is for cars. One correct solution that will definitely not be introduced in heavy goods vehicles is electric drive systems. Although they may perhaps make even more sense for local delivery vans than they do for cars, depending on energy taxes and tolls, for trucks

the best way of achieving CO<sub>2</sub> neutrality is by using biofuels. However, these fuels will continue to be in short supply even with industrial-scale production and the first signs of competition for resources between goods transport on the roads and in the air are already emerging.

Anyone who wants to take a closer look at the links between drive systems, markets and logistics concepts will find the “Transport and Logistics” issue of our Automotive Agenda, which is appearing to coincide with the IAA, an interesting read. You can try an excerpt at [www.automotive-agenda.de](http://www.automotive-agenda.de).

I am looking forward to the opportunity of discussing with you at the IAA the latest technical solutions to the challenges that I have outlined in this editorial.



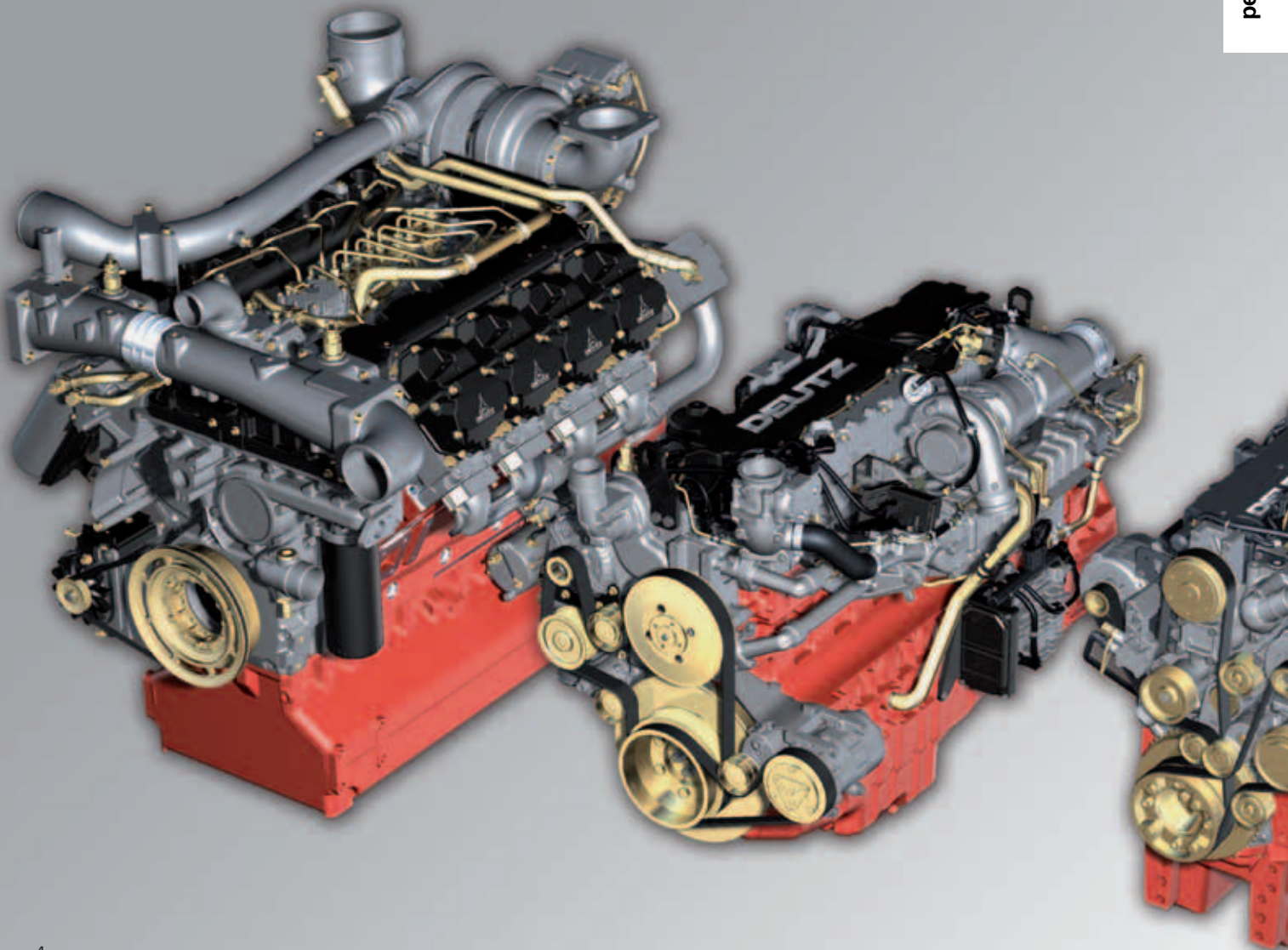
**JOHANNES WINTERHAGEN**, Editor-in-Chief  
Wiesbaden, 17 August 2010



# THE NEW DEUTZ TIER 4i ENGINES

The limit values stipulated by exhaust legislation under Tier 4i or EU Stage IIIB for mobile machinery with a power of more than 130 kW will become valid in the USA and in the EU on January 1, 2011. In comparison to today, these limit values entail a reduction in particulate by up to 90% and nitrogen dioxide emissions by 50%. Deutz has applied several technical concepts to its engines of displacement classes 6 to 16 litres, in order to comply with Tier 4i and Stage IIIB. This first part of the article describes the aspects design and durability, you will find the second part in the MTZ issue 11/2010.

personal buildup for Force Motors Ltd.



## AUTHORS



**DR.-ING. WERNER BICK**  
is Head of Platform 4-8L at  
Deutz AG in Cologne (Germany).



**DIPL.-ING. MARKUS KÖHNE**  
is Head of Platform <4L and >8L  
at Deutz AG in Cologne (Germany).



**DIPL.-ING. ULRICH PAPE**  
is Head of Testing and  
Application Engineering at Deutz AG  
in Cologne (Germany).



**DR.-ING. HANS-JOSEF SCHIFFGENS**  
was Head of Research &  
Development at Deutz AG  
in Cologne (Germany).

## REQUIREMENTS

Hence, all manufacturers of engines for the off-road market are faced with enormous technical challenges, which can only be overcome with revised engines, extended electronic control and the use of complex exhaust aftertreatment.

As a provider of engines in the on-road and off-road area with displacement between 2.9 and 16 l and power between 25 and 520 kW, Deutz has refined existing concepts for Tier 4i and EU Stage IIIB, while implementing new technology to this end [1, 2]. In comparison to engines of the previous generation, the development has focussed on:

- : increasing the specific power
- : increasing the ignition pressure resistance
- : increasing the thermal load capability and conversion to cooling gallery pistons (TCD 6.1 L6)
- : increasing the cubic capacity (TCD 7.8 L6)
- : increasing the maximum injection pressure
- : improving the crankcase ventilation and oil separation (TCD 12.0 V6 or TCD 16.0 V8).

The 11/2010 edition will examine the different combustion processes as well as the exhaust aftertreatment components for the engines more closely. ❶ summarizes the technical data of the Deutz Tier 4i engines in the power range above 130 kW.

### TCD 6.1 L6 ENGINE WITH SCR FOR TRACTORS

The TCD 6.1 L6 is a refinement of the TCD 2012 L06 engine and was conceived both for industrial applications as well as for use in tractors. The tractor variant is described here as representative.

Deutz is the first engine manufacturer for the agricultural machinery segment to introduce selective catalytic reduction (SCR) for exhaust aftertreatment in the exhaust level Tier 4i/Stage IIIB. The decision to use SCR for the agricultural machinery segment was made in particular under the aspect of avoiding thermal regeneration of a particulate filter as well as of the high requirements in comparison to construction machine applications in respect to power and torque over wide sections of the load profile and the comparatively good availability of “Ad Blue” (aqueous urea dilution) in the market.

Increasing the ignition pressure is especially advantageous for achieving an optimum fuel consumption. Increased power in comparison to the previous engine TCD 2012 L06 and the associated higher thermal load on the powertrain means that considerably stricter requirements are placed on the engine components. In order to meet at the same time the much more stringent requirements for lower product costs, the decision was made to transfer the cylinder head concept of the TCD 2013 L06 4V successfully used in the commercial vehicle segment since 2006 to the smaller engine series, ❷.

The cylinder head concept corresponds to the Deutz-typical L-flow design, i.e. charge air intake from above and exhaust outlet on the left side in respect to the flywheel side of the engine. The water jackets have been designed for better cleaning of the raw parts without a cast dome for the centrally positioned injector. The partition between the water jacket and the injection/fuel cavities is via a copper sleeve. The leak fuel is recirculated centrally via a fuel line integrated in the cylinder head.



ENGINES > 130 kW		TCD 6.1 L6		TCD7.8 L6		TCD12.0 V6	TCD16.0 V8
ENGINE VARIANT	–	Agri	Industry	Agri	Industry	Industry	Industry
NUMBER OF CYLINDERS	–	6		6		6	8
DISPLACEMENT	l	6.1		7.8		12.0	16.0
CYLINDER BORE	mm	101		110		132	
STROKE	mm	126		136		145	
RATED POWER	kW	203	180	285	250	390	520
NOMINAL SPEED	rpm	2100	2300	2200	2200	2100	2100
RATED TORQUE	Nm	920	747	1235	1085	1774	2365
PEAK TORQUE	Nm	1170	1000	1490	1400	2130	2890
AT SPEED	rpm	1450	1450	1500	1450	1400	1400
MAX. SPECIFIC POWER	kW/l	33.3	29.7	38.6	32.3	32.8	32.5
BMEP @ PEAK TORQUE	bar	24.2	20.7	24.2	22.7	22.5	22.9
MIN. BSFC	g/kWh	200	210	198	200	196	198
BSFC RATED	g/kWh	212	222	212	219	217	219

① Technical data Deutz engines >130 kW for Tier 4 interim

The injection system of the TCD 6.1 L6 has been significantly revised to improve the particulate emissions. In comparison to the previous version, the maximum injection pressure has been increased from 1600 bar to 2000 bar for the versions with high power. The new 2000 bar system is based on the Deutz common-rail system successfully used in series production since 2006. Besides the PF high-pressure pumps typical for the system, a new injector forms the core of the revised injection system. The CRIN 3 injector from Bosch exhibits significantly reduced leakage volumes in comparison to its predecessor (CRIN 2) and therefore provides the option of reducing the plunger diameter of the high-pressure pumps in such way that the fuel quantity balance allows representation of a peak power of 300 kW (in the TCD 7.8 L6). Apart from in the TCD 6.1 L6, the new 2000 bar injection system is also generally used in the TCD 7.8 L6.

In order to meet the high requirements for power and torque as well as use the good fuel consumption of the SCR process over the entire characteristic map shortly after starting as well, the exhaust gas temperature before the catalytic converter in operation must be increased as quickly as possible to a level in the range 250 to 300 °C. To fulfil these requirements, Deutz has developed a turbocharger with electrical waste gate actuator together with Borg Warner Turbo Systems. The turbocharger system with exhaust line for the

TCD6.1 L6 series is shown in ②. The electrical rapid waste gate adjustment controlled via CAN bus ensures precise regulation of the charge pressure in the entire engine map.

**TCD 7.8 L6 ENGINE WITH DPF FOR USE IN THE CONSTRUCTION MACHINE**

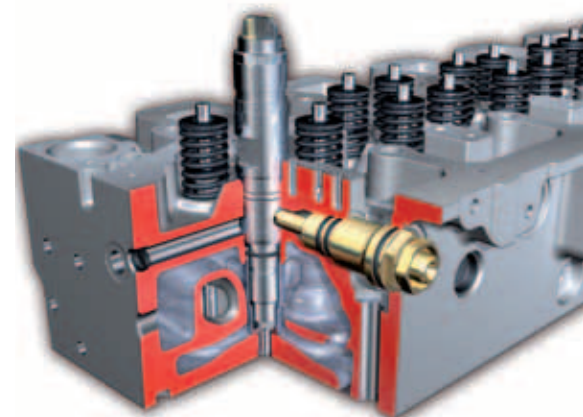
The TCD 7.8 L6 engine represents a refinement of the TCD 2013 L06 engine and works in the same way as the TCD 6.1 L6 both for the agricultural machinery segment and for use in construction machines each with their own combustion process. The essential feature of the new engine is the increased cubic capacity in comparison to the TCD 2013 L6 from 7.2 l to 7.8 l.

A system with externally cooled EGR and a diesel particulate filter (DPF) with active regeneration were selected for the industrial application. This means the diverse off-road applications no longer have to use additional operating media.

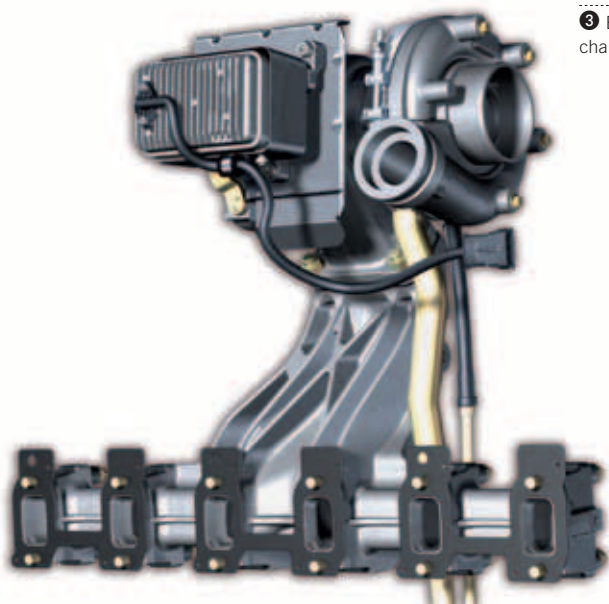
The EGR system has been designed for the 6-cylinder engines as a double-flow modular concept, which is used as the same part both for the TCD 6.1 L6 series and the TCD 7.8 L6 series. The main elements are the EGR cooler, the EGR flap, the peak pressure valve, the flap actuator, as well as a Venturi system for measuring the EGR mass flow. An essential design feature of the module is the omission of

the otherwise standard corrugated pipes, which both increase the installation complexity and negatively affect the product costs. The fastening is on the gas inlet side directly on the exhaust manifold and on the gas outlet side using a bracket on the crankcase, which is designed as a “loose bearing”. The concept chosen provides the option of a complete preassembly and hence a significantly reduced installation time on the engine assembly line.

For reliable and fault-free operation of the engine with particulate filter in construction machines, a burner is necessary to increase the exhaust gas temperature in line with requirements, this enabling a reliable regeneration of the loaded particulate filter under all operating conditions.



② TCD 6.1 L6 cylinder head



⑤ Exhaust manifold with turbo charger and electric actuator

Above all, reference is made to the applications with long-lasting low load operation here.

The burner system developed by Deutz itself with the required air and fuel supply is shown in ④. Besides the actual burner, an electrically driven air pump, a metering unit for the primary and secondary fuel supply as well as lines for air and fuel are necessary. The electric drive of the air pump ensures the requisite air supply to the burner for a regeneration of the particulate filter also when operating the engine at low speeds in the idling range. The burner is designed as a partial-flow burner. The partial flow of combustion air fed separately via the air pump and the fuel are combusted directly in the burner, thereby increasing the exhaust gas temperature. After reaching a sufficiently high exhaust gas temperature, extra fuel is injected via a second injection pipe in the burner, which does not combust directly, however, but is converted chemically in the diesel oxidation catalyst (DOC) upstream of the particulate filter. Thanks to this further exhaust gas temperature increase directly before the particulate filter, the necessary regeneration temperature is then reliably reached.

#### TCD 12.0/16.0 V6/V8 ENGINE WITH SCR

The TCD 12.0 V6 and TCD 16.0 V8 engines are derived from the TCD 2015

series as V-engines with a cylinder displacement of 2 l. For exhaust level Tier 4i or EU Stage IIIB, the engines retain the basic dimensions of the previous versions, but have been revised in essential parts.

Both units operate with an SCR system and dispense with exhaust gas recirculation.

This emission concept was defined on the basis of the packaging conditions in the segments covered by these engines, because it reduces the installation space requirements for the exhaust aftertreatment system and allows the machine manufacturer to retain the cooling system of the previous engine versions.

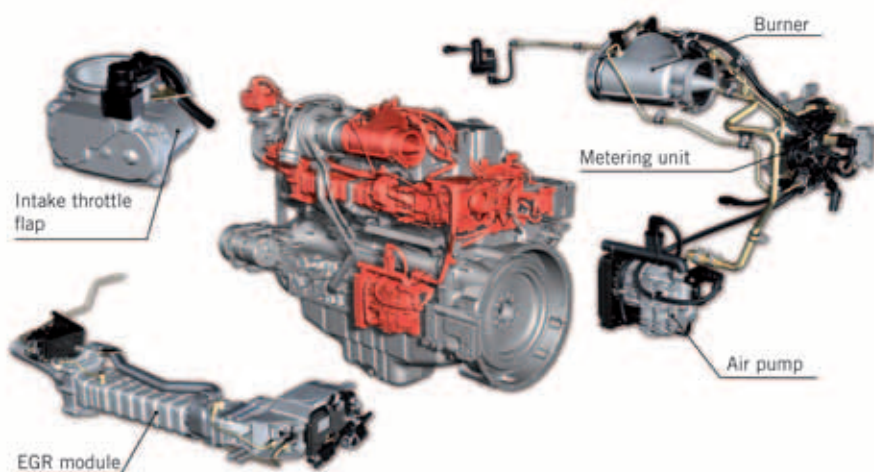
The increased mean combustion temperature in comparison to its predecessor

has been countered via improved piston cooling as well as a re-adjustment of cylinder liner and piston rings.

The low level of engine out emissions is achieved via an optimized combustion process and the use of a Bosch common rail system of the latest generation. The system comprises the high-pressure pump CPN-5, which can provide a maximum injection pressure of up to 2000 bar, two forged rails (V6) or a single rail (V8) as well as solenoid controlled injectors.

The high-pressure pump is driven by a wheel set via the camshaft gear wheel of the engine and is located in the rear part of the inner V. In comparison to its predecessor with unit pumps and a separate camshaft for injection control, the crankcase and the engine timing have been significantly simplified, ⑤.

A further module for achieving engine out emissions is the closed crankcase ventilation. An electric disk separator is used for the first time in an industrial engine, which is located in a space-saving constellation in the inner V. The blow-by gas containing oil is routed from the crankcase into the disk separator, flowing through the latter radially from inside to outside. The oil accumulates on the 98 rotating disks and is cast centrifugally outwards and returned from there to the crankcase. The cleaned gas flow leaves the disk separator via a constant-pressure valve and is returned to the combustion chamber. The disks rotate electrically in the entire engine map at a constant speed of 12,000 rpm, the system thereby achieving separating efficiencies > 98 % for smallest droplet

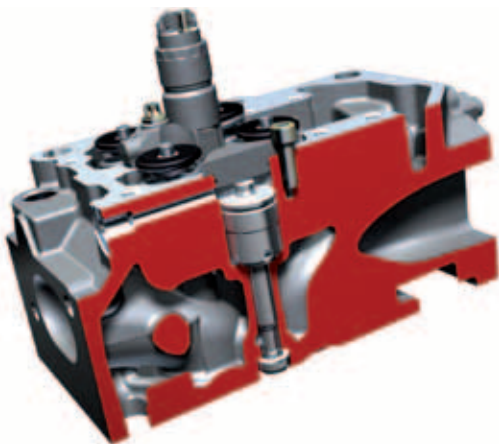


④ Deutz burner system

sizes (0.4 µm). In contrast to conventional separating systems, droplet sizes down to the aerosol range are therefore separated off reliably. The majority of particles < 0.4 µm consist of evaporated and re-condensed lube oil droplets, they contain much less lube oil components with a tendency to accumulate and thus remain uncritical for the compressor cleanliness.

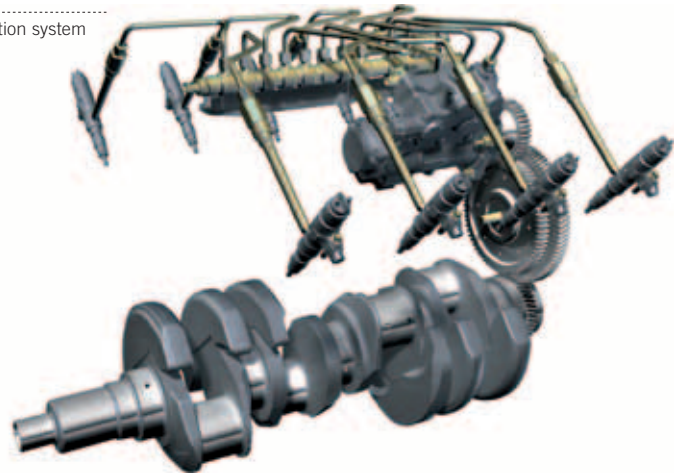
The TCD 12.0 V6 and TCD 16.0 V8 engines have individual cylinder heads that can be installed on either cylinder bank with four valves per cylinder, which are actuated via forked rocker arms and push rods. The cylinder heads have been redesigned for exhaust level Tier 4i/EU Stage IIIB. Besides integration of the common rail injectors, which are fuel supplied at the sides via an inlet connector, the cylinder heads optionally have an additional valve, which is used as engine brake. The brake valve, whose seat is a machining variant in the cylinder head, is operated with engine oil pressure and enables a bypass bore into the exhaust port, 6.

On the exhaust side, the TCD 12.0 V6 and TCD 16.0 V8 engines have waste gate turbochargers. For emission level Tier 4i or EU Stage IIIB, their layout has been fundamentally revised, with water-cooled electrical actuators being used for operating the waste gate, as in the in-line Deutz engines. This resulted in simplification to the design as well as a significantly improved transient behaviour in comparison to the predecessor, which had a fixed turbocharger with separate pneumatic bypass valve.



6 TCD 16.0 V8 cylinder head with brake valve

5 Distribution and injection system



**FUNCTION AND DURABILITY TESTING**

The function and durability testing is based on the long-standing experience from Deutz engine developments and has been supplemented further by the additional requirements of Exhaust After Treatment Systems (EATS).

The development of new specifications for EATS corresponded in particular to the specific requirements from the diverse off-road applications. The overview in 7 shows the content of the function and durability testing for all engines with EATS.

**PISTON TEMPERATURES**

Adaptation of the SCR combustion process to the TCD 6.1 L6 Agripower engine represented a challenge regarding mechanical validation of the basic engine. The higher thermal and mechanical stresses associated with SCR combustion in comparison to EGR combustion call for extensive functional examination in the powertrain. As an example, the temperature field measurement at the piston (PTM) is to be examined here. While standard piston temperature measurements using “temp-plugs” can only provide a static record of the maximum temperature, the “online” PTM measuring method also allows transient temperature variations to be recorded at all critical points of the piston.

The measured values enable a detailed calibration of the piston calculation model, while engine protection strategies for critical application and surrounding boundary conditions for field use can also be devised.

The calculated FEA temperature field for the pistons of the Tier 3 engine without cooling gallery reveals piston bowl rim temperatures just below the critical limit for aluminium materials under the new boundary conditions of the Tier 4i SCR combustion. For comparison of the calculation, a PTM measurement with the previous series pistons without cooling gallery was therefore conducted at the beginning of the Tier 4i combustion development. The temperatures thus ascertained confirmed the critical temperature level in the area of the piston bowl rim and the necessity to introduce a cooling gallery. Repetition of the PTM with the cooling gallery piston confirmed a significant reduction in temperature as expected, 8.

**TURBOCHARGER AND CONNECTION**

Owing to the installation space requirement typical of tractors for a small engine width, the turbocharger of the TCD 6.1 L6 Agripower must be located above the valve cover. The resultant so-called “swan neck” of the exhaust manifold, 3, represents a special challenge for the turbocharger and the electrical actuator from a vibrational point of view. Besides the usual turbocharger validation, e.g. oil leak tightness test and installation temperature survey, the shaft motion track of the turbocharger rotor assembly had to be measured for this particular installation position.

To examine the operational reliability under all operating conditions and tolerances occurring in the tractor, compressor and turbine wheel were provided with a

ENGINE MECHANICS DURABILITY TEST	FOCUS OF TESTING	DURATION
VIBRATION DURABILITY TEST	Vibration validation of add-on parts and systems	
FULL-LOAD DURABILITY TEST	Wear to crank drive, valve train, bearings	
CYCLE DURABILITY TEST	Thermo-mechanical alternating loads: cylinder head, cylinder head gasket, turbocharger, exhaust line, EGR cooler, pistons	
RELEASE DURABILITY TEST	Final program run for entire engine	
		Total 62,000 h
<b>EXHAUST GAS AFTERTREATMENT</b>		
SCR CRYSTALLISATION DURABILITY TEST	Low load operation	
SCR HIGH-TEMPERATURE DURABILITY TEST	High-temperature operation	
DPF REGENERATION CYCLE	Regeneration durability testing	
DPF FIELD CYCLE	Software and data setting (e.g. soot loading model)	
DPF COLD CHAMBER	Cold start & cold operation	
		Total 8,500 h
<b>FUNCTION TEST</b>		
MOTOR MECHANICS	Component & system testing	
THERMODYNAMICS APPLICATION	Data setting & map application	
EXHAUST AFTERTREATMENT APPLICATION		
		Total 45,000 h
<b>FIELD TEST</b>		
REPRESENTATIVE TEST SPECIMENS	Function & durability under field conditions	
		Total 45,000 h
		Total amount 160,500 h

7 Deutz Tier 4 interim engine test bench and field validation

maximum imbalance and the bearing clearance set to the maximum dimension. The turbocharger provided with an inductive measuring system for recording the shaft motion track was now operated under “worst case” conditions at extremely low lube oil pressure and temperatures in transient measuring cycles and the operational reliability of the turbocharger was demonstrably ensured.

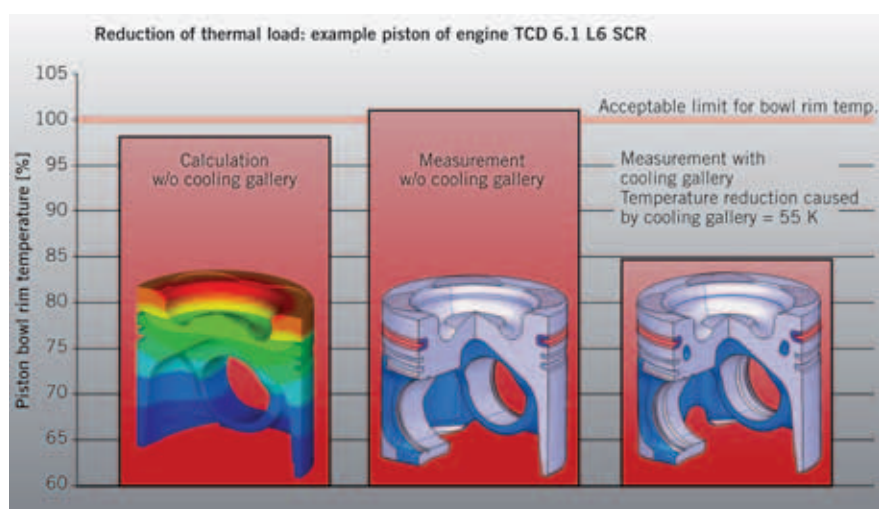
### EXHAUST AFTERTREATMENT COMPONENTS

The significantly higher requirements for the exhaust aftertreatment components in off-road application in comparison to on-road is above all due to higher shock loads and tougher load cycles. The mechanical durability was tested in component tests based on the real values measured in the vehicle. In this way, durability of the components could be reliably ensured.

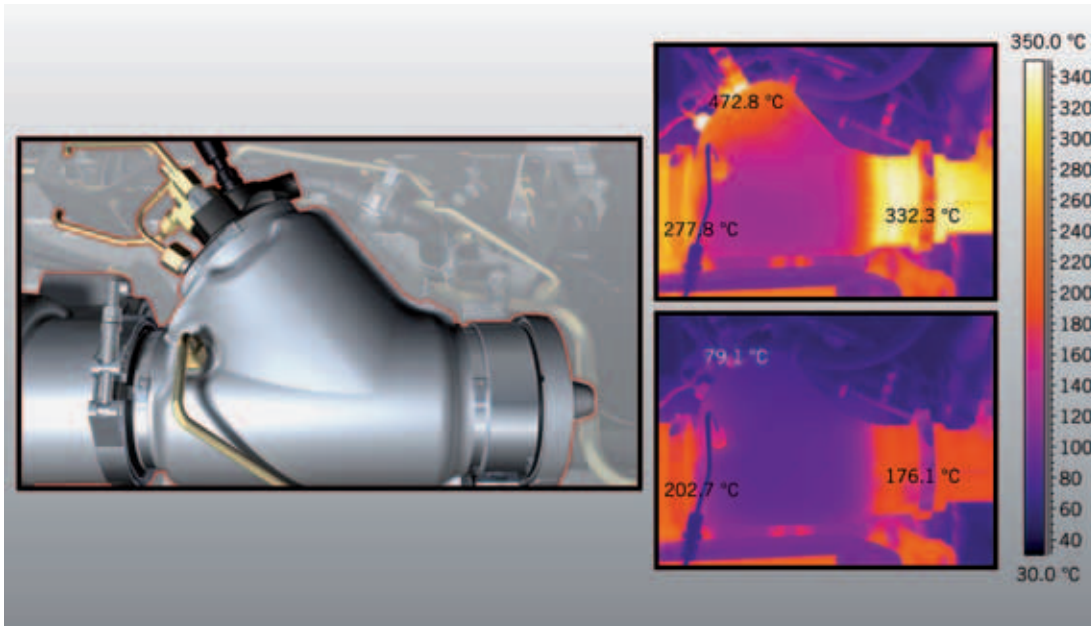
New tests for ensuring the function and durability have been developed for the

Deutz burner system. The functional validation comprises both component tests for the media supply and the ignition components as well as the overall system testing on a burner test bench developed in-house. The regeneration capability at

all operating points in the engine map under stationary and highly-transient conditions was also verified at high altitude under extreme temperature conditions. To ensure the thermal material strength, extreme temperature amplitude tests have



8 Piston thermal stress



9 Burner in thermal shock testing

been conducted. 9 shows the temperature amplitudes. The durability of the overall system was verified via shaker tests and special engine test bench endurance trials (lifetime test).

New test standards compatible with the high requirements of off-road applications have also been defined for the DPF component tests jointly with the system suppliers. “Worst case” load spectra for the (thermo-)mechanical stress on the exhaust aftertreatment components in field measurements were therefore determined in the early phase of the development, these forming the basis for the service life design:

- Component tests/test bench at supplier:
- : hot-shaker test
  - : thermal shock test
  - : pipe bending fatigue test
  - : service life test.
- System tests/test bench at engine manufacturer, 10:
- : loading – regeneration test (substrate life cycle test)
  - : field simulation (software & data input for soot loading model)
  - : cold cycle test (cold start & cold running performance).
- The service life test corresponds to the real loads of the “worst case” application. The harmful elements thereof ascertained

in the field are transferred to a real time test on a hot-shaker test bench, taking into consideration a safety factor. The complex harmful mechanisms of the above test are summarized as a whole in 10.

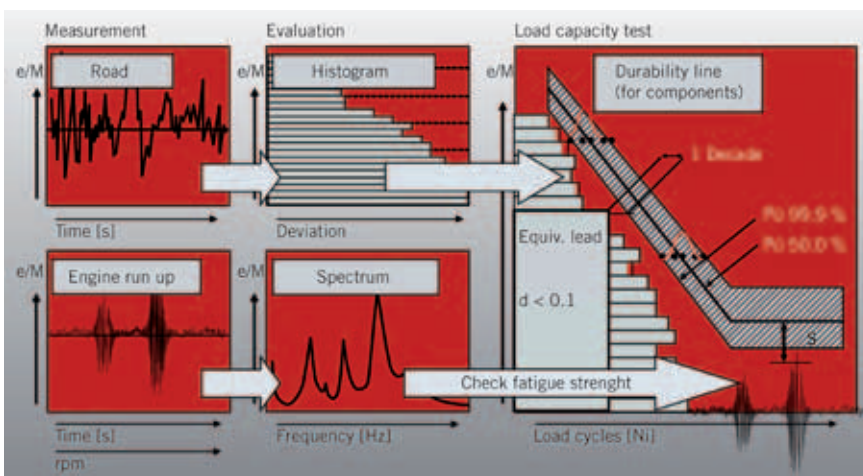
**SUMMARY**

The Deutz engines with powers above 130 kW have been revised in essential parts for exhaust level Tier 4i/Stage IIIB, their most recent form enjoying a leading position technically ahead of the competition. In the range from 130 to 520 kW, it was possible to further increase the power by up to 15 % depending on the series, while the specific fuel combustion could be reduced by up to 6 %. The measures for Tier 4i/Stage IIIB lay the foundations for the next development phases set to ensure that the engines reliably comply with the exhaust classes Tier 4 final or EU Stage IV.

**REFERENCES**

[1] Bülte, H.; Schiffgens, H.-J.; Broll, P.; Beberdick, W.: Technologiekonzept von Deutz zur Einhaltung der Grenzwerte der Abgasstufe US EPA Tier 4 und EU Stufe IV für Motoren in Mobilien Arbeitsmaschinen. 17. Aachener Kolloquium Fahrzeug- und Motorentechnik 2008, Aachen, 2008

[2] Bülte, H.; Schiffgens, H.-J.; Broll, P.; Schraml, S.: Abgasnachbehandlungskonzepte für Motoren in mobilen Arbeitsmaschinen gemäß der Gesetzgebung US Tier 4 und EU Stufe IV – Technologien und Applikationen. 18. Aachener Kolloquium Fahrzeug- und Motorentechnik 2009, Aachen, 2009



10 Determining the component service life from load populations (source: Tenneco)

# BOOSTING CIRCUITS WITH THE NEWEST KNOWLEDGE.



© 2009 creative republic & Rantow Frankfurt / iStock

personal buildup for Force Motors Ltd.



**LEADING TECHNICAL KNOWLEDGE, WHICH  
PUTS AUTOMOTIVE ELECTRONICS INTO GEAR.**

Electronics are the motor for innovation in automotive engineering. **ATZ elektronik** delivers the newest findings on electric mobility, high performance electronics, energy management, testing, human-machine interaction, consumer automotive electronics, and anything else that would electrify automobile developers. Geared for professionals who seek unique in-depth information.

More information at: [www.ATZonline.de/leseprobe/atze](http://www.ATZonline.de/leseprobe/atze)

**ATZ elektronik**



## THE NEW 4.6 L V8 GASOLINE ENGINE FROM MERCEDES-BENZ

Mercedes-Benz is poised to introduce a new generation of the V6 and V8 gasoline engines. Autumn 2010 will see the successful V6 engines with the internal model designation M272 and the M273 V8 engines replaced with a completely new engine family on a phased basis beginning with the CL-Class and followed by the S- and E-Class.

## AUTHORS



**DIPL.-ING. GERHARD DOLL**  
is Senior Manager Development  
Basic Engine M 276/M 278 at  
Daimler AG in Stuttgart (Germany).



**DIPL.-ING. ANTON WALTNER**  
is Senior Manager Combustion  
Development Gasoline Engines  
at Daimler AG in Stuttgart  
(Germany).



**DIPL.-ING. PETER LÜCKERT**  
is Director Gasoline Engine  
Development at Daimler AG  
in Stuttgart (Germany).



**DIPL.-ING. ROLAND KEMMLER**  
is Senior Manager Calibration  
Gasoline Engines at Daimler AG in  
Sindelfingen (Germany).

## OBJECTIVES

The new engines with the model designation M 276 for the V6 engine and M 278 for the V8 engine are systematically based on modularisation and technological development.

The use of flexibly deployable technological modules permits the fulfilment of the different market and legal requirements worldwide and guarantees the sustainability of the engine family for the future. The successful V6 and V8 gasoline engines with the internal model designation M 272 and M 273 rolled out across all Mercedes-Benz vehicles in the medium-size and luxury class since 2004 will now be replaced by a new family of engines. The new V6 has the model designation M 276 and the new V8 the model designation M 278. The new engines fulfil the following requirements:

- : high-performance engine offering exclusive driving characteristics and benchmark-oriented fuel consumption targets
- : fuel consumption-optimised technical equipment including third-generation direct injection as well as stop/start functionality
- : the highest levels of acoustic and vibration comfort
- : fulfilment of current emissions regulations worldwide with potential for the future

- : modular concept for the integration of turbocharging and hybridisation
- : fuel compatibility up to an ethanol content of 25 % and, as an additional module, up to 85 %
- : provision of a further performance module.

The purpose of the newly developed V8 engine – which is described below – was to introduce a new engine based on the tried-and-tested M 273 engine design that best meets these requirements.

In order to reduce fuel consumption and CO<sub>2</sub> emissions, the main development emphasis was therefore placed on further developing the direct injection system featuring spray-guided combustion and piezo injectors, successfully introduced in series production at Mercedes-Benz, as well as on reducing the power consumption of auxiliary devices such as a scaled-down water pump, use of a regulated oil pump, a flow-controlled high-pressure fuel pump, generator management and second-generation thermal management as well as the reduction of friction losses in the engine and cylinder head, ❶.

## DESIGN CHARACTERISTICS

Despite significantly higher engine loads, suitable further development made it possible to use the tried-and-tested basis of the predecessor engine and to carry over important production-relevant characteristics, ❷.



❶ Technologies used in the new M 278 V8 gasoline engine

		M 278 DELA 46	M 273 KE 55 (PREDECESSOR)
TRANSMISSION		7 gear automatic	7 gear automatic
NO. OF CYLINDERS		V8	V8
BANK ANGLE		90°	90°
VALVES/CYLINDER		4	4
DISPLACEMENT	cm <sup>3</sup>	4663	5461
BORE	mm	92.9	98
STROKE	mm	86	90.5
CYLINDER GAP	mm	106	106
COMPRESSION	ε	10.5	10.5
CONROD LENGTH	mm	146.5	148.5
MAIN BEARING DIAMETER	mm	64	64
BEARING WIDTH	mm	20.6/24	20.6/24
CRANK PIN DIAMETER	mm	52	52
BEARING WIDTH	mm	19.6	19.6
PISTON COMPRESSION HEIGHT	mm	32.35	28.1
NOMINAL POWER, RATED RPM	kW rpm	320 5250	285 6000
NOMINAL TORQUE, RATED RPM	Nm rpm	700 1800-3500	530 2800-4800
MAX. BOOST PRESSURE	mbar	900	-
ENGINE WEIGHT DIN 70020 GZ	kg	220	195
CERTIFICATION FUEL		Eurosuper RON 95	Eurosuper RON 95

② Comparison of key data of the M 278 with that of the predecessor engine

**CRANKCASE AND ENGINE**

Despite additional increased loads, the engine still has a die-cast aluminium crankcase with aluminium/silicone cylinder liners. Basic and connecting rod journal diameters were adopted from the predecessor engine, while the piston compression height was raised by just under 4 mm for load reasons. By reducing the stroke and shortening the connecting rod by 2 mm, it was possible to retain the interior height of the crankcase. The high compression ratio of 10.5:1 of the naturally aspirated engine remains unchanged despite the use of turbocharging.

**CYLINDER HEAD AND ENGINE TIMING**

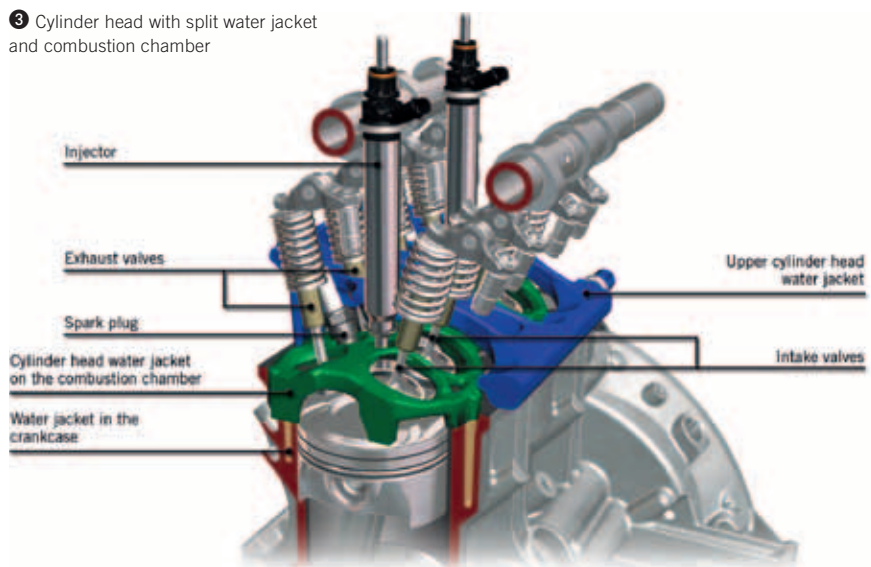
The tried-and-tested basic cylinder head design featuring the compact, low-friction roller cam follower valve control was largely carried over from the predecessor engine.

Due to the higher combustion chamber load and in order to achieve the desired high compression ratio along with an excellent centre of combustion position, the heat transfer on the combustion chamber roof was significantly improved. The required flow optimisation was realised by means of a two-piece water jacket, ③.

The development of the functional and production-oriented design of the cores and the cylinder head using unprecedentedly small core cross-sections represented a particular challenge for the Development and Manufacturing departments.

The new V8 is equipped with a completely new silent chain timing assembly. The aim on the one hand was to ensure a compact design so as to further reduce the crash-relevant overall height of the

③ Cylinder head with split water jacket and combustion chamber



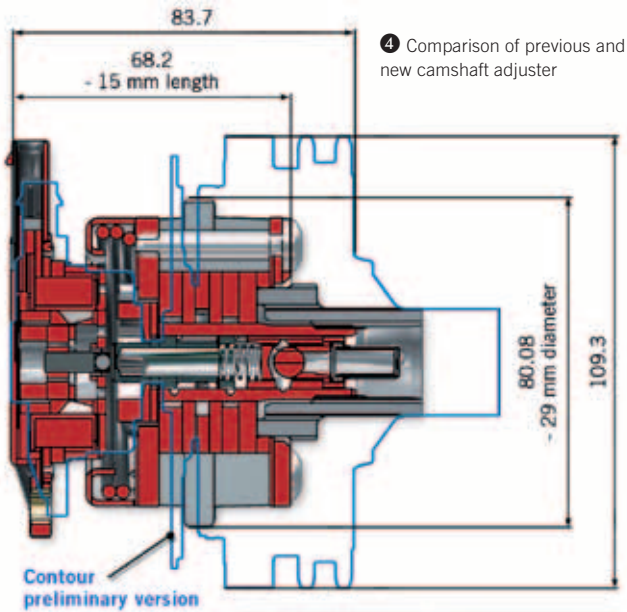
engine in particular, while at the same time further optimising the tried-and-tested good acoustic and durability characteristics as well as the chain friction on the other. The further development of the hydraulic vane-type camshaft adjuster was an important aspect in terms of installation space requirements and weight optimisation.

The significant improvements in relation to weight, installation space and function can be clearly seen in ④. In order to ensure an optimum level of wear and leakage, the use of steel was retained. Even so, weight was nearly halved compared with the previous status.

**COOLANT CIRCUIT AND THERMAL MANAGEMENT**

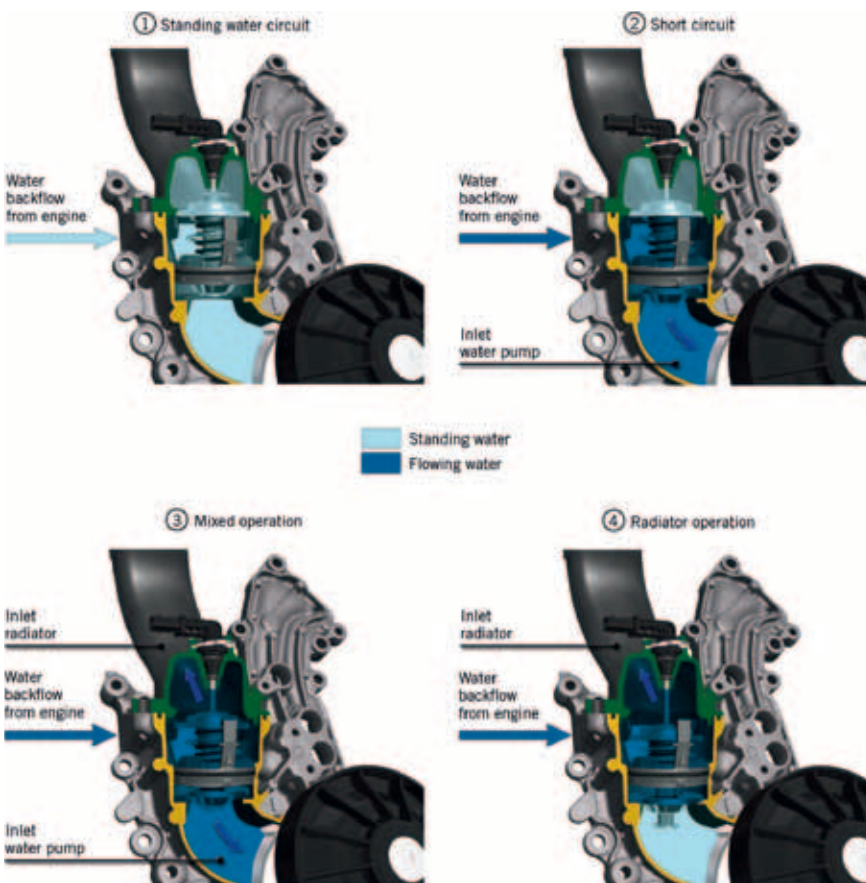
The new V8 engine incorporates efficient thermal management based on the following components: A highly efficient and compact coolant pump, an unrestricted coolant circuit and an electrically regulated thermostat which can set different water control temperatures according to the engine’s characteristic map. Its special design allows it to interrupt the flow of coolant while the engine reaches its operating temperature, which means that coolant is not circulated in the crankcase and cylinder head during this phase.

An additional electrically activated valve also blocks the heating circuit during this phase, preventing it from acting



④ Comparison of previous and new camshaft adjuster

	New version	Preliminary version
Advance angle [°KW]	40	40
Adjustment speed	135 %	100 %
Adjustability from bar	1.0	1.4
Weight [g]	930	1755



⑤ Optimised thermal management based on switch on / switch off water circuit

as a possible bypass. ⑤ shows the concept of this two-disc thermostat in its four control phases.

The improvements achieved in fuel consumption result on the one hand from the reduced power consumption by the water pump during the standing water phase and on the other from the faster warming-up of the oil and water in the engine.

### OIL CIRCUIT

The new V8 is equipped with a completely new vane-type oil pump featuring automatic flow control based on two map-controlled electrically activated main oil duct pressure stages. The controlled oil pump as the heart of the concept was developed in-house as a modular and universally applicable complete system. The system is also manufactured in-house, ⑥. At this point, there are two characteristics that need to be highlighted, specifically:

- : the aluminium oil pump housing and aluminium intermediate flange are anodized thus ensuring long-term wear resistance and low leakage play
- : an additional external gear pump acting as an intake stage for the turbocharger oil return lines guarantees reliable drainage of the turbocharger.

With the two switched compression stages of 2 bar respectively 4 bar the lubrication and cooling points of the engine are supplied in line with the engine load and engine speed in absolute terms and particularly in the partial load range using significantly lower drive power than would be possible with an uncontrolled pump.

Whereas all lubrication and cooling points in the engine are supplied with the maximum amount of oil at 4 bar in the high pressure stage, the volume flow in the low pressure stage of 2 bar is reduced to the absolute minimum required. At the same time, oil sprayers for cooling the piston underbody are shut off since the selected opening pressure is not reached.

⑦ uses the example of the NEDC to illustrate the percentage reduction of drive power in the controlled pump compared to that of a conventional oil pump.

The mean value shows that the oil pump drive power falls to below 35 % of that of the fixed pump.

**GAS EXCHANGE**

⑧ shows the entire scope of components and their extremely compact arrangement, which contributes significantly to the excellent dynamic response to load demands.

Since it was possible to accommodate the hot gas ducting with the turbochargers on the outsides of the cylinder heads, this enabled the intercooler module with its air/water intercooler and charge-air distributor to be located compactly inside the V of the engine.

The two damper filters are symmetrically arranged above the cylinder heads.

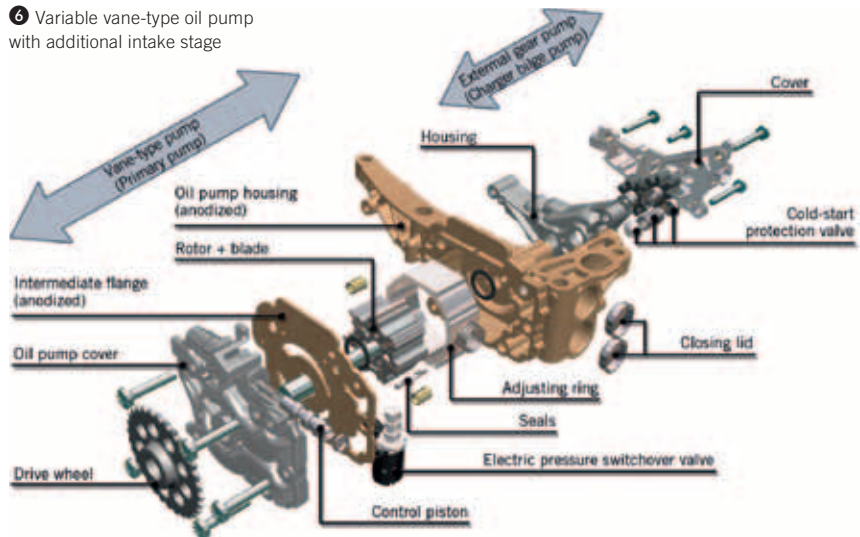
The supply to the compressors and the connection from the compressors to the central intercooler is realised using extremely thin-walled hydroformed stainless steel tubes which perfectly satisfy the requirements of installation space, weight and pressure stability.

Charge regulation takes place using a single butterfly valve fitted between the outlet of the intercooler and the inlet into the charge air distributor at the rear of the engine.

**TURBOCHARGING**

The two waste-gate turbochargers are an assembly consisting of a cast steel part containing the turbine, waste gate and gas distribution for the first cylinder and a welded double-walled pressed steel manifold for the gas distribution to cylinder two to four on each side. For space-saving reasons, an exhaust pipe that con-

⑥ Variable vane-type oil pump with additional intake stage

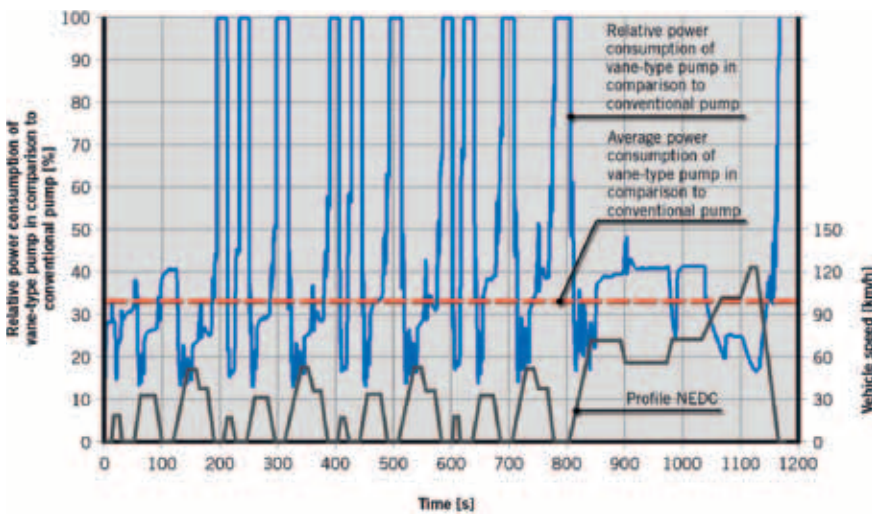


nects turbine outlet and the exhaust system is pre-assembled on the turbocharger, ⑨. The turbine and compressor are optimised to meet the conflicting objectives of achieving a good response on the one hand and a full-load response that benefits fuel consumption on the other. Another important aspect relating to control response, dynamics and emissions optimization was the use of a vacuum-operated waste gate enhanced by a mechanical vacuum pump to ensure that vacuums are created as quickly as possible. A pleasing fringe effect of choosing this extremely rapid control system was the ability to omit a deceleration air valve on the compressor. The double-walled sheet metal exhaust manifold and an additional double-walled exhaust pipe

from the turbocharger outlet leading to the separating point for the hot end of the vehicle exhaust system guarantee a swift response of the catalytic converters.

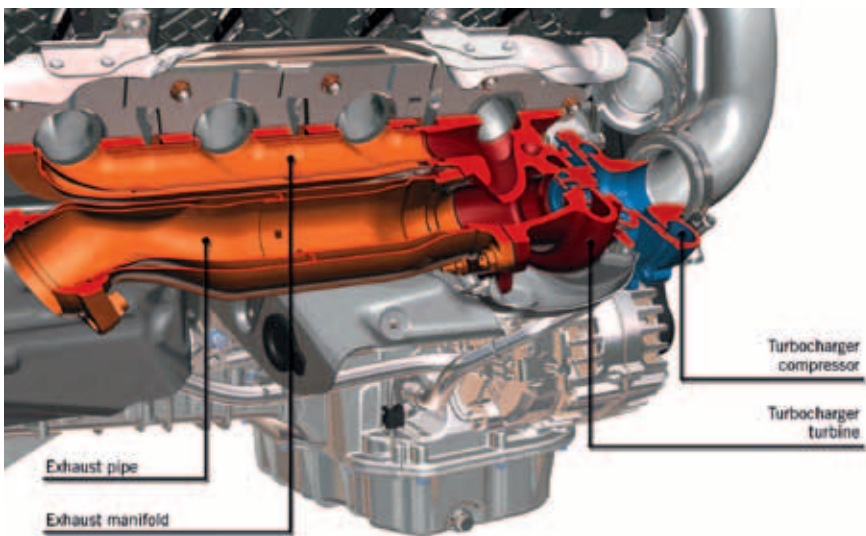
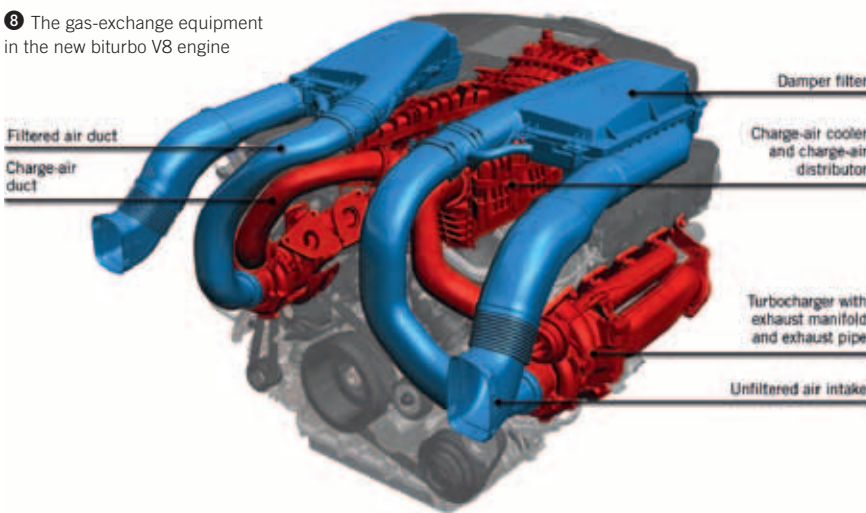
**INJECTOR AND COMBUSTION SYSTEM**

The third-generation direct injection system was further developed based on experience gained with the current M 272 engine. The common rail pressure can be varied between 120 and 180 bar depending on the operating mode. The newly developed high-pressure injector with direct control by means of a piezo actuator is capable of delivering up to five extremely precise injections per cycle and forms the basis of the newly developed combustion system.

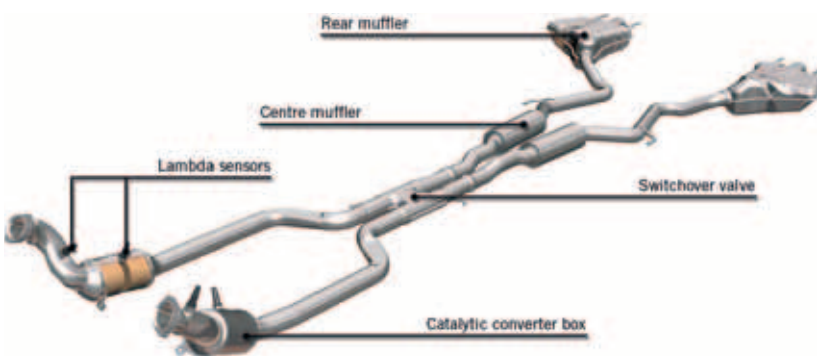


⑦ Power consumption of the new variable oil pump in comparison to conventional oil pump

8 The gas-exchange equipment in the new biturbo V8 engine



9 Configuration of exhaust gas distribution and turbocharger on the new biturbo V8 engine



10 The exhaust system of the new 4.6 l biturbo engine M 278 in the S-Class

Naturally, the objectives in developing the combustion system for the new V8 engine were to lower fuel consumption and emissions on the one hand while providing the kind of NVH response ex-

pected of a premium 8-cylinder engine on the other. The basic elements were:

- : a compact combustion chamber with a central spark plug and central injection valve

- : optimum cooling of the combustion chamber by designing the water jacket accordingly
- : rapidly and precisely operating injection valve offering multiple injections during a cycle
- : optimised charge movement in the combustion chamber by means of suitable configuration of the intake duct and the piston crown
- : fully exploiting the possibilities offered by the extremely accurate multiple injections from the piezo-actuated injector
- : realising an extremely high compression ratio of 10.5:1, resulting in particular from the aspects mentioned above
- : use of the multi-spark ignition system depending on the operating point.

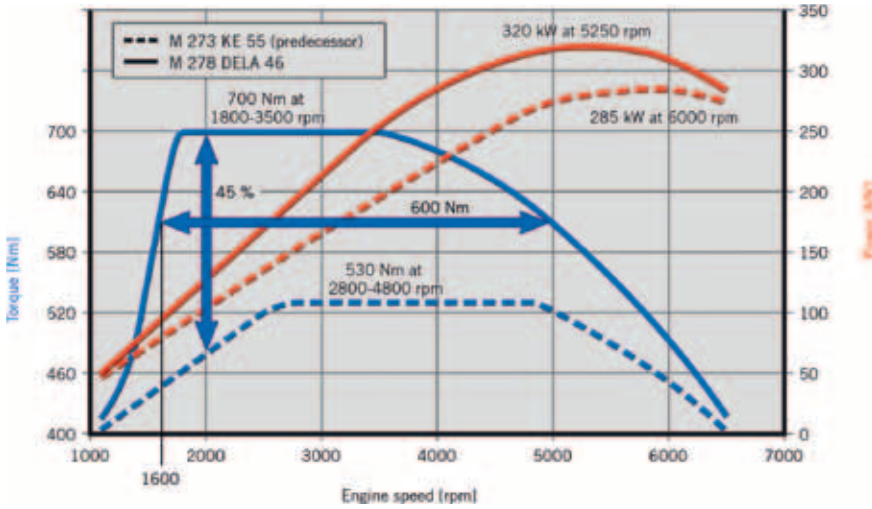
Taking into account the core sales markets for this engine – in which low-sulphur fuel is not available, thus making lean stratified operation impossible – the engine uses homogeneous direct injection, i. e. the engine operates predominantly in the range  $\lambda = 1$ .

The excellent and easily controllable mixture preparation by the new piezo injectors offers an unprecedented degree of control over the ignition and combustion process in order to optimise fuel consumption, emissions and noise development.

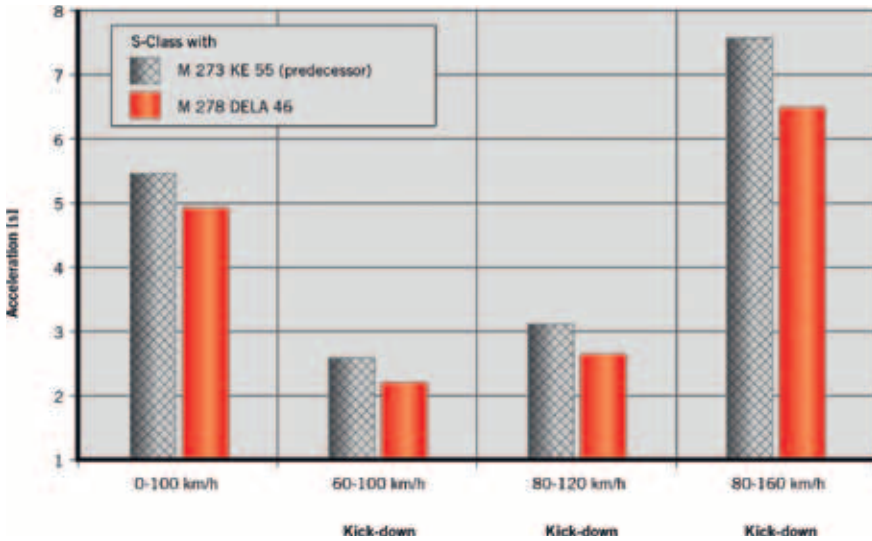
Beneficial side effects of this include excellent cold start characteristics and an optimised catalytic converter heating strategy without a secondary air delivery system. To ensure the optimum mixture formation during the catalytic converter heating phase, up to 5 injections are delivered per intake. Together with the lean combustion chamber  $\lambda$  here and the delayed ignition, it was possible to dispense with a secondary air delivery pump to ensure a rapid light off of the catalytic converters, despite the use of a turbocharger (which acts as an additional heat sink).

## EMISSION CONTROL

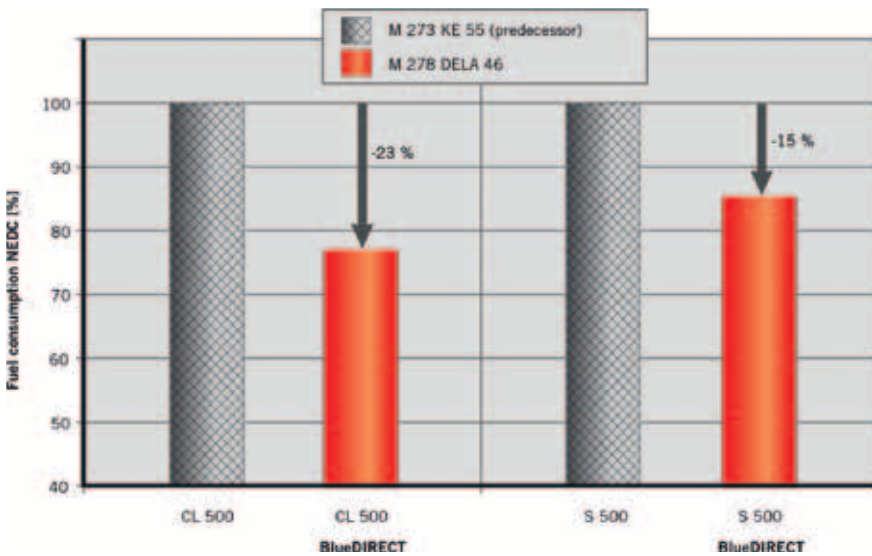
The challenge in developing the exhaust system, 10, for the M 278 was in overcoming the high mass flow rates combined with high temperatures. Looking ahead to the future, the exhaust system also had to offer the potential to meet the emissions requirements around the world during the next decade.



① Power and torque compared with the predecessor engine



② Comparison of performance values, kick-down



③ Comparison of vehicle fuel consumption of the current engine M 278 DELA 46 and the previous M 273 KE 55 engine

The near-engine mounted catalytic converter boxes each contain 2 ceramic monoliths with a volume of around 1.5 l. The cell density is 600 cpsi in the front monolith and 400 cpsi in the rear one, both are provided with a Pd/Rh coating.

For control purposes, linear O<sub>2</sub> sensors are arranged in front of both catalytic converters with planar sensors fitted between the two bricks.

The acoustic components are fitted further along the exhaust system. Noise attenuation begins in the underbody with a switchover valve featuring a monochoque design.

This is followed by two separate centre mufflers designed as Helmholtz resonators which contain additional sound absorption wool. The two rear mufflers contain a reflection chamber and additional sound absorption wool.

Damper weights are used to optimize the NVH response. The pipe routing and acoustic components were optimized so that it was possible to achieve virtually the same exhaust back pressure value of the predecessor engine even though the mass flow rate has increased by around 30 %.

**START-STOP SYSTEM**

The new V8 engine is equipped for the relevant markets with the in-engine Mercedes-Benz-start-stop function. This is a combination of an engine-stop function, which switches off the engine based on activating operating parameters when the vehicle is at a standstill and the foot brake is applied, and a swift direct-start engine function when the foot brake is released.

The direct-start function uses the fact that the selected piezo injection valve, coupled with precise timing of the injection and ignition, enables the first compression stroke of a cylinder to be used to achieve controlled combustion.

An accurate sensor system combined with finely tuned engine management enables the detection of the very first cylinder TDC and ensures a smooth engine run-up to speed regardless of the highly dynamic intake manifold pressure.

The engine control system manages the activating operating parameters and ensures that the engine is only switched

off if specific conditions are fulfilled. For example, the starter battery must have sufficient energy. Likewise, the engine must have reached the required operating temperature to ensure optimum emission control. The same applies to the interior temperature desired by the driver: If it has not yet been reached, the engine is not switched off when the vehicle is at a standstill. The management system for the vehicle power supply ensures that active audio, telephone or video functions are not interrupted by the ECO start/stop function. A yellow "ECO" symbol indicates to the driver that the ECO start/stop function is activated, but that one of the criteria above is temporarily preventing the engine from being switched off. If all the necessary conditions are fulfilled, the "ECO" symbol switches to green.

#### ENGINE RESULTS, PERFORMANCE AND FUEL CONSUMPTION

Alongside the other internal project targets such as quality, deadlines and costs, the results experienced in the truest sense of the word by the customer are extremely important.

In addition to examining the absolute key figures, it is always interesting to make comparisons with the predecessor product. ❶ shows the torque and power profile under stationary full load.

In this respect, the design focused in particular on the delivery of high torque even at low engine speeds and on avoiding any disadvantages in terms of fuel consumption during moderate output increases under full load.

As a result, the increase in torque at 2000 rpm compared with the previous engine still amounts to 45 %, with an exceptional 600 Nm available between 1600 rpm and 5000 rpm.

The overall design delivered advantages in terms of specific fuel consumption across wide areas of the characteristic map for the new turbo engine, especially in the most relevant driving area.

The performance data compared with the previous engine in the same vehicle, ❷, confirm the development of longitudinal dynamics with excellent figures for the traditional yardsticks of the 0-to-100 km/h dash or kick-down acceleration in the lowest possible gear.

Furthermore, the design and characteristics of the engine guarantee effortless driving with sporty performance available when desired.

In spite of the downsizing, drivers will benefit from a pleasant downspeeding effect during real-life driving conditions.

Despite the very noticeable improvements in vehicle dynamics, it was possible to make further significant progress on the fuel consumption front.

The certified standard consumption figures of the S-Class and CL-Class vehicles to be equipped as first with the new engine in conjunction with the further optimised automatic transmission 7G-Tronic will be between 15 % and 23 % lower than the predecessor engine, ❸.

#### SUMMARY

With the new biturbo V8 engine, Mercedes-Benz has succeeded in implementing a design which, in addition to providing outstanding performance values along with the highest degree of comfort, also appropriately addresses environmental issues and economic viability.

The use of a range of innovative technology modules such as third-generation spray-guided direct injection combined with multi-spark ignition and a direct stop/start system results in fuel consumption values that set new benchmarks for the combustion engine in this class.

## THANKS

The Authors would like to thank Dr.-Ing. Ralph Weller, Dipl.-Ing. Hartmut Weckenmann and Dipl.-Ing. Helmut Herwig for their effort on this article.

# THE NEW GENERATION OF THE AUDI 3.0 L V6 TDI ENGINE



personal buildup for Force Motors Ltd.

## PART 1 – DESIGN AND MECHANICS

Following on from Audi's 2003 production launch of the first generation of the 3.0 l V6 TDI engine, 2010 now marks the launch of the second generation – a completely newly developed unit successfully combining low fuel consumption, low emissions, high power output along with significantly reduced engine weight. This accomplishment is based on a large number of innovative solutions, focused particularly on minimising friction and on lightweight construction. The familiar Audi four-valve combustion method has been thermodynamically modified. The fuel injection system is an updated piezo-inline common rail unit delivering up to 2000 bar maximum rail pressure. The turbocharger has also been modified to provide enhanced spontaneity. In the following design and the mechanics of the new engine are described, the second part in the MTZ 11 deals with thermodynamics, application and exhaust treatment.

## AUTHORS



**DIPL.-ING. RICHARD BAUDER**  
is Head of Diesel Engine  
Development at Audi AG in  
Neckarsulm (Germany).



**DIPL.-ING. ANDREAS FRÖHLICH**  
is Head of Design for V6 Diesel  
Engines at Audi AG in Neckarsulm  
(Germany).



**DIPL.-ING. DANILO ROSSI**  
is Head of Mechanics Development  
for V6 Diesel Engines at Audi AG in  
Neckarsulm (Germany).

## LOW EMISSIONS, LESS CONSUMPTION

V6 TDI engines have become an Audi tradition. The success story began in 1997, with the world's first four-valve 2.5 V6 TDI engine featuring a distributor-type injection pump. In late 2003 came the first V6 TDI with common rail fuel injection – a 3.0 l engine with a chain as the timing drive. In 2004 this in turn led to the lower-power 2.7 l variant. Both engines have since undergone an evolutionary stage, and are successfully deployed on the market in a variety of models, not just from Audi but across the VW Group. Over 1.6 million V6 TDI engines have been produced to date.

In 2010, the second generation of the 3.0 TDI engine will be introduced. An engine with a power output range from 150 to 184 kW and a torque spread of 400 to 550 Nm. State-of-the-art diesel technology with the piezo-inline common rail

system delivering up to 2000 bar rail pressure, consistent thermal management, extensive measures to optimise friction and the start-stop system, in combination with new eight-speed automatic transmissions, make the new engine a low-emission unit which also offers outstanding fuel economy. This ensures customers can enjoy top-class driving pleasure without troubling their conscience.

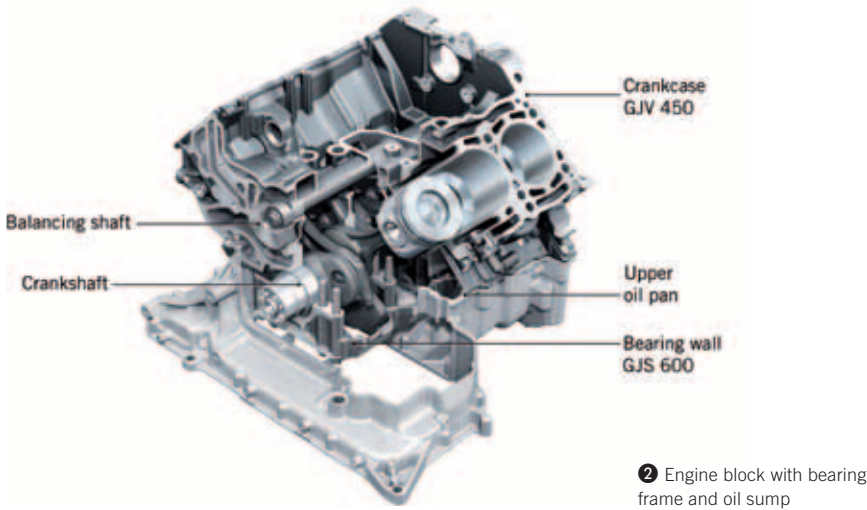
The engine's weight has been reduced by a substantial 25 kg compared to the predecessor generation. The key factors in this are innovative solutions in relation to lightweight construction as well as the use of lightweight materials such as magnesium, aluminium and plastic.

## DESCRIPTION OF THE ENGINE

The new V6 engine features a 90° V angle and a 90 mm cylinder spacing. With an 83 mm bore and a stroke of 91.4 mm,

MAIN DIMENSIONS AND FEATURES OF THE ENGINE		
PRIMARY DIMENSIONS	UNIT	
CONSTRUCTION	–	V6 engine with 90° V angle
DISPLACEMENT	cm <sup>3</sup>	2967
STROKE	mm	91.4
BORE	mm	83.0
STROKE/BORE RATIO	–	1,10
COMPRESSION RATIO	–	16.8:1
CYLINDER DISTANCE	mm	90
CRANKSHAFT	–	forged, four main bearings
MAIN BEARING DIAMETER	mm	65.0
CONNECTING ROD BEARING DIAMETER	mm	60.0
CONNECTING ROD LENGTH	mm	160.5
VALVE DIAMETER		
– INLET	mm	28.7 (2 x)
– OUTLET	mm	26.0 (2 x)
INJECTION	–	Common Rail, 1800/2000 bar (Bosch CRS 3.2/3.3) with piezo-injectors and CP4.2 high pressure pump
EXHAUST GAS TURBOCHARGER		Garrett VTG 2056 (150 kW) / Garrett VTG 2260 (175/184 kW) with variable turbine geometry, electrical controller
IGNITION SEQUENCE	–	1, 4, 3, 6, 2, 5
POWER	kW	150 – 184 kW at 4000/min
TORQUE	Nm	400 – 550 from 1250 – 3000/min
EMISSION LEVEL	–	EU5
WEIGHT ACC. TO DIN 70020 GZ	kg	193
ENGINE EFFECTIVE LENGTH	mm	437.0

① Technical data



engine capacity is 2.967 l. Depending on vehicle equipment and transmission combinations, power output ranges from 150 up to a maximum of 184 kW. Torque ranges from 400 to 550 Nm. Thanks to the compact engine package with the two-piece gearbox-side chain drive, it has been possible to achieve an extremely short overall length of just 437 mm between the gearbox flange and the front edge of the oscillation damper.

To achieve performance and torque figures as well as emission targets, the familiar Audi four-valve combustion method was further developed. The latest generation of the Bosch common-rail system is used, with a maximum rail pressure of 2000 bar. The main technical features are summarised in ❶.

**CRANKCASE**

The crankcase design principle employed on all Audi V-configuration diesel engines has been retained in the new engine generation, ❷. Consequently, the material used is once again vermicular graphite cast iron (GJV-450). This choice was based on the need for high strength and durability under the given geometric conditions of just 90 mm cylinder spacing. The tried and proven construction principle of the bearing frame was also employed for the crankshaft bearing for reasons of strength and rigidity. The material used is nodular graphite iron (GJS-600). The weight of the cylinder crankcase assembly has been cut by 8 kg compared to the predecessor generation based on reductions in wall thickness and on design opti-

misations aimed at achieving a more lightweight construction.

For reasons of packaging, all lateral water ducts were integrated into the engine block. Unlike on its predecessor, the water pump housing was moved from the engine block to the aluminium sealing flange in order to save weight. The crank chamber is enclosed by an ignition force-free oil sump top. Die-cast magnesium is used for the first time as the material for the oil sump top. The weight advantage compared to aluminium is 1.8 kg. The chosen high-rigidity design concept, featuring a GJV crankcase, bearing frame and raised oil sump, offers major benefits not only in terms of weight but also with regard to acoustics, and as such represents the best design principle for Audi.

In order to attain the optimum cylinder shape in motor operation, the crankcase is plate-honed. To do so, in cylinder bore finishing the mounted cylinder head is simulated by honing plates. The almost optimally round bore in motor operation enables a significant reduction in piston ring pre-tension along with low blow-by values. The resultant reduction in mechanical friction plays a major role in improving the efficiency of the new engine generation. As the final cylinder bore machining step, the UV photon imaging process familiar from the predecessor engine is used. Consequently, the new engine too guarantees low oil consumption right from the beginning.

**CRANKSHAFT DRIVE**

The crankshaft forged from 42 CrMoS4 is of split-pin design in order to attain identi-

cal spark gaps on the 90° V-configuration engine. To provide sufficient strength, both the main bearing and conrod bearing pins are induction-hardened. The area of the 30° split pin poses a particular challenge in this respect.

The redesigned crankshaft plays a key role in saving weight on the engine as a whole. By omitting the centre counterweights and introducing crank pin lightening bores, a weight reduction of 2 kg compared to the predecessor generation was achieved.

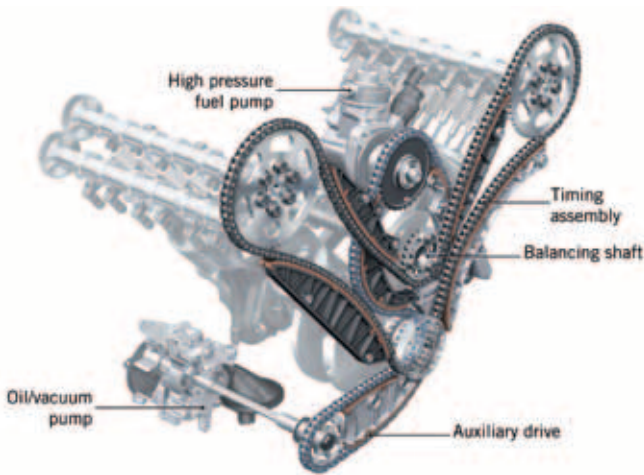
The forged conrods made of 36 MnVS4 are obliquely split and cracked. The aluminium pistons are executed with a salt-core cooling duct and splash oil cooling in order to provide optimum cooling of the bowl lip and ring package.

Lead-free materials are now used in the new generation for the main bearing and conrod bearing shells. At ignition pressures up to 185 bar this imposes particular demands on production tolerances as well as in terms of the cleanliness of the individual components and the assembly processes.

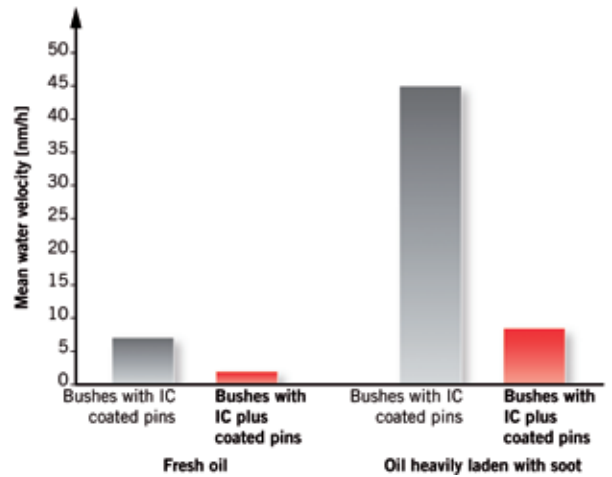
**CHAIN DRIVE**

One of the key features of Audi's V-engine family – the gearbox-side two-track chain drive – has been further optimised on the new V6 TDI, ❸. The layout of the chain drive is new. A relatively long bush chain, with 206 links, is used to drive the two inlet camshafts and the balancing shaft in the timing drive. The chain has a highly wear-resistant coating on the pins, the so-called IC plus coating. This is a further enhanced chromium carbide layer up to 20 µm thick. ❹ shows the rate of wear for chains with conventional chromised pins and IC plus-coated pins as determined with the aid of radionuclide technology. With oil heavily laden with soot, the rate of wear and thus chain elongation is reduced by up to 80 %. Even after rigorous, protracted tests, the elongation does not exceed an outstanding 0.08 %, the maximum permissible limit value being 0.5 %.

The auxiliary drive chain is also executed as a bush chain. It drives the high-pressure injection pump positioned at the rear in the inner V as well as the oil and vacuum pump which are accommodated in a common housing. The new chain layout enabled the number of chains and



③ Chain drive with drive for high-pressure pump, balancing shaft and oil/vacuum pump



④ Chain wear rate

chain tensioners to be reduced from four to two compared to the predecessor generation. The omission of two intermediate gears, as well as the new high-pressure pump drive concept with no additional toothed belt drive, not only makes assembly much simpler but also greatly reduces friction and weight. The new design saves 4 kg in weight compared with the predecessor engine.

### CYLINDER HEAD AND VALVE GEAR

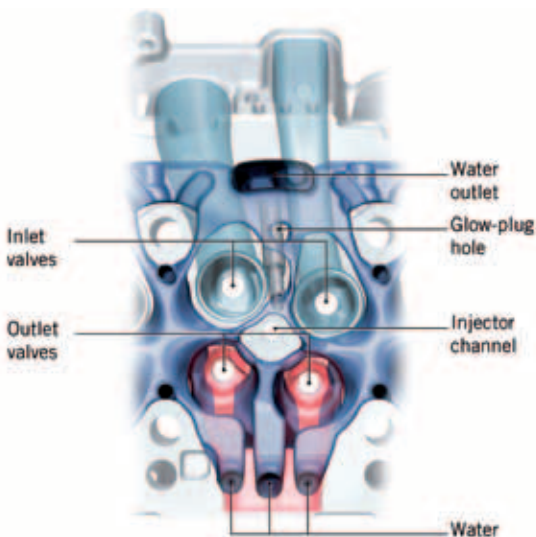
The familiar Audi four-valve combustion method, featuring one tangential and one charging duct on the inlet side and two exhaust ducts converged into a Y-pipe, has been adopted from the predecessor

generation. The inlet ducts have been further optimised in terms of swirl and throughput, largely by way of swirl chambers on the valve seat.

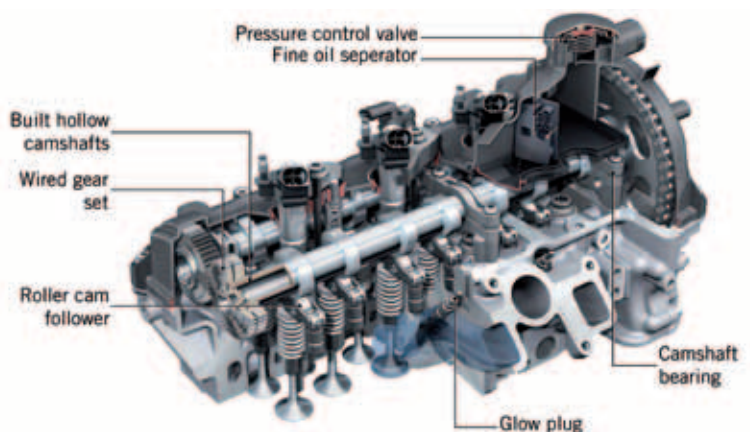
In order to keep the component temperatures close to the valve bridges at a with-standable level despite the increased power output, the cross-flow cooling concept for the cylinder head has been modified. The exhaust valves have been spread apart and reduced in size, so as to increase the cooling water flow cross-section. In addition, the water chamber as a whole has been designed so as to enable targeted water flow at high speeds, thus providing optimum cooling in the areas close to the combustion chamber, between the valves and the injector channel. Water enters on

the exhaust side via the three separate ducts for each cylinder. The main flow is fed between the exhaust valves and is then distributed throughout the remaining valve bridges, ⑤. The intricate structure of the water chamber around the injector channel and between the inlet valves requires utmost precision during the core-making process and when positioning in the mould. The new design enabled the maximum temperatures in the hottest area between the exhaust valves to be reduced by some 10 K, despite the increase in power output.

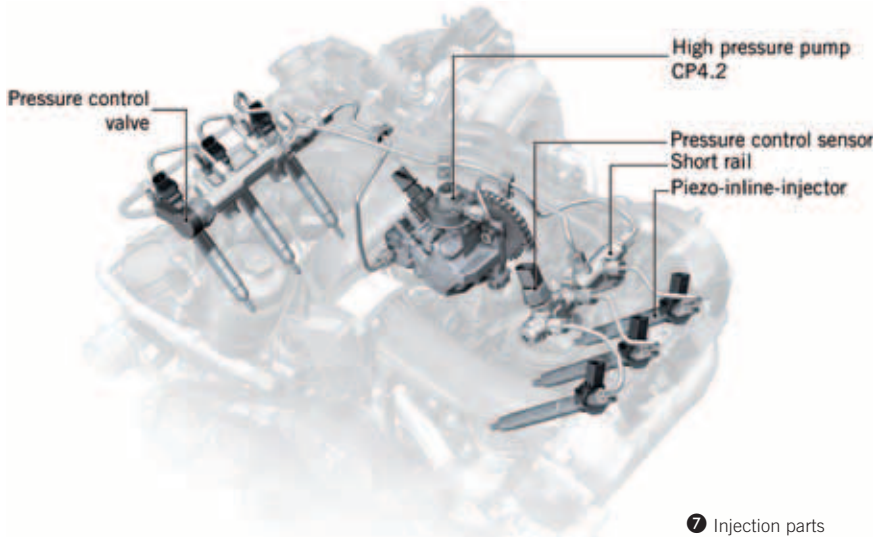
Following cylinder head assembly, the constructed hollow camshafts are mounted on the cylinder heads as a package with split double-bearing blocks, ⑥.



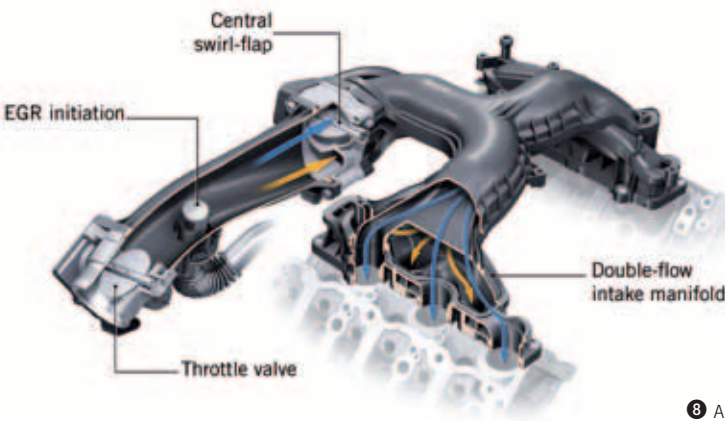
⑤ Cylinder head cooling – bottom view



⑥ Cylinder head with attachment parts



7 Injection parts



8 Air ducting

This assembly sequence permits the use of camshafts without specific clearance for fitting the cylinder head bolts and at the same time allows for a tight camshaft position. The exhaust camshafts are driven by tensioned gear wheels, for acoustic reasons. The valve actuation by low-friction roller cam followers has been adopted from the predecessor generation. To optimise the friction of the valve drive, the camshaft bearing diameters were additionally reduced from 32 to 24 mm.

This design principle also meant that the cylinder head, in AISi10MgCu 0.5, could be made much flatter. In combination with the lightweight plastic cylinder head cover, it was possible to reduce the weight of the two cylinder heads by 3 kg, despite the significant increase in specific power output of the engine as a whole.

Additionally, the engine breather system is integrated into the cylinder head covers with a fine oil separator.

**INJECTION PARTS**

The chosen high-pressure fuel injection system is the latest Bosch common rail system, with up to 2000 bar injection pressure and piezo-inline injectors, 7. Depending on power output and fit spec, the maximum rail pressure is 1800 or 2000 bar, combined with the matching nozzle flow rate. To save weight, the forged rails are extremely short.

The rail pressure is generated by a latest-generation two-stamp high-pressure pump – the so-called CP4.2 – with an aluminium housing. The high-pressure pump is located on the gearbox side in the inner V beneath the turbocharger. It is driven by

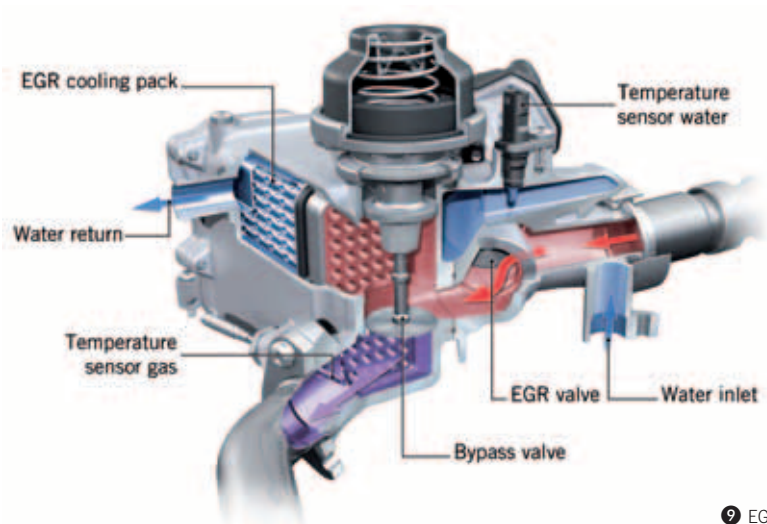
a simplex chain directly from the crankshaft. To synchronise the delivery to the injection, a transmission ratio of 1:0.75 to the crankshaft was selected. To reduce chain forces, the pump mounting on the engine is phase-oriented.

Oil circuit and engine block ventilation As a means of improving efficiency, the regulated oil pump already familiar from the predecessor generation, featuring two pressure stages, was deployed. New, however, is the pump combination. The oil pump and vacuum pump are housed in a single unit. Installation in the oil sump enabled an ideal package solution to be implemented. The two pumps are driven by the gearbox-side chain drive by way of a plug-in shaft. The breather system of the new engine generation has been relocated from the inner V into the cylinder heads. Both cylinder head covers incorporate coarse and fine oil separators, 6.

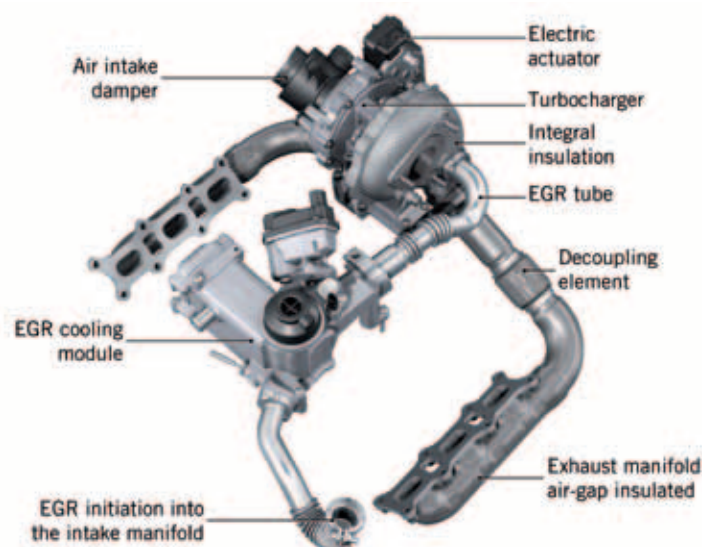
**AIR INTAKE**

The transfer point for the vehicle-side air ducting to the engine is the throttle body on the front of the engine, 8. It was possible to position the throttle body in such a way that its position in all vehicle systems is identical, meaning identical components can be used for the engine-side air ducting. Attached to the throttle valve is a short plastic air duct, into which the recirculated exhaust gas is also routed by way of a thermally insulated stainless steel sheet construction. The geometry of the exhaust gas intake means deposits on the inner walling of the plastic pipe are avoided at all operating points, while at the same time, a good mixture is guaranteed.

The swirl control for the new engine generation is provided by just one central flap instead of the six individual flaps used previously. Consequently, downstream of the central swirl control flap the intake manifold is of dual-flow design as far as each of the two cylinder banks. For this purpose, the intake manifold in plastic (PA6) is of triple-shell construction and friction-welded. The intake manifold geometry was optimised to the individual cylinders in terms of pressure loss and uniformity of air flow distribution based on multiple CFD calculation loops. The reduced pressure loss is advantageous in terms of power output, fuel consumption and spontaneity.



9 EGR system



10 Exhaust manifold, turbocharger and EGR module

## EXHAUST GAS RECIRCULATION

The EGR (exhaust gas recirculation) system plays a key role in safeguarding conformance to emissions standards. The EGR system, optimised to minimise pressure loss and so attain high recirculation rates, draws off the exhaust gas from the turbocharger housing upstream of the turbine. All the exhaust gas recirculation function elements are housed in the EGR module, comprising the EGR valve, EGR cooler and bypass valve, 9. The electrically actuated EGR valve located on the hot side has been redeveloped. To reduce the pressure loss, the seat diameter of the valve has been increased from 27 mm in the predecessor generation to 30 mm.

The cooling power enhanced tubular stainless steel EGR cooler is built-in to the

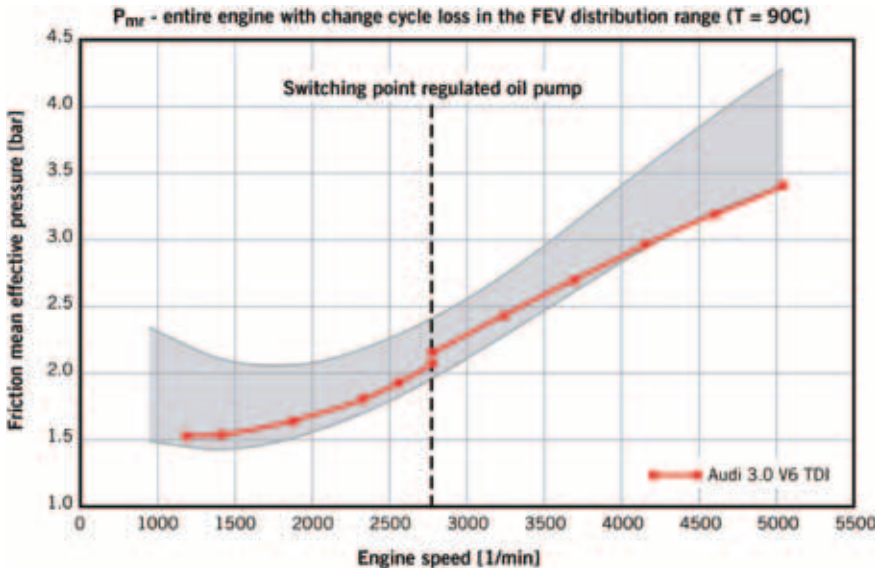
aluminium housing of the module. For EGR cooler bypass, a pneumatically operated lift valve is used instead of a flap. The guaranteed leak-tight seating of a lift valve – as opposed to a flap, with its unavoidable gap – is of major benefit in delivering maximum cooling power. The design-related disadvantage of higher pressure loss was avoided by skilful execution of the inflow and outflow.

An EGR temperature sensor is located in the exhaust gas outlet of the EGR module, which helps to keep the exhaust temperature to a minimum downstream of the cooler. The aim of keeping recirculated exhaust gas as cold as possible in order to maximise the reduction in  $\text{NO}_x$  emissions is thus accomplished; at the same time, condensation is prevented from forming if gas temperatures are too

low. The pressure loss of the complete EGR system has been reduced by around 10 % compared to the predecessor generation, despite the increase in cooling power. This has resulted in emission and consumption benefits based on a broader usable EGR map with high EGR rates, without activating the throttle valve to assist inflow.

## EXHAUST MANIFOLDS AND TURBOCHARGERS

The two exhaust manifolds of the new V6 TDI are executed as a one-piece air-gap-insulated construction, including isolating elements from the cylinder head flange to the flange of the turbine housing, 10. As a result, exhaust gas heat losses in the heat-up phase are minimised.



① Friction mean effective pressure in the FEV distribution range for all engines analysed

To implement the power range between 150 and 184 kW, there are two turbocharger variants featuring specifically adapted rotor assemblies and compressor trims. In all variants the mounting of the rotor assembly was further enhanced to reduce friction loss. As a result, fast response and uniformity of torque build-up was implemented. In order to optimise flow acoustics, in all applications a pulsation damper is built-on to the turbocharger at the compressor inlet.

**WATER CIRCUIT AND THERMAL MANAGEMENT**

To enhance efficiency, particular attention during the development process was paid to the engine’s heat balance. In addition to the powerplant heating up as quickly as possible thanks to the coolant not being circulated in the warm-up phase, the benefits of thermal management were to be secured for all engine operating ranges.

The cooling circuit of the new Audi V6 TDI is therefore executed as a split cooling system, meaning the flow through the cylinder crankcase and the cylinder heads is routed in two separate parallel cooling circuits. A detailed description of the operating principle will be given in the second part of this article in the MTZ 11.

**DRIVE FOR AUXILIARIES**

A poly-V belt drive operates the alternator, air conditioning compressor, water pump and, depending on the vehicle fit spec, also the power steering pump. The crankshaft drive gear is executed as a damper pulley. Due to the increased demands of start-stop operation it was necessary to further enhance the elastomer compound. By lowering the belt tension, it was possible to reduce the bearing forces on idler pulleys and belt pulleys, which resulted in reduced friction losses. A freewheel on the alternator additionally dampens vibrations during the starting process.

**MECHANICAL FRICTION LOSS**

The friction mean effective pressure characteristic with the gas exchange losses of the entire engine is presented in ①; the new V6 TDI is at the lower end of the FEV reference distribution range of all diesel engines analysed. This is one of the key factors in the increased efficiency of the new engine generation.

The relevant features of the new V6 TDI engine in terms of optimising friction and gas exchange are:

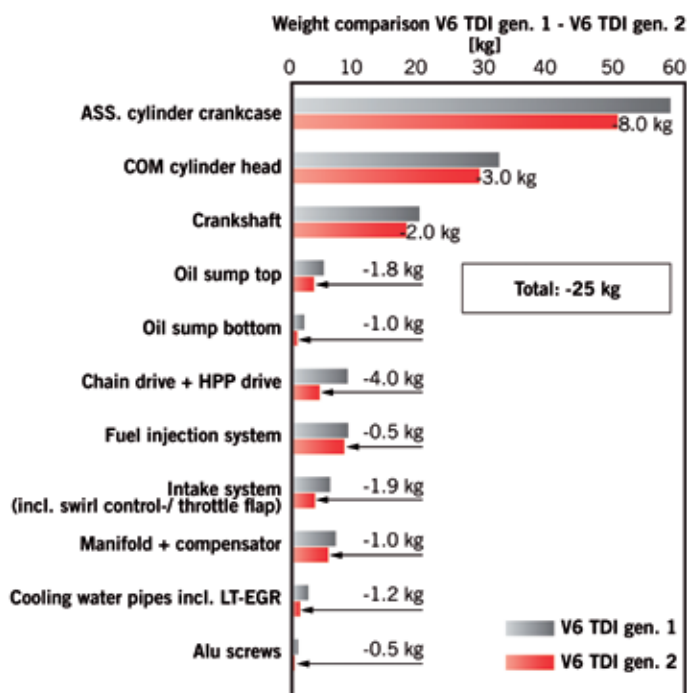
- : Piston rings and cylinder barrel: Plate honing of the cylinder barrels significantly improved the true run-

ning of the bore in engine operation. As a result, it was possible to reduce the tangential forces of the piston rings by around 35 %.

- : Chain drive: Optimised layout with just two instead of the previous four chain drives and additional chain force reduction.
- : Valve drive: New camshaft bearing concept with individual bearing blocks and reduced diameters.
- : De-throttled intake manifold, optimised inlet ducts and turbocharging: These components greatly reduce gas exchange losses, particularly effectively in the upper engine speed range.
- : Adjustable oil pump: As introduced for the predecessor generation, a vane pump with volumetric flow control and two pressure stages is used [5]. The delivery characteristic is varied by a pivot-mounted adjuster ring in order to adapt the volumetric flow of the pump to the actual demand of the engine. The lower pressure level is increased to a maximum engine speed of 2500 rpm, dependent on the engine load, oil temperature and other operating parameters.

**ENGINE WEIGHT**

Consistent application of lightweight construction techniques and the new



12 Weight reduction – engine components

engine design has enabled the weight as per DIN 70020 GZ to be reduced by 25 kg overall relative to the predecessor generation to 193 kg as per DIN 70020 GZ. Only by saving weight on virtually all components was it possible to achieve this minimum weight, 12. The short, compact design produces additional secondary weight effects throughout the vehicle which are beneficial in terms of front axle loading and thus enhance driving dynamics.

The intelligent design meant that not only a very short, but also a very lightweight, V6 diesel engine could be realised, combined with the high strength advantages of a cylinder crankcase made of vermicular graphite cast iron. Consequently, the appropriate development steps have now already been initiated to meet even higher demands in future.

### SUMMARY

Audi TDI engines have always had to be very short and compact in order to ensure optimum vehicle design. With the new generation of the Audi V6 TDI, Audi is once again setting a milestone in the development of diesel engines. State-of-the-art diesel technologies have been combined with consistent lightweight design. The engine's weight has been reduced by a substantial 25 kg compared

to the predecessor generation. Many detailed solutions to minimise friction help the engine to achieve very low consumption figures in the respective vehicle systems.

The new engine offers outstanding power and torque figures of 184 kW and 550 Nm respectively at maximum output. The V6 TDI also convinces with its superb engine acoustics and refinement. The V6 TDI engine has been designed

today to meet the needs of future developments in terms of performance, emissions and consumption.

### REFERENCES

- [1] Bauder, A.; Clos, R.; Hatz, W.; Hoffmann, H.; Pözl, H.-W.; Reichert, H.J.: The new V-configuration engines from Audi. Vienna Engine Symposium 2002
- [2] Bauder, R.; Reuss, T.; Hatz, W.; Pözl, H.-W.: The new V6 TDI from Audi. Vienna Engine Symposium 2004
- [3] Anton, C.; Bach, M.; Bauder, R.; Franzke, G.; Hatz, W.; Hoffmann, H.; Ribes-Navarro, S.: The new 3.0 l V6 TDI engine from Audi, Part 1, Design and Mechanics. In: MTZ 65 (2004) No. 7
- [4] Bauder, R.; Brucker, D.; Hatz, W.; Lörch, H.; Macher, A.; Pamio, Z.-G.; Reuss, T.; Riegger, R.; Schiffgens, H.-J.: The new 3.0 l V6 TDI engine from Audi part 2: Thermodynamics, application and exhaust treatment. In: MTZ 65 (2004) No. 9
- [5] Bauder, R.; Bach, M.; Köhne, M.; Streng, C.; Hofmann, H.; Rossi, D.: The new 3.0 l V6 TDI engine in the Audi Q5. In: ATZ extra – The new Audi Q5 (2008)
- [6] Bauder, R.; Bach, M.; Fröhlich, A.; Hatz, W.; Helbig, J.; Kahrstedt, J.: The new generation of the 3.0 TDI engine from Audi. Vienna Engine Symposium 2010

## THANKS

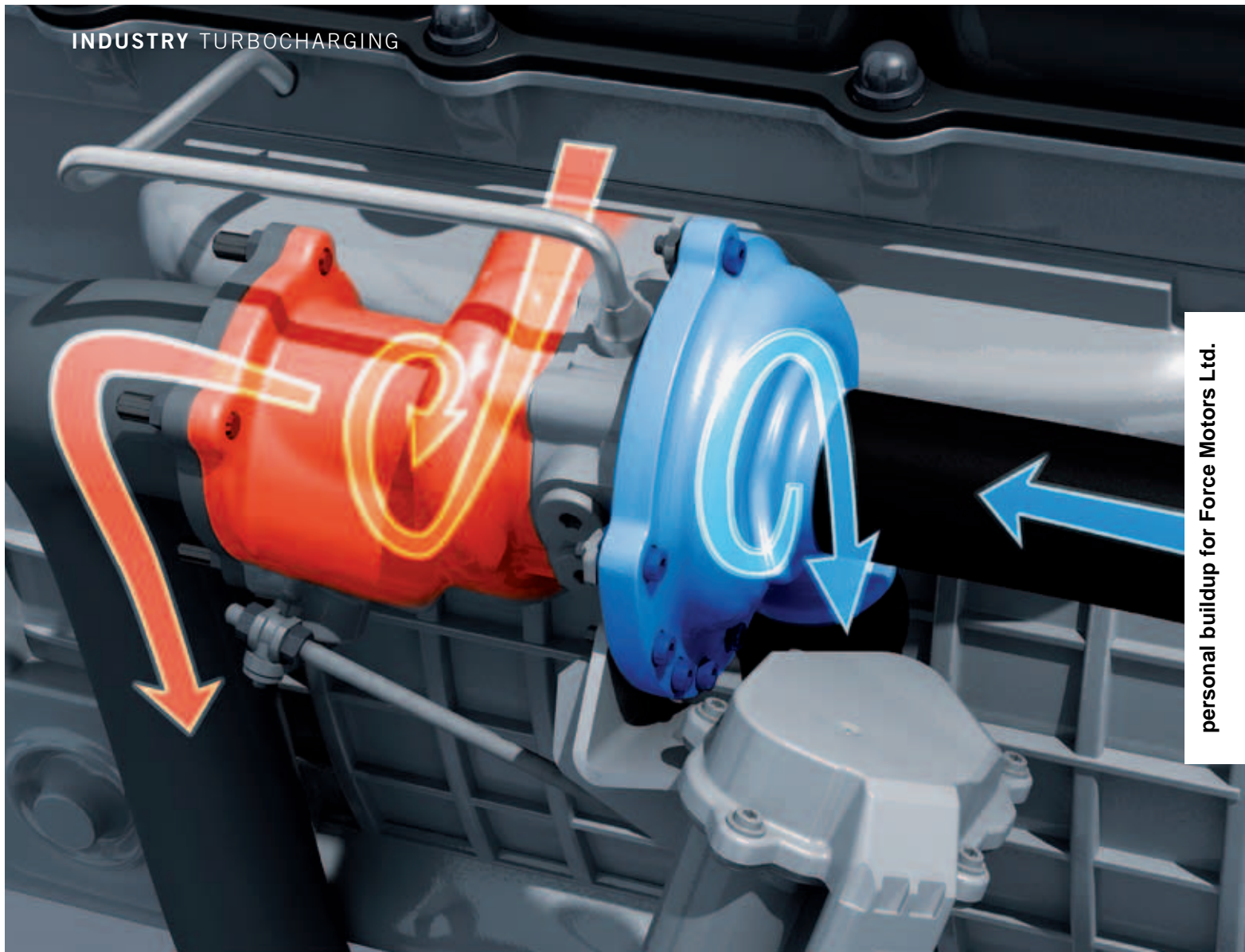
In the preparation of this paper additionally have collaborated:

Dipl.-Ing. Manfred Bach, Head of Diesel Engine Design at Audi AG in Neckarsulm (Germany).

Dipl.-Ing. Jan Helbig, Head of Mechanics Development for Diesel Engines at Audi AG in Neckarsulm (Germany).

Dipl.-Ing. Jens Ortwein, Senior Engineer in Mechanics Development for the V6 TDI at Audi AG in Neckarsulm (Germany).

Dipl.-Ing. Gerd Seifried, Senior Design Engineer for the V6 TDI at Audi AG in Neckarsulm (Germany).



## TURBOCHARGER DESIGN FOR ELECTRICAL WASTEGATE ACTUATION TO MINIMIZE LEAKAGE

Exhaust gas turbochargers are a major part of current strategies for reducing CO<sub>2</sub> emissions – especially in the gasoline engine. To optimally support downsizing and downspeeding, turbochargers must react as fast as possible, and the exhaust gas volumetric flow to the turbine must be exactly adjustable with a wastegate. Electric motor actuation is advantageous here. However, it places specific requirements on the wastegate which Continental has taken into account in its new generation of turbochargers.

## AUTHORS



**ACHIM KOCH**

is Director Turbocharger Engineering at Continental AG in Regensburg (Germany).



**HARTMUT CLAUS**

is Director Sales and Customer Application at Continental AG in Grünstadt (Germany).



**DIRK FRANKENSTEIN**

is Manager Turbocharger Design at Continental AG in Grünstadt (Germany).



**ROLAND HERFURTH**

is Project Leader Half Moon Wastegate at Continental AG in Regensburg (Germany).

## REQUIREMENTS

With its increasing thermodynamic efficiency, the internal combustion engine makes a contribution to reducing mobility-dependent CO<sub>2</sub> emissions. Downsizing and downspeeding with a lower axle ratio play key roles especially for the gasoline engine, as they shift operation to more favorable load points i.e. higher mean pressures. Based on a naturally aspirated engine with a corresponding power characteristic, the combination of a turbocharger and direct injection enables reductions in fuel consumption of approximately 20 %.

However, to provide a fuel-efficient vehicle with a downsized engine and good drivability, the turbocharger must have a favorable transient behavior. Especially in the lower engine speed range with a low exhaust gas volumetric flow, the spontaneous support for the gas exchange cycle is essential.

As a result, the leakage at the turbocharger wastegate (WG) must be viewed as especially critical. Particularly at low volumetric flows, disproportionately high leakages on the closed wastegate are hardly acceptable, as they delay the response of the turbocharger. Furthermore, in other parts of the engine map the focus shifts to the exact control of turbine charging with exhaust gas.

Two development goals can be derived from this: First, the leakage at the wastegate must be minimized. Second, the elec-

trification of the wastegate with a close connection to the engine control system is particularly advantageous. However, this assumes a specific optimization of the wastegate for this type of actuation. Continental has realized both development goals with its newly developed SK turbocharger product range [1].

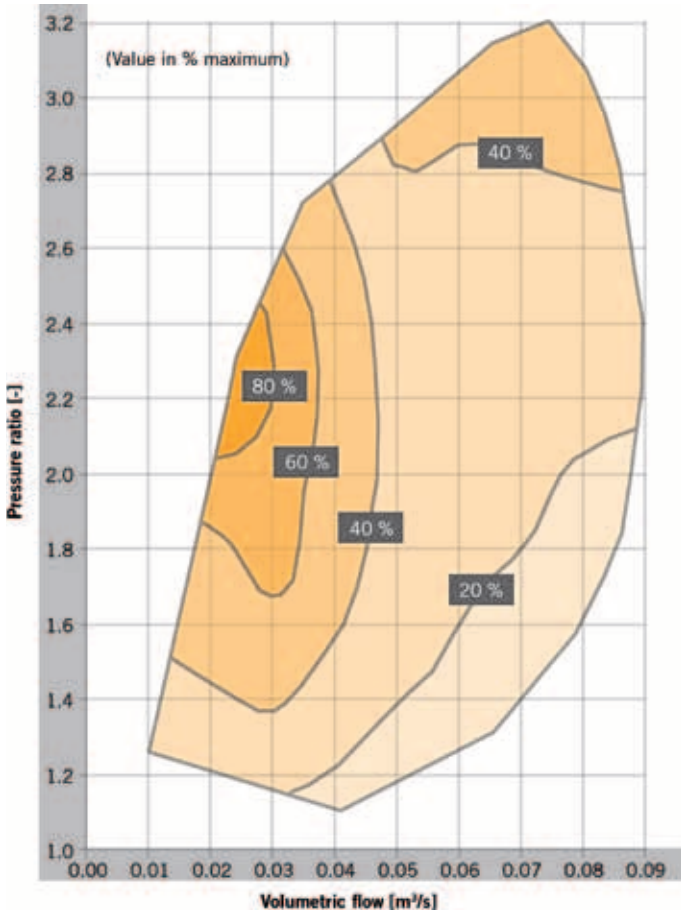
## SK TURBOCHARGER DESIGN

The new turbocharger generation consists of water-cooled units. The newly developed modular design is available with turbine diameters from 29.9 mm to 59.6 mm, and therefore covers a broad engine performance range between approximately 50 kW and 250 kW per turbocharger. A graduation of the turbine diameters in small steps and the modular design of the SK turbochargers enable optimal adjustment of inertia and capacity to the respective application, and therefore an excellent transient behavior can already be realized at engine speeds lower than 2000 rpm. This good suitability for making application-specific adjustments is one of the reasons for the turbochargers' high thermodynamic efficiency.

The structural integrity of the components is designed for exhaust gas temperatures of up to 1050 °C in order to avoid the need to enrich the mixture at high engine loads for reasons of component protection. First the SK1 series with turbine diameters from 30 to 38 mm for engine powers of up to approximately 100 kW will go into series



① Water-cooled exhaust gas turbocharger of the SK1 series for gasoline engines with half moon valve as wastegate



② Due to reduced axial gaps of the labyrinth seals, SK turbochargers achieve low blow-by

the wastegate. However, the specific optimization of the wastegate creates the best conditions for an energy-efficient operation with electric motors.

**ELECTRIC MOTOR WASTEGATE ACTUATION**

An electric operation of the wastegate provides several advantages: One advantage is that the valve can be operated without restriction. In contrast to pneumatic actuators with boost pressure operation i.e. without a vacuum pump, the electric actuation is independent of the force of the control pressure which has to exceed the hold-closed force of the valve closing spring. A flexible control of the wastegate position results in fuel efficiency improvements in parts of the engine map. In addition, the operation with an electric motor is faster and can be controlled more precisely with an integrated position sensor. Another advantage is the reduced complexity, as no pressure hoses need to be installed.

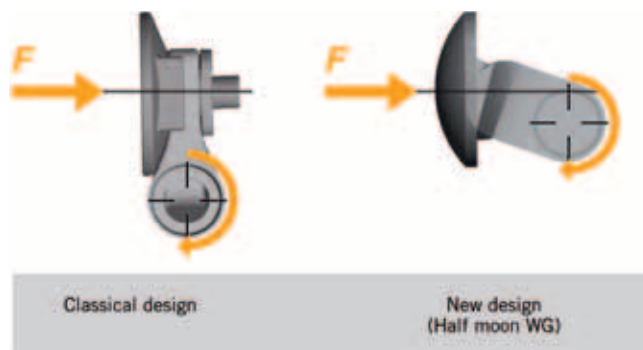
However, as the output of electric motors decrease as the temperature increases, the remaining closing force is a critical variable when the winding limit temperature is reached. Due to the ohmic resistance which increases with the rise in temperature and the decreasing generator constant, servomotors must therefore be dimensioned in accordance with their output at the winding limit temperature. With common valve designs, this would result in unacceptably large, heavy and expensive motors, which would also require a disproportionately large amount of electrical energy. Furthermore, motors with a high output at the winding limit temperature also have a too large closing force at low temperatures which may lead to component damage. For this reason, Continental has chosen a new valve design for this purpose, which requires considerably less closing force and is therefore ideally suited for an operation with a compact electrical motor.

production, ①. In contrast to existing designs, these turbochargers enable a fully automated assembly from one direction.

The design characteristics include the patented core design with unusually large cooling duct cross sections for improved cooling and tribology. The mounting of the shaft on floating bush bearings is favorable, even in case of an oil shortage. Both features increase the service life and reliability of the unit. The compressor impellers are milled in the interest of an optimized

service life and improved acoustics. Two labyrinth seals, mounted in separate grooves on the compressor and turbine sides, have small axial gaps and thus facilitate a correspondingly low blow-by by sealing off the shaft and help to comply with strict emission limits, ②. The large divided oil chamber combines excellent oil leak tightness with an optimised oil drain-off behavior.

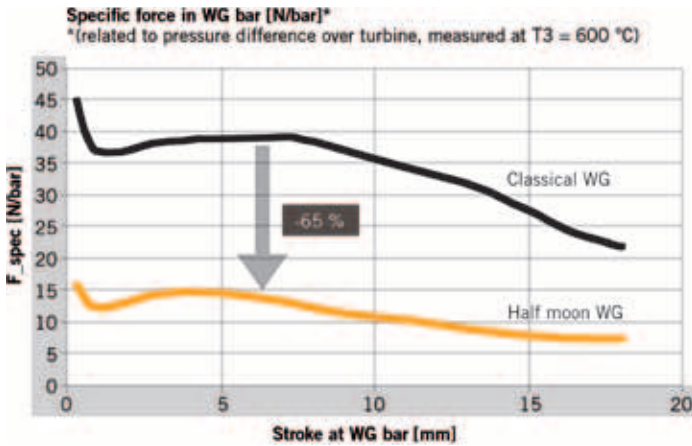
Both, a purely pneumatic and an optional electrical actuation, can be used to operate



③ Operating principle of a common valve flap (on left) and of the half moon valve (on right)

**WASTEGATE WITH HALF MOON VALVE DESIGN**

In common wastegate valves, the valve plate opens in flow direction. Therefore, the effective lever arm between valve plate and rotational axis remains almost constant. This is different for the half moon valve, where the spherical-shaped



④ Actuating force for the half moon valve and for a classical waste-gate valve

domed flap plate makes a swinging movement. The pivot point of the flap is slightly offset behind the flap plate. Due to this geometry the flap does not open in the direction of attack from the gas pressure with its rotating movement, but instead swings out of this direction, ④. As a result, the gas forces act only on the flap via a short lever arm. The closing movement is supported by a spring, which generates approximately 15 Ncm on the actuator rod at the closing point.

**POSITIONING FORCES AND LEAKAGE BEHAVIOR**

Following this design, a small force is sufficient to firmly close the flap. Measurements on the hot gas test bench have shown that the required specific force at the actuator rod for the half moon valve is 65 % less than the actuating force for a classical valve, ④. For the SK turbocharger the Continental model NG2 electric actuators were chosen, because they easily supply this force up to their maximum operating temperature of winding at 230 °C despite their compact dimensions.

The actuator is a DC motor with a two-stage spur-gear transmission. It is controlled directly by a full bridge from the engine control unit (ECU) with ± 12 V. The effective acting voltage is set by the pulse duty factor of a PWM signal. A sensor measures the angular position of the actuator rod and outputs a sensor voltage between 0.5 and 4.5 V to the ECU, where the position control of the actuator takes place.

The flow characteristic of the half moon valve has advantages over common valve designs. At the start of the valve opening,

the increase in the gas flow through the half moon valve has considerably flatter slope and is more linear and therefore offers a good controllability. Measured on the stroke of the wastegate actuator rod, the half moon valve also permits a higher flow rate at the end of the opening movement, ⑤.

A key advantage of the half moon valve is its considerably lower leak rate. With an actuating force of just 80 N, the flap already shows a sealing capacity due to its beneficial geometry which is much better than that of classical valves. Even with a considerably higher actuating force, ordinary valves show more leakage than the half moon valve, ⑤.

The low amount of leakage enables the turbocharger to utilize the available exhaust gas mass flow better for the tur-

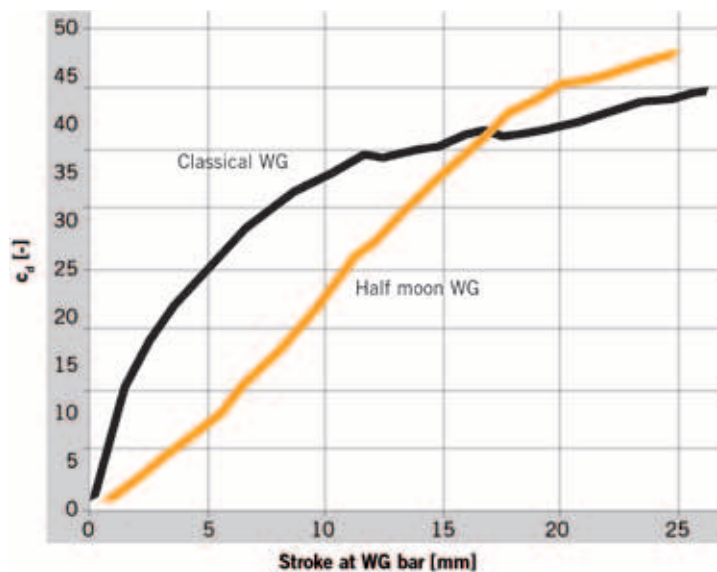
bine output. As a result, the available power for the compressor increases, and the boost pressure increases accordingly. This closed wastegate position occurs in parts of the engine map where good transient behavior is demanded. Leakage and torque measurements on an engine have confirmed this effect.

**VALIDATION OF TURBOCHARGER DESIGN**

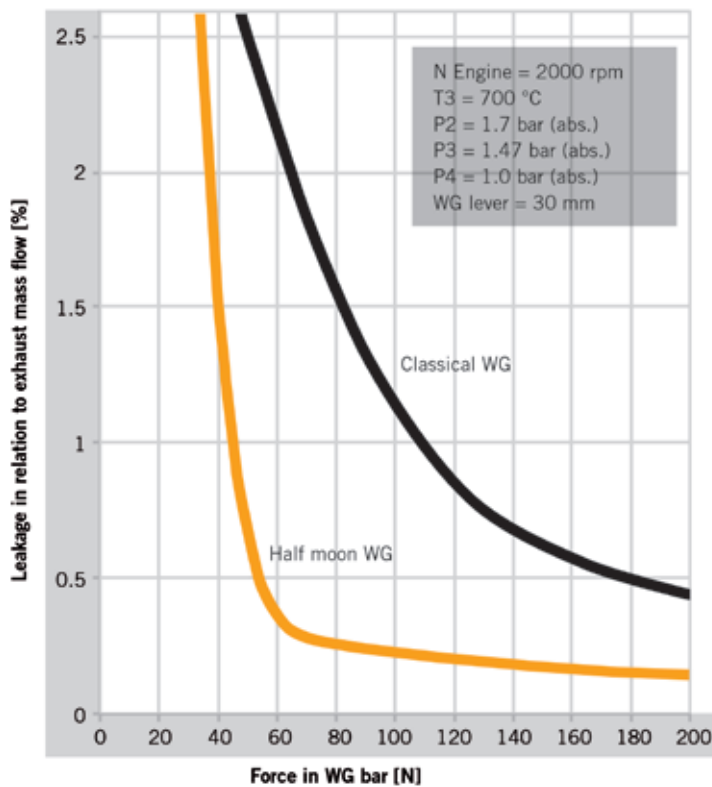
The turbocharger was tested extensively in the course of the development of the new turbocharger generation. For example, the units were subjected to various load collectives at the combustion chamber test bench. In the process, the maximum component temperatures were recorded with a tightly woven network of 55 measuring points and compared in detail with the simulation results.

The combustion chamber test bench used is additionally equipped with a device for the sudden switchover from hot gas to cold air. With this function the turbochargers were subjected to a thermal shock endurance test. Following its completion, the resistance to cracking of the turbine casing was checked and the measuring results were compared with the thermo-mechanical simulations.

Subsequently the operating behavior of the turbochargers was checked with a prototype engine. Here one focus was placed on the forces on the actuator rod and the exhaust gas pressure measure-



⑤ Comparison of the flow behavior of a classical valve and a half moon valve flap



6 Comparison of the leakage for a classical valve and for the half moon valve flap

ment. The tests during engine operation showed that the specific actuating forces on the rod were lower and more linear than initially expected following the measurements on the hot gas test bench. The reasons for this are vibrations and exhaust gas pulsations which reduce the influence of friction on the valve behavior.

**SUMMARY AND OUTLOOK**

Due to the advantages for fuel efficiency, exhaust gas turbocharging will prevail on the gasoline engine in the years to come, as this technology also enables good drivability for smaller engines. The requirements for turbocharged engines in respect of the transient behavior and the seal tightness of the units increase which make new design approaches advisable.

Many details of the Continental SK turbochargers have therefore been optimized. In addition to the reliability, above all the thermodynamic efficiency and the option of a fully automated assembly are characteristic for the SK turbochargers. Due to the

graduation of the turbine diameters in small steps and the program specific development of the compressor side, the modular product line can be specifically matched to individual engines. The generic validation for the size SK1 has been successfully completed.

With the new half moon valve wastegate geometry, the SK turbochargers are optimally prepared for the use of a compact electrical actuation. The low actuation forces in conjunction with the minimized leakage and the linear flow characteristic of the valve create the conditions for efficient, precisely controllable exhaust gas turbocharging. The faster pressure buildup reduces the time to torque, and the minimized leakage improves the torque offered in the lower engine speed range and increase the downspeeding potential.

**REFERENCE**

[1] Schwerdel, U., Koch, A., Claus, H., Frankenstein, D., Held, J., Kaufmann, A., Herfurth, R.: Neuer Turbolader mit elektrischer Waste-Gate Verstellung. 14. Aufladetechnische Konferenz, Dresden 2009

# IT'S TIME FOR EXPERT KNOWLEDGE WITH NEW FLEXIBILITY. ATZ eMAGAZINE.



© creative republic / Rentop Frankfurt - 2010

personal buildup for Force Motors Ltd.



## THE FASTEST INFORMATION IS DIGITAL.

**ATZ eMagazines** are loaded with the newest findings in research, development and production for the automotive industry, for every branch and specialty. Delivered to your e-mail as PDF, **ATZ eMagazines** are fast and up-to-date. Easily find topics with keyword searches, read up on feature articles in the online archives or create a PDF with extracted information. As a subscriber, you also receive **ATZ autotechnology** free of charge.

[www.eMagazine.ATZonline.com](http://www.eMagazine.ATZonline.com)

### ORDER NOW AND GET UP TO SPEED ON THE NEWEST KNOWLEDGE:

311 10 504

- ATZ** (11 issues / € 269,-)\*     **ATZ ELEKTRONIK** (6 issues / € 131,-)\*  
 **MTZ** (11 issues / € 269,-)\*     **ATZ PRODUKTION** (4 issues / € 131,-)\*

\* annual subscription rate

to the following e-mail address:

E-MAIL (please write legibly)

FIRST AND LAST NAME

COMPANY

DEPARTMENT

POSITION

ADDRESS

POSTAL CODE / CITY

COUNTRY

DATE / SIGNATURE

Simply fill in the form and fax it to **+49 (0) 611.78 78 - 4 07**  
or send it via E-mail at [SpringerAutomotive@abo-service.info](mailto:SpringerAutomotive@abo-service.info)

If you have any questions, please do not hesitate to contact us.  
Phone **+49 (0) 611.78 78 - 151**



personal buildup for Force Motors Ltd.

# SYSTEMS DEVELOPMENT FOR FUTURE PASSENGER CAR DIESEL ENGINES

By setting up a fully indicated, modern passenger car diesel engine, Mahle has created the basis for systematically testing current and future engine technologies. The experimental set-up has both an integrated high- and low-pressure EGR circuit and an open engine control unit, thus enabling efficient development of new systems under real-world conditions. The advantages of this comprehensive approach are illustrated below, using the example of different EGR technologies tested.



## AUTHORS



**PATRIC GENIESER**  
is Project Manager, Corporate Advanced Engineering at Mahle International GmbH in Stuttgart (Germany).



**DR. ALFRED ELSÄSSER**  
is Head of Testing, Corporate Advanced Engineering at Mahle International GmbH in Stuttgart (Germany).



**DR. DAVID GURNEY**  
is Principle Engineer Simulation, Research & Development at Mahle Powertrain Ltd. in Northampton (Great Britain).



**DR. MARCO WARTH**  
is Head of Diesel Engine Development, Research & Development at Mahle Powertrain Ltd. in Northampton (Great Britain).

## MOTIVATION

The requirements for improvements in energy efficiency (ACEA 2012) and reductions in emissions (Euro 6, etc.) are the primary cause of further increases in the complexity of modern diesel engines. In order to optimise the various components and assemblies, and their interaction with each other, a comprehensive approach to the diesel engine as a system is more necessary than ever. Using the example of different EGR technologies, both the potential of the “engine test bench” as development tool and that of various systems for further reductions of emissions and fuel consumption are demonstrated in the following.

## TEST SETUP

The basis of the experiments is a modern, fully indicated four-cylinder common-rail diesel engine with VGT turbocharger, cooled high-pressure EGR, diesel oxidation catalyst and diesel particulate filter, ❶. A cooled low-pressure EGR circuit was added in order to analyse the potential of different EGR concepts, ❷. The applied exhaust gas measurement technology is used for analysing both stationary and transient emissions.

Additionally, the diesel throttle flap was replaced by a fast rotating charge air valve (SLV) from Mahle, which opens and closes the charge air path continuously. The associated SLV electronic synchronises the closing point relative to the engine cycle (“phase” for short, ❸). Due to the temporary drop in charge air pressure when running in SLV mode, the negative scavenging pressure gradient increases, and so does the exhaust gas recirculation rate [1].

## ENGINE CONTROL UNIT

The following requirements are key for an electronic control unit in order to be able to efficiently develop a complete engine system:

- : stationary and transient operation
- : free access to all actuators and sensors
- : flexible integration of new (sub-)systems
- : independence of OEMs and controller manufacturers.

These requirements are optimally fulfilled by the Mahle Flexible ECU. The system is based on the AFT Protronic control unit platform [2]. The corresponding software toolchain allows automated and secure code generation, using Simulink functional models, while the components on the functional level are developed in-house. Similar to a production ECU, a torque structure is used for this diesel application, with an additional control concept based on cylinder pressure currently under development. The characteristic production engine map is emulated across the entire oper-

<b>SPECIFIC POWER OUTPUT</b>	[kW/l]	50
<b>STROKE-TO-BORE RATIO</b>	[-]	1.18
<b>COMPRESSION RATIO</b>	[-]	16.5
<b>EMISSION STANDARD</b>	[-]	Euro 5

❶ Technical data of the test engine

ating range. Integrated application interfaces allow direct control of individual actuators. Diagnostic functions with flexible error handling, emergency shut-downs and diesel particulate regeneration using a loading model with temperature control, are examples of already implemented functions that go beyond regular combustion control.

**SIMULATION AND ANALYSIS**

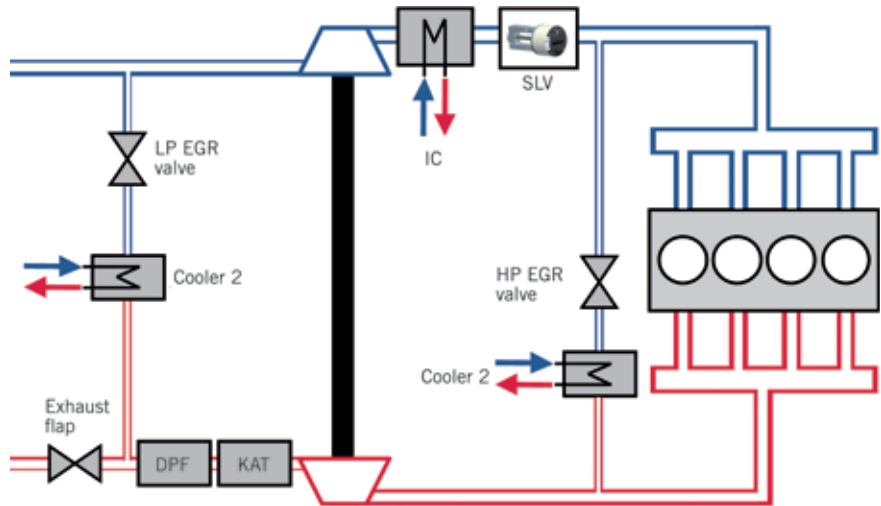
In order to investigate the potential of various technologies without performing expensive, time-consuming real-world tests, and to support the analysis of testing data, a thorough engine model has been set up in a 1D simulation program and validated across the entire operating range. Supported by an integrated combustion model, predictions about the engine combustion and emissions behaviour can be calculated. As the comparison of time-resolved pressure traces for low-pressure and high-pressure signals shows in the example, ④, the model correlates adequately in both trends and absolute values with the test data.

Evaluation and analysis of the measured data using gas exchange and combustion analyses is an efficient means for interpreting the results, thus e.g. allowing to describe the influence of highest EGR rates on combustion and emissions.

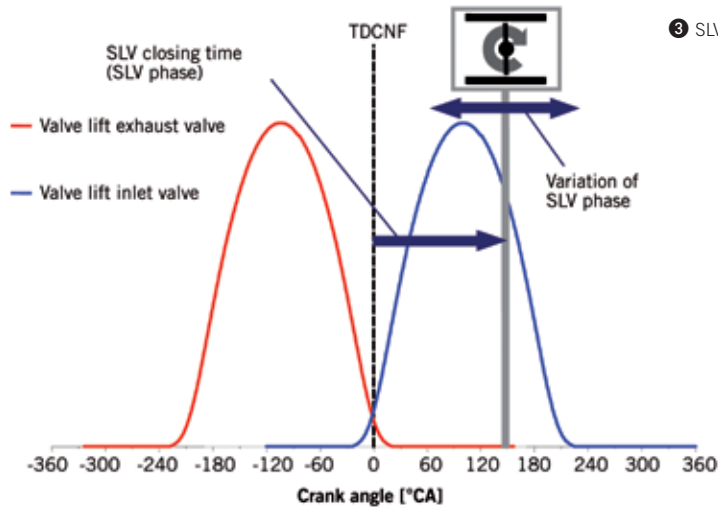
**EGR TECHNOLOGIES**

The engine scavenging pressure gradient is responsible for the external recirculation of exhaust gas. If the gradient is negative, exhaust gas will flow back into the intake air path, given the EGR valve is opened. In order to meet future NO<sub>x</sub> emission limits (e.g., Euro 6) with engine internal measures, the negative scavenging pressure gradient present in major areas of the MVEG must be further intensified. In principle, this can be done for the cooled high-pressure EGR by increasing the exhaust back pressure (e.g., VGT actuator) or by lowering the charge air pressure (e.g., diesel throttle flap). In order to minimise the losses associated with a constant throttling diesel throttle flap, a SLV is used for the tests listed here.

Using the example of operating point 1 (OP1: 3.2 bar bmep at 1500/min), it is shown that in order to meet Euro 6 NO<sub>x</sub>



② Test setup with SLV and cooled HP- and LP-EGR



③ SLV functional principle

engineering targets with internal combustion measures only, the SLV phasing, VGT actuator position, injection timing and pressure were optimized, ⑤, using both the Mahle Flexible ECU and design of experiments. Additionally to the reduction in NO<sub>x</sub> emissions, the comprehensive optimisation also led to improved fuel consumption and reduced soot emissions.

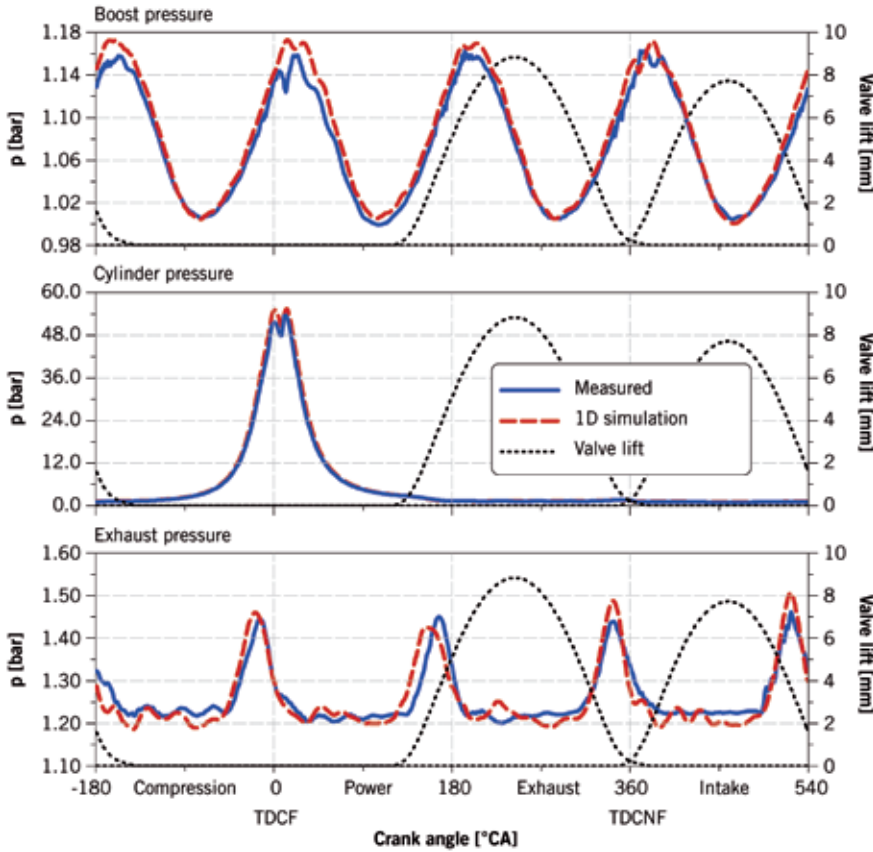
Reduction of NO<sub>x</sub> emissions can primarily be traced back to two phenomena caused by the SLV. The temporary pressure gradient, which is generated by the rotating SLV, leads to a increased EGR rate, whereas the cylinder pressure drops due to the an early intake closing realised simultaneously (“Miller Cycle”). The combination of these two phenomena causes a decrease in peak cylinder pressure, and thus in NO<sub>x</sub> emissions, ⑤. The combined application of these internal

combustion engine measures is the key to achieving Euro 6 emission targets over the entire MVEG relevant operating map.

In order to analyse the potential of HP and LP EGR systems, as well as combinations of the two, identical test runs at characteristic operating points within the engine operating map were carried out. Results for three characteristic operating points (OP) of a modern diesel engine are shown below.

- : OP1 – low-load range: 3.2 bar bmep at 1500/min (MVEG)
- : OP2 – medium-load range: 6.4 bar bmep at 2000/min (MVEG)
- : OP3 – full-load range: 19.2 bar bmep at 2000/min (US06).

The test layout shown ② was used for these tests, i.e. the cooled HP EGR system including a SLV and a series production system for the LP EGR was used. When



4 Pressure curve correlation

operating with combined EGR, the LP EGR valve was initially fully opened and the  $\text{NO}_x$  target values were set using the exhaust back pressure valve. The LP EGR rate is then lowered by continuously opening the exhaust back pressure valve, while simultaneously increasing the HP EGR proportion by selecting the appropriate SLV phasing to implement the  $\text{NO}_x$  target values desired, 6.

In the low-load range, the pure HP EGR has advantages with regard to fuel consumption at constant  $\text{NO}_x$  and particulate matter (PM) emissions. The pure LP EGR in contrast generates significantly higher fuel consumption figures, due to the essential increase in exhaust back pressure and the associated increase in gas exchange work. Another advantage of HP EGR in this operating point is the higher intake air temperature, as the admixture of warm exhaust gas has a positive effect on compression ignition at lower loads.

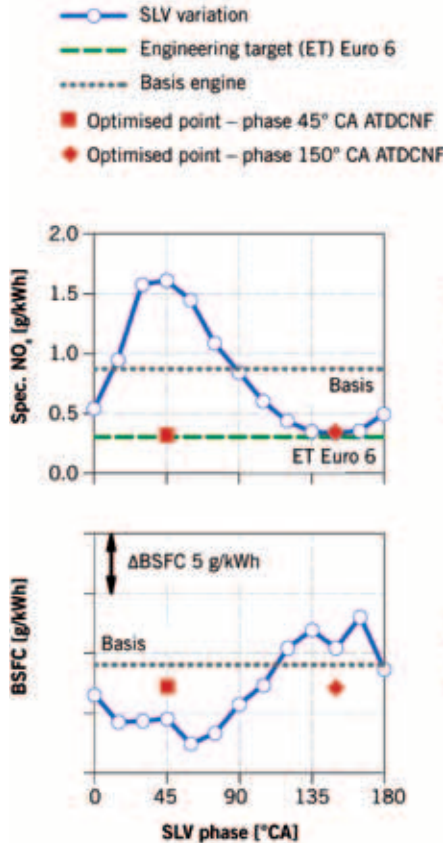
For the medium-load range and low  $\text{NO}_x$  emission levels, LP EGR has an increasing advantage with regard to fuel consumption and particulate matter,

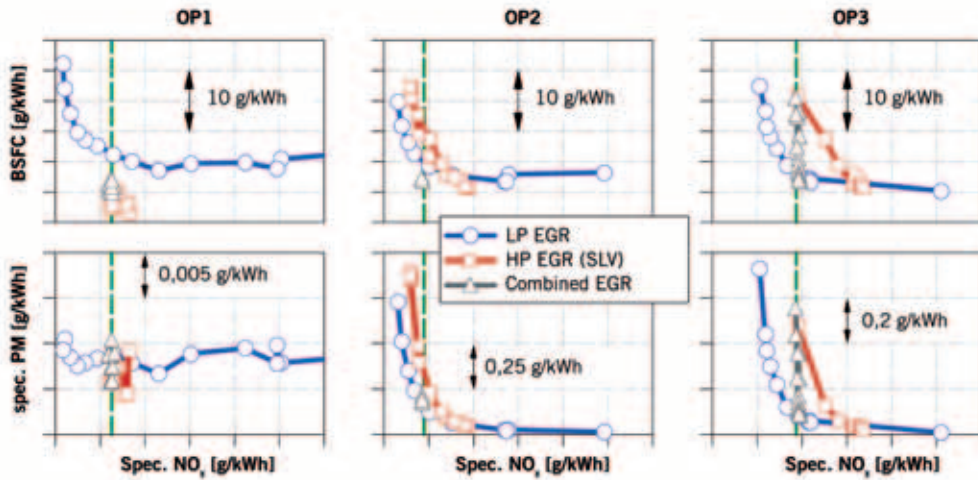
which is also evident in the gradient of the trade-off from HP to LP EGR. With a combination of both EGR systems however, the result is a fuel advantage for constant  $\text{NO}_x$  and PM emissions.

A comparison of the systems at high loads shows significant advantages for LP EGR. Due to the large scavenging pressure gradient at peak torque, the exhaust gas can be recirculated without additional measures. The thermodynamic advantage of LP EGR is that there is no loss of enthalpy at the turbine, so that the maximum possible charge air pressure remains available at all times. Furthermore, the recirculated exhaust gas is cooled twice, 2. On top, the additional pipe length of the air path has a positive effect on homogenisation, and therefore on the uniformity of the EGR distribution.

On the basis of the tests presented here, the following recommendation is made for the various EGR technologies tested: including internal combustion measures, a combined EGR system shows the greatest potential for the Euro 6 and US Tier 2 emission regulations, 7.

5 Variation of SLV phasing (OP1)





⑥ EGR technologies at characteristic operating points (OP)

VALVE TRAIN VARIABILITY

As is known from literature [3,4,5], IC engine emissions can also be lowered by means of variable valve trains, especially particulate matter and nitrogen oxide emissions. The former can be reduced by an optimisation of the charge motion – analogous to the swirl flap – thanks to the improved mixture homogenisation. The function of the swirl flap is thereby substituted by the variable valve train. The adaptation of variable intake valve timing, similar to early or late intake closing („Miller/Atkinson cycle“), primarily reduces the NO<sub>x</sub> emissions. The reduction of the effective compression ratio is shifted to the compressor, whereby lower in-cylinder temperatures, and thus lower nitrogen oxide emissions, can be achieved.

For this purpose, Mahle can implement a technology already used in series production for gasoline engines: the Cam-In-Cam

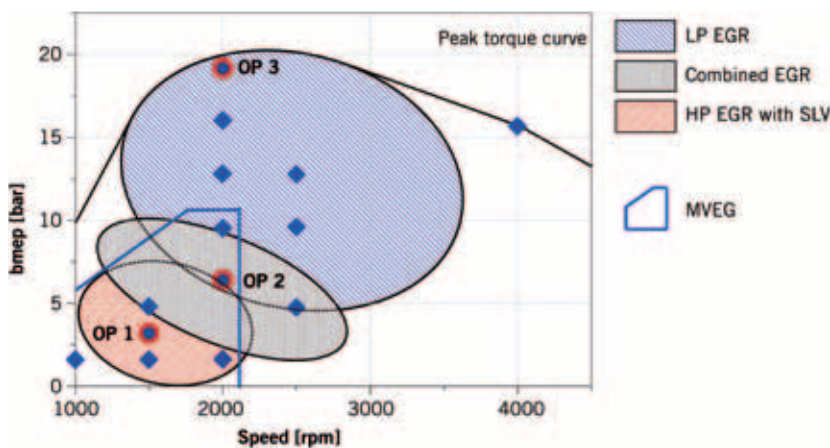
(CIC) [6,7]. With CIC, two camshafts are nested together – within the package constraints of one camshaft. The outer element is a shaft with fixed cams. Within this shaft, there is an inner camshaft with adjustable lobes connected to the outer shaft. Using a hydraulic cam phaser, the position of the inner camshaft lobes can be rotated relative to the lobes on the outer camshaft. With a CIC installed on the intake side, all of the effects mentioned above can be implemented, ⑧, by a relative phase adjustment ( $\varphi_{CIC}$ ) between the individual intake valves (IV). The CIC can be integrated in the existing package constraint of the cylinder head.

Simulation results of the swirl numbers achievable using the CIC – hereafter shown as swirl ratio (angular velocity of swirl to crank shaft speed) – are shown in ⑧. Compared to a conventional swirl flap, the swirl numbers over an engine cycle with intake CIC show the potential to further increase swirl number levels.

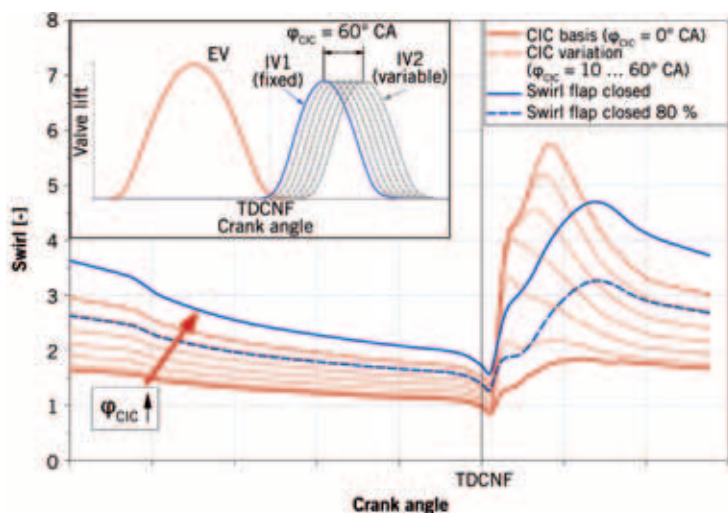
TOTAL SYSTEM OPTIMISATION

The previous tests and the results obtained can be used to derive possible optimisations for future diesel engines, using a wide range of technologies. For example, in order to implement an internal combustion measures solution meeting Euro 6 NO<sub>x</sub> emissions limits, the entire EGR system including pressure levels in the intake air and exhaust gas side pre and post turbocharger must be considered. This includes, in addition to the regular HP / LP EGR valve and cooler design, the inlet port and duct geometry, the turbocharger as well as expanded operating modes due to new controller functions optimisation.

Mahle is currently testing the following approaches in its development programs:  
 : improvement of EGR strategy by using the SLV to meet future legislative emission requirements and reduce fuel consumption at the same time



⑦ EGR technologies



OP1: Swirl as a function of the crank angle, using CIC technology and the swirl flap

- : fast control of the EGR rate in transient engine operation – engine cycle resolved adaptation of EGR rates
- : optimisation of the air intake and turbocharging system – adaptation of the turbocharger to the highest EGR rates
- : next generation EGR valves and coolers – reduction in overall pressure losses in EGR systems
- : improved inlet port and duct geometry for uniform EGR rate distribution
- : cylinder-selective mfb-control (mass fraction burned), using the Mahle flexible ECU
- : gas exchange optimisation using a variable valve train (CIC) – reduction in raw emissions and fuel consumption
- : improvement of “classical” engine components (pistons and piston rings) – reduction in frictional losses, increased durability and improvement in fuel consumption.

#### REFERENCES

- [1] Mahr, B.; Warth, M.; Rückauf, J.; Elsäßer, A.: „Innovatives Abgasrückführsystem zur kosten- und verbrauchseffizienten Erfüllung zukünftiger Emissionsvorschriften“, 30. Wiener Motorensymposium, 2009, Wien
- [2] Eckmann, M.: „Prototyping-Plattform – jetzt offen für Serienwerkzeuge“, ATZ 02/2009 Jahrgang 4; S. 40-44
- [3] Broda, A.; Rieping, M.; Eilts, P.; Elsäßer, A.; Genieser, P.: „Active Air Management with High Speed Flap for DI-Diesel Engines“, SAE Paper 2008-01-1345, 2008
- [4] Tomoda, T.; Ogawa, T.; Ohki, H.; Kogo, T.; Nakatani, K.; Hashimoto, E.: „Improvement of Diesel Engine Performance by Variable Valve Train System“, 30. Wiener Motorensymposium, 2009, Wien
- [5] Bression, G.; Baudrand, O.; Pacaud, P.: „Innovative VVA scavenging concept for Diesel engines: A promising way for downspeeding“, SIA Conference Diesel Engines, 2010, Rouen
- [6] Schneider, F., Lettmann, M.: „Mahle Cam-In-Cam, die neue Lösung für variable Ventilsteuerzeiten“, Aachener Kolloquium Fahrzeug- und Motorentechnik, 2007, Aachen
- [7] Schneider, F.; Kreisig, M., Dingelstadt, R.: „Torqueboost Cam-In-Cam – ein kompaktes System zur Drehmomentsteigerung mittels variabler Auslassöffnungsdauer“, 10. Stuttgarter Symposium, 2010, Stuttgart

#### SUMMARY AND OUTLOOK

By setting up an advanced diesel engine prototype with an open ECU, Mahle was able to reduce internal combustion nitrogen oxide emissions down to Euro 6 limits, while maintaining the raw soot emissions of the baseline engine (Euro 5). The extensive analysis of different EGR technologies, together with both a recommendation for an EGR application with the focus across the entire characteristic engine map and tests on variable valve trains, illustrate the advantages of this comprehensive approach in the development of new systems for next generation passenger car diesel engines.



## FUTURE EXHAUST EMISSION MEASUREMENT TECHNOLOGY REQUIREMENTS

While in the past – especially in emission roller dynamometers – the emphasis used to be on integrated measurement of emissions via bag using CVS systems, the transient course of emissions in the cycles is increasingly becoming relevant for the development. As a result, FEV Motorentechnik GmbH and the Chair for Combustion Engines, RWTH Aachen University, are working together on optimizing these measurements.



**AUTHORS**



**DR.-ING. YVES ROSEFORT**  
is Project Manager at  
FEV Motorentechnik GmbH  
in Aachen (Germany).



**DR. RER. NAT. BERNHARD LÜERS**  
is Technical Specialist at  
FEV Motorentechnik GmbH  
in Aachen (Germany).



**DR.-ING. MICHAEL WITTLER**  
is Senior Engineer at the Institute for  
Combustion Engines VKA RWTH  
Aachen University (Germany).



**DIPL.-ING. MATTHIAS SALMEN**  
is Scientific Assistant at the Institute  
for Combustion Engines VKA RWTH  
Aachen University (Germany).



**MARTIN SIMM**  
is Student Assistant at the Institute  
for Combustion Engines VKA RWTH  
Aachen University (Germany).

**CHALLENGES**

As exhaust emissions standard are increasingly becoming more stringent, the requirements for the measurement technology that are being used are increasing as well. While raw emissions are decreasing on the one hand, the measurement of catalytic converter efficiency becomes more and more important. This not only applies to engine test stands, but also to exhaust emission roller dynamometers that are used for passenger car certification.

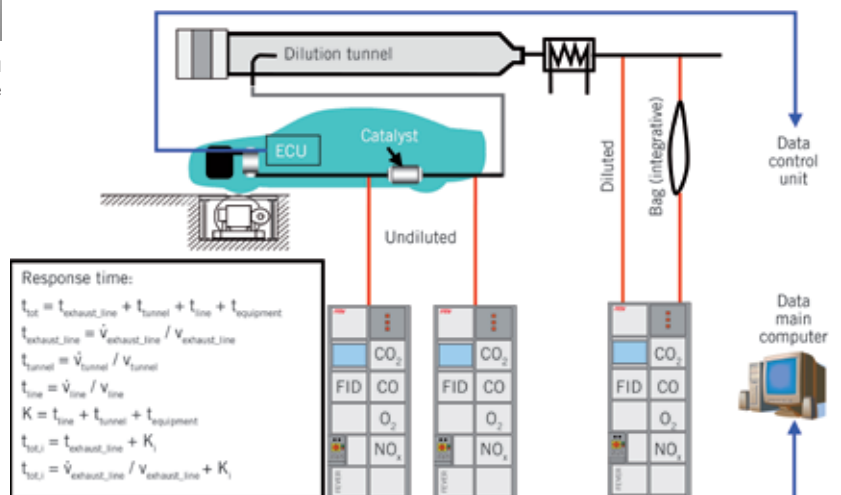
In addition to the rising demands when it comes to measuring accuracy, the evaluation in particular plays an important role. Various measures are used to ensure that the measurements from diluted and undiluted exhaust can be compared for transient cycles as well. In addition to humidity correction, steady-state and non-steady-state response times, corrections based on samples taken, as well as synchronization and integration of different measurement data formats are important.

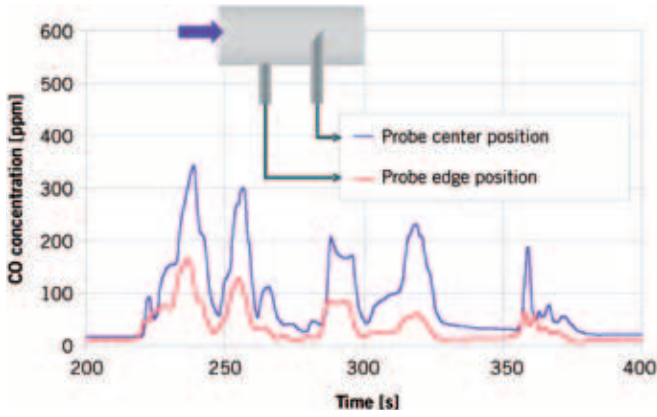
An evaluation program by FEV allows us to perform calculations necessary for transient evaluations. The steady-state and non-steady-state response times are automatically corrected in the program. This results in a considerable improvement in measuring accuracy, which we were also able to verify in comparisons to measurement made with the help of a CVS system (Constant Volume Sampling).

In addition to the legally prescribed exhaust emission measurement technology that is used to measure the diluted exhaust [1] (diluted and bag) of the last measurement cabinet, ❶, two additional exhaust emission measurement cabinets are used for the roller dynamometer under consideration for measuring the undiluted exhaust upstream and downstream of the catalytic converter. While the undiluted and the diluted stretches are continuously recording the concentration, the bag analysis merely permits an integrative measurement, which can only be split up into individual phases by using several bags.

To permit a transient measurement with adequate accuracy, optimized measuring probes, mass flow determinations, corrections, and the integration of different data sources are necessary in addition to an exact measurement technology. In the following, we will explain the optimization options that are available.

❶ Exhaust emission measurement schematics





② Influence of the sampling probe

**MEASURING PROBE**

The objective is to take a representative sample from the exhaust by means of suitable probe design and positioning. A suggestion for this can be found for example in ISO 8178, which we adapted/applied here in simplified form using chamfered probes in the center of flow [3]. In order to also permit measurements in the inhomogeneous range with plug-flow characteristics (e.g., downstream of catalytic converters), FEV has developed multi-hole probes that are taking samples based on the weight per unit area. They are producing representative results here.

Sampling from plug-flow ranges is necessary in order to be able to take measurements in standard exhaust systems, where minimum distances cannot be observed. Exhaust sampling in the wall-area of the pipe leads to incorrect measurements due to catalytic effects, ②.

**DETERMINATION OF THE MASS ON THE ROLLER DYNAMOMETER**

In order to be able to record emission mass flows online, the total mass flow in the system must be known in addition to the concentration course.

Various air and fuel mass flow measuring instruments are available on the stationary test stand to determine the exhaust mass flow. They cannot be used on the vehicle without making changes to the air system. This is why a tracer measurement with the CVS system is typically used in exhaust emission roller dynamometers.

Since the volumetric flow in the dilution tunnel is known as a matter of principle, the exhaust volume flow rate and thus also the mass flow can be calculated by measuring the CO<sub>2</sub> concentration downstream of the last exhaust aftertreatment component in the CVS system, in the intake air, and in the exhaust. Due to the

relatively high concentration, CO<sub>2</sub> is used here for the determination.

As an alternative, measurement by means of ultrasound has been found to be a very exact method for determining the exhaust mass flow. This method is also used on the roller dynamometer by the Chair for Combustion Engines (VKA). This measurement technology does not require any large-scale response time correction.

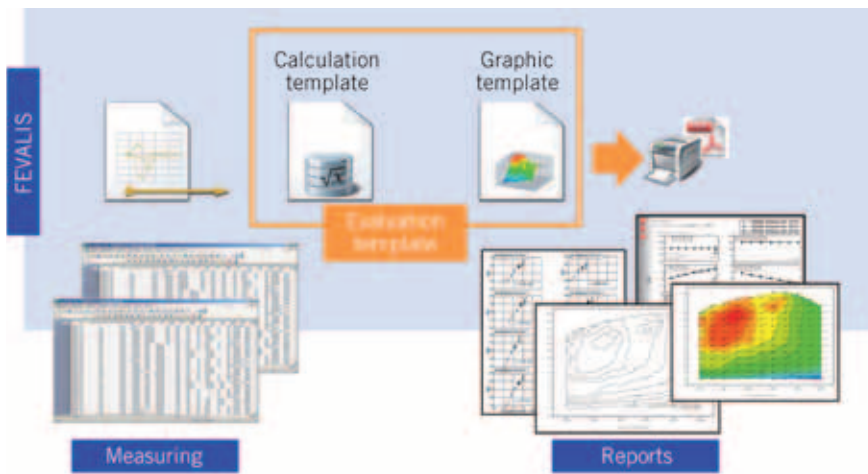
**CORRECTION OF SAMPLE QUANTITIES TAKEN**

Since the sample quantities that are being taken have an impact on both the subsequent volumetric flow rate measurement and the dilution ratio upon entering the CVS system, the results must be corrected accordingly.

**COMPUTATION OF ADDITIONAL MEASURED DATA**

Inherent test bed data are transmitted to the measurement data acquisition system. The data from the application system are typically recorded separately and must be synchronized with the test stand data and set to the same frequency. Additional factors can now be calculated based on all of the raw data.

If we want to analyze engine processes, catalytic converter efficiencies, integrated emissions, or the correlation between diluted/undiluted CO<sub>2</sub> measurements (tracer measurements), the emissions must relate to a defined measuring point. We have chosen a measuring point at the outlet of the turbine or the exhaust manifold here.



③ Fevalys– automated from the measurement results to the report

**RESPONSE TIME CORRECTION**

The response time, ①, is defined as the time that is elapsing between the change of an input factor (load, rotational speed, etc.) and the measurement of the change of the output factor (e.g., exhaust composition). It is mainly influenced by the following:

- : the positioning alongside the exhaust emission system ( $t_{\text{exhaust\_line}}$ )
- : the length of the sampling lines ( $t_{\text{line}}$ )
- : the sampling flow rates ( $t_{\text{line}}$ )
- : the volume of the measuring cell ( $t_{\text{equipment}}$ )
- : electronic signal processing ( $t_{\text{equipment}}$ )
- : the CVS system (if available) ( $t_{\text{tunnel}}$ ).



④ Fever exhaust emission measuring engineering system

The exhaust takes a certain time  $t_{tot}$  to get from the engine block to any measuring point. The response times  $t_{tunnel}$ ,  $t_{line}$ ,  $t_{equipment}$  are, by approximation, exclusively functions of geometry and volumetric flow and therefore for the most part constant. This results in a constant response time ( $K_i$ ) for the particular measuring point and gas component  $i$ .  $t_{exhaust\_line}$  describes the gas travel time up to the sample removal or up to the inlet level of the CVS system during measurement in the undiluted exhaust. This time is independent from the component and changes as a function of the exhaust volume flow rate with a given volume of the exhaust system section.

This response time correction also has a major impact on the mass flow determination by means of the  $CO_2$  tracer method.

### FEVALYS

The introduced response time correction was implemented in a prototype based on the development of the new FEV evaluation software Fevalys and could therefore

already be validated in practical work. The implementation based on Fevalys is only the first step here for expanding the product by a trend-setting evaluation method for exhaust emission measuring engineering. Fevalys is based on the technology by National Instruments Diadem and implements the automated evaluation at the touch of a button ranging from acquiring various types of data formats and sources and applying a calculation catalog to creating a standardized report, ③. In the process, Fevalys shows the perspectives of the evaluation method. It permits an online evaluation as early as during the test run with early identification of errors and deviations in the measurement and in the evaluation chain. In addition to this, the consistent automation also increases the reliability and efficiency of the evaluation process and, by means of guided analysis such as the graphic data inspection, function chains become tangible starting from the effects down to their causes. The new methodology in modal emission measurement thus lays an important foundation here.

### FEVER

Based on more than 20 years of experience in operating our own exhaust emission measuring engineering systems, the FEV-Emission-Rate Fever as well as Fever FTIR systems were created in 2006 for the continuous analysis of undiluted engine exhaust gas.

Due to the modular design and simple accessibility to all components from the front side, the Fever concept is highly flexible, which makes the configuration required for the measuring tasks a lot easier, ④. Fever contains the following main features:

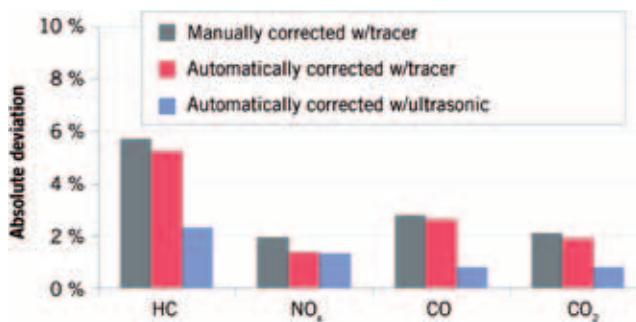
- : exhaust measurement system for diesel and gasoline engines

- : modular system design with complete access on front (system can be set up with the rear side facing the wall), electric indicator board with extendable front, gas connections from above or below, integrated temperature conditioning as an option
- : easy to roll without additional installation effort involved, integrated gas transport and conditioning module, standard functions and standard communication for all analyzers, user-friendly touch screen for all functions, fully integrated FTIR module as an option, diagnostic socket located on front in door aperture, versions available for diluted or undiluted measurement, can be integrated via AK protocol commands or TCP/IP interface.

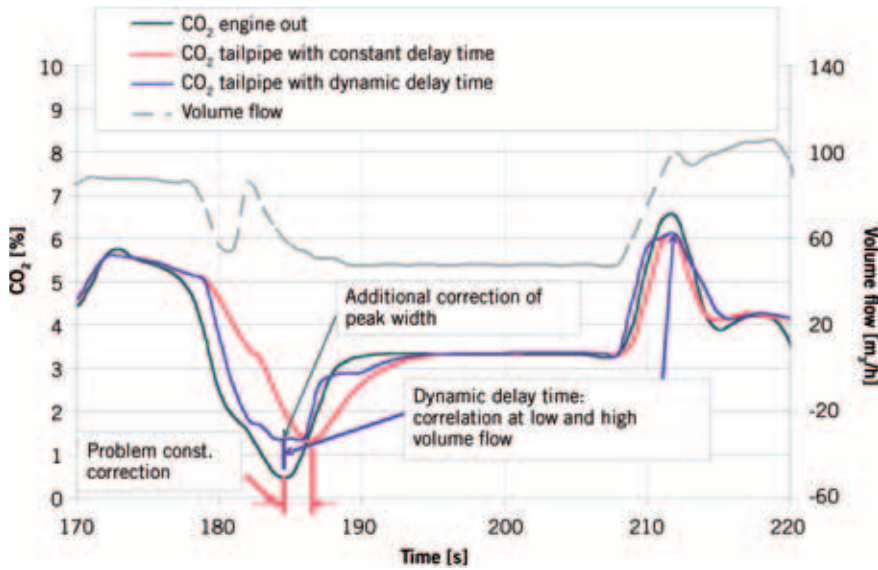
The system can be fitted as a system with one or two exhaust measuring lines and with up to ten individual analyzer channels. In addition to the standard systems for measuring the exhaust components THC, NO/NO<sub>2</sub>/NO<sub>x</sub>, CO<sub>2</sub>, CO, and O<sub>2</sub>, additional analyzers as well as an FTIR system can be integrated. Due to the switchover of the measuring gas, it has become easier to use the Fever system for emission measurement in several sampling points.

### RESULTS

With the help of the described measurement technology and corrections, NEDC vehicle tests were analyzed to see whether the emission measurement using the CVS system (bag) and the continuous undiluted measurement are matching. The measurements were performed on the climatic roller dynamometer of the VKA, ①. ⑤ compares the manually corrected results (constant response time elements) as well as the automatic response time



⑤ Influence of the response time correction and the mass flow determination on measuring accuracy



6 Influence of the dynamic response time correction on the comparability of two sampling positions

correction (all response time elements) on the basis of different mass flow measurements. The automatic response time correction is thereby based on the cross-correlation [2] of the particular concentration measurements with a comparison function, which comprises several input factors that depend on dynamic handling characteristics. The automatic response time correction is comparable to the best possible manual correction; however, its quality is the same regardless of the individual person making the correction. Furthermore, response time changes are automatically compensated through drifts in the system (depending on level of soiling, change of measurement configuration). The response time elements that are not constant lead to only minor improvements in accuracy, but they are the elements that actually permit the automatic response time correction. The ultrasonic measurement leads to further improvement.

Even if the signals are used for the simulation, these additional corrections are important, since time synchronization becomes possible for both small and large volumetric flows. We can see this when we take a look at the match between the CO<sub>2</sub> concentration course of two measuring points with a distance of approximate

3 m upstream and downstream of the catalytic converter, 6. The measurements correlate significantly better due to the dynamic response time correction.

**CONCLUSION**

Due to the optimization of individual variables (measuring probes, mass flow determination, response time correction, and corrections of the sampled measurement gas quantities), the measuring accuracy for the samples taken from undiluted exhaust can be improved considerably.

Using a prototype, the automatic response time correction for constant and dynamic response times were integrated into the Fevalis evaluation software by FEV. By using this software, it was possible to achieve an accuracy comparable to the best possible manual correction, but with the advantage of having an automatic compensation of response time changes and constant quality.

**REFERENCES**

[1] Richtlinie 91/441/EWG des Rates vom 26. Juni 1991  
 [2] Butz, T.: Fouriertransformation für Fußgänger; 2007  
 [3] DIN EN ISO 8178-1: Hubkolben-Verbrennungsmotoren – Abgasmessung – Teil 1; 1996

# ATZ live

## NEW ENGINES

Powertrains for commercial vehicles and off-highway, marine and stationary applications

## FUEL INJECTION AND COMBUSTION PROCESS

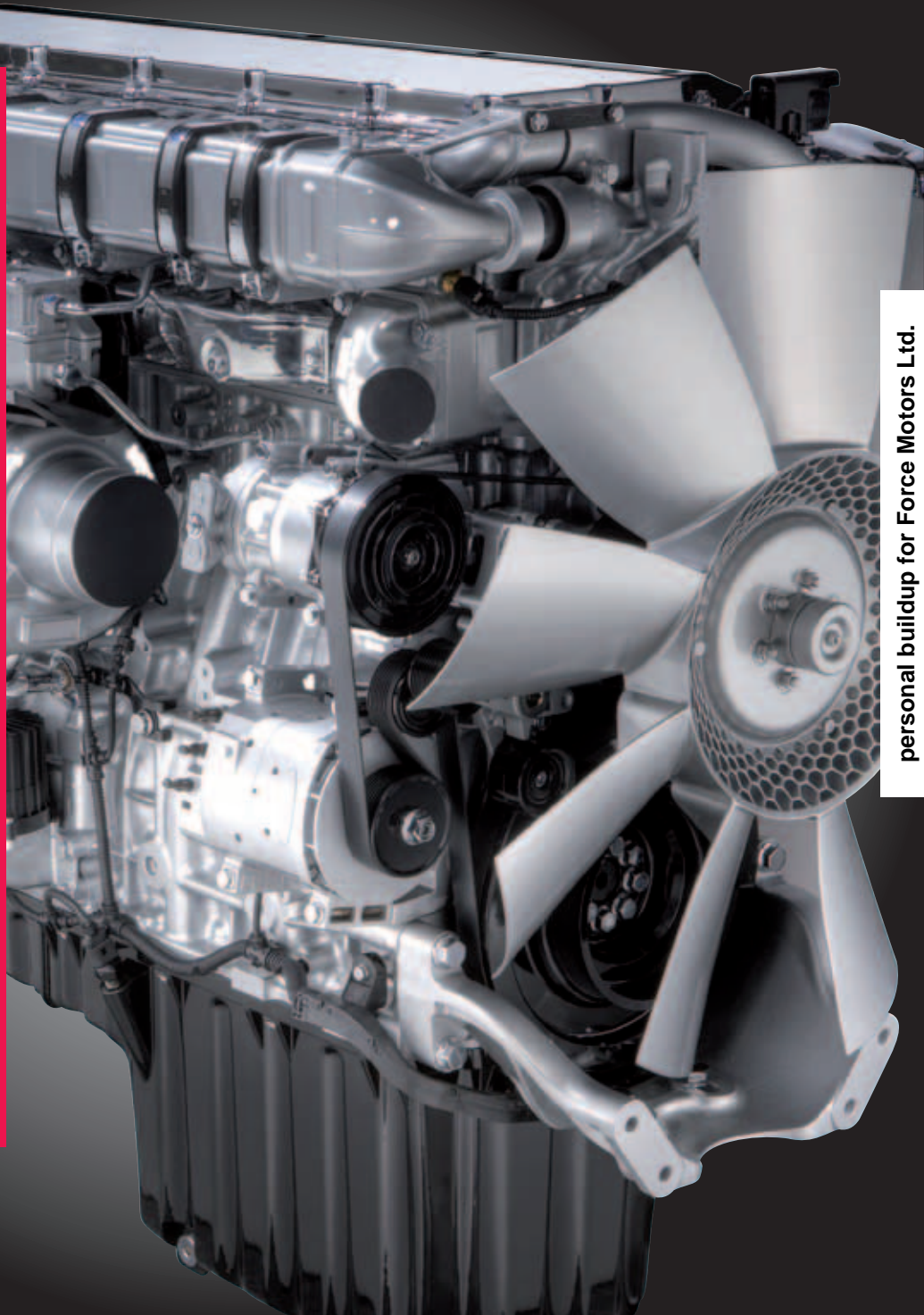
Concepts for fuel-efficient and clean engines

## ALTERNATIVE POWERTRAINS

Innovative solutions for the future

/// FACTORY TOUR

Mercedes-Benz Mannheim Plant



personal buildup for Force Motors Ltd.

# Heavy-Duty, On- and Off-Highway Engines

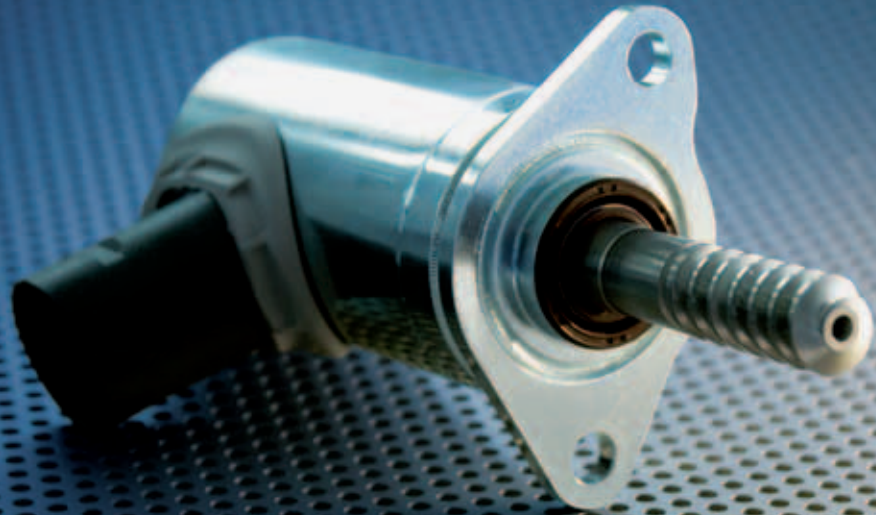


Euro 6 / Tier 4 – and what comes next?

MTZ Conference – On-/Off-Highway Engines 2010

23 and 24 November 2010 | Mannheim

PROGRAM AND REGISTRATION  
[www.ATZlive.de](http://www.ATZlive.de)



## NEW VALVETRONIC ACTUATOR FOR THE MINI TURBO ENGINE

To optimise the needed space, weight and functional integration, BMW Group and PSA Peugeot Citroën switched to brushless DC technology for the fully variable valve control in the process of further developing the “TwinPower” turbo engine. Sonceboz Automotive SA, in cooperation with Moving Magnet Technology, the subsidiary for research and advance development in the area of actuators and sensors, has developed a suitable new brushless DC motor with redundant, digital angle measurement. The fully automated production of such a complex and highly stressed electrical actuator was and is at least just as challenging as its development and qualification.

## AUTHORS



**DANIEL SIGG**  
is Business Unit Manager EC  
Motors at Sonceboz Automotive SA  
in Sonceboz (Switzerland).



**DR. JÜRGEN SCHNEIDER**  
is Department Manager Engine  
Electric at BMW AG  
in Munich (Germany).



**GAËL ANDRIEUX**  
is EC Motors Development Manager  
at Sonceboz Automotive SA  
in Sonceboz (Switzerland).

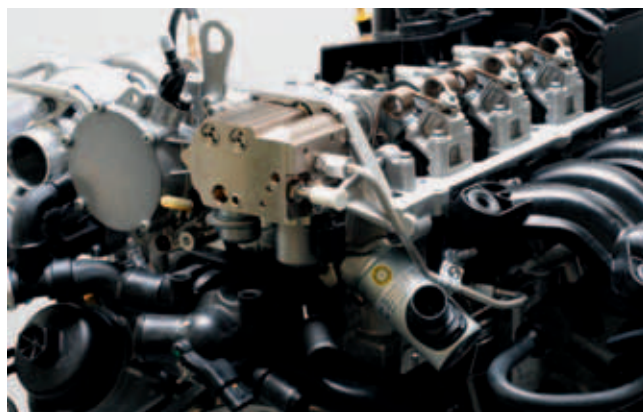
## HISTORY OF FULLY VARIABLE VALVE CONTROL AT BMW

To meet the demand for a technology usable worldwide to further reduce fuel consumption of gasoline engines, BMW in 2001 brought “Valvetronic” onto the market [1]. In this design, system demand control is performed by a fully variable mechanical valve train, an electric actuator and an electronic controller. A reduction of consumption of 12 % compared to the predecessor motor completely fulfilled the performance target. This established a new basic technology for all BMW gasoline engines. Since then, the Valvetronic has become standard in all BMW engine series, from four-cylinder to twelve-cylinder.

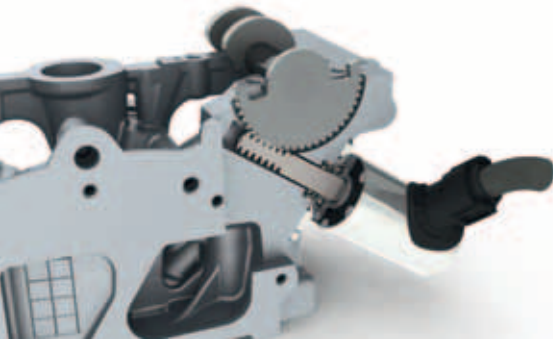
The Valvetronic has been further developed and optimised in the meantime and is now in the third generation [2]. Further product development has focussed on reducing charge-cycle losses and friction as well as optimising combustion. In the electronic system, the focus was placed on minimising the number of control systems and individual components used to achieve cost advantages and optimise the installation size. The Valvetronic was first used in Mini engines in 2006. To take the special package situation of the transversely installed 1.6 l four-cylinder engine into account, a special variant of this servomotor, suitable for external installation on the cylinder head, was developed, ❶.

As is typical for the third-generation Valvetronic, here, too, the necessary position sensors were integrated redundantly in the servomotor. The power electronics needed for control found their place in the engine management system and so formed a unit that was as economical as it was compact. To make optimal use of the very limited space in the new Mini’s engine, the focus in the design of the new servomotor was on keeping the installation dimensions as small as possible while simultaneously achieving high torque and dynamics.

To be able to use all the advantages of the latest BMW engine construction set, the Valvetronic for the new 1.6 l Mini engine was combined with a gasoline direct injection as well as a turbocharger with “TVDI” technology (Turbocharging Valvetronic Direct Injection). The new Mini “TwinPower” turbo engine thus uses the same fuel-saving motor technology as the new 3.0 l six-cylinder engine with turbocharger, for example. Moreover, thanks to a further increase in performance over its pre-



❶ Installation of the Valvetronic EC motor on the cylinder head



2 Mechanical integration of the EC motor



3 Exploded view of the new BLDC motor

decessor engine, it provides the typical BMW driving fun. To achieve this, a new electrical actuator for the Valvetronic is needed. In addition, the consistent further development of electrical and electronic technology with the goal of constantly increasing integration markedly reduced system components and complexity. This allowed a further increase in stability and reliability which directly benefits the end customer.

**CHANGE FROM DC BRUSH MOTOR TO BRUSHLESS DC MOTOR**

In a Valvetronic an eccentric shaft sets the intake valve stroke, 2. In the previous layout of the Mini 1.6 l engine this eccentric shaft was driven by a classic DC motor. A separate sensor recorded the position of the shaft at the shaft end. BMW’s specifications for this small four-cylinder TVDI engine were: compact installation with high torque and high dynamics, long service life as well as full integration of all the sensors. The sensor was to be integrated into the motor so that only a single ten-pin connector was needed and the motor diameter could be reduced from 61 to 42 mm. The torque was simultaneously increased to achieve additional functional reliability. The mass moment of inertia also had to be reduced to make cylinder-individual adjustments for greater actuator dynamics.

Under these general conditions, in particular the significantly high ambient temperatures and vibrations, it was soon apparent that only a brushless DC motor (BLDC motor) would be acceptable, 3. The high tolerance for vibrations and the possibilities for weight reduction through minimisation of the space used were the distinguishing

	UNITS	VVT2 <sup>(1)</sup>	VVT3
ROTOR INERTIA	J [10 <sup>-6</sup> kgm <sup>2</sup> ]	55	12
TORQUE CONSTANT	Kt [mNm/A]	20	20
MECH. TIME CONSTANT	T [ms]	26	1.97
MOTOR CONSTANT	Km [mNm/W <sup>1/2</sup> ]	45	78
RESISTANCE	mOhms	190	65
DIAMETER X LENGTH	mm x mm	ø61 x L91	ø42 x L85
MASS	kg	1.00	0.65
TORQUE PER KG	Km/m [mNm/W <sup>1/2</sup> /kg]	45	120
VOLUMIC TORQUE	Km/V [mNm/W <sup>1/2</sup> /mm <sup>3</sup> ]	1.7E-04	6.6E-04
INTEGRATED SENSORS		None	2 redundant sensors

(1): Estimated figures

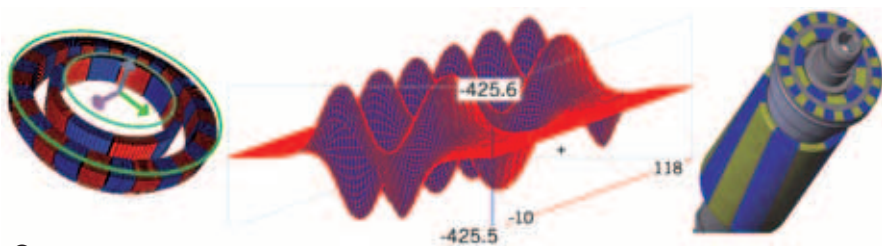
4 Comparison of DC motor VVT2 versus BLDC motor VVT3

features of this design. This also facilitated mechanical integration. A comparison of the classic VVT2 DC motor with the new VVT3 BLDC motor is depicted in 4.

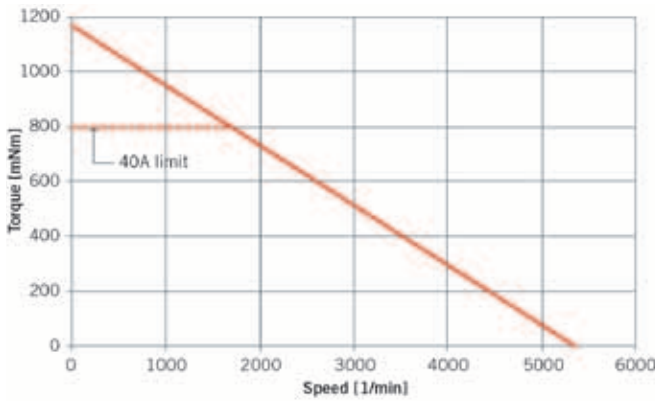
**SIMULATION VERSUS PROTOTYPE CONSTRUCTION**

The project also faced an extremely tight time schedule. And so it was not possible to approach the optimal design through various experimental models. The exact product definition as well as the design had to be found through purely numerical models. For example, the motor constant

of exactly 2 % had to be simulated with the development software from Moving Magnet Technology (MMT). The relevant know-how and wide-ranging experience in this area made it possible to start the out-of-tool B prototypes before all measurements were complete on the A prototypes. In defining the redundant sensor, the decision was made for a magnetic encoder with two solenoid coils, 5. The outside track was to have double resolution compared to the commutation sensors. Here, too, it was necessary to first evaluate feasibility based on a three-dimensional magnetic simulation, but



5 Rotor and magnet field modeling



6 Torque characteristics

then, using a model, to determine the precision and the influences of the external rotor on the internal rotor as well. MMT then took over fast implementation of the magnetising device. In this way, the calculated values were achieved from the start.

Due to challenging vibration requirements, numerical simulation was also used to determine mechanical strength. This meant that optimisation of the motor flange could begin even before delivery of the B-sample using purely numerical models.

Various simulations were performed to define the optimal injection points and also improve the mechanical characteristics of the flow lines for the complex injection moulding process, in which the connector is formed and the sensitive contacts of the three motor pins on the coil windings are overmolded.

Despite the intensive use of simulation tools, certain characteristics had to be improved for the B prototypes based on the

test results. The existing theoretical models helped find concrete solutions very quickly. In retrospect, such a fast development was possible only because these numerical models and simulations were used and comprehensive know-how was already available. The gain in time from the simulations made it possible to achieve the specified development time for the new small BMW four-cylinder engine.

**IMPROVEMENT OF PERFORMANCE AND TORQUE**

The specifications for space, weight, vibration resistance, torque and dynamics in accordance with 4 could all be achieved. The sensor could be integrated into the specified space. The mechanics with resetting mechanism required nominal 0.2 Nm. But to have a corresponding torque reserve even for a cold start or long-term wear, a torque of up to 0.8 Nm

was used, 6. Power monitoring in the controller avoided overheating of the actuator.

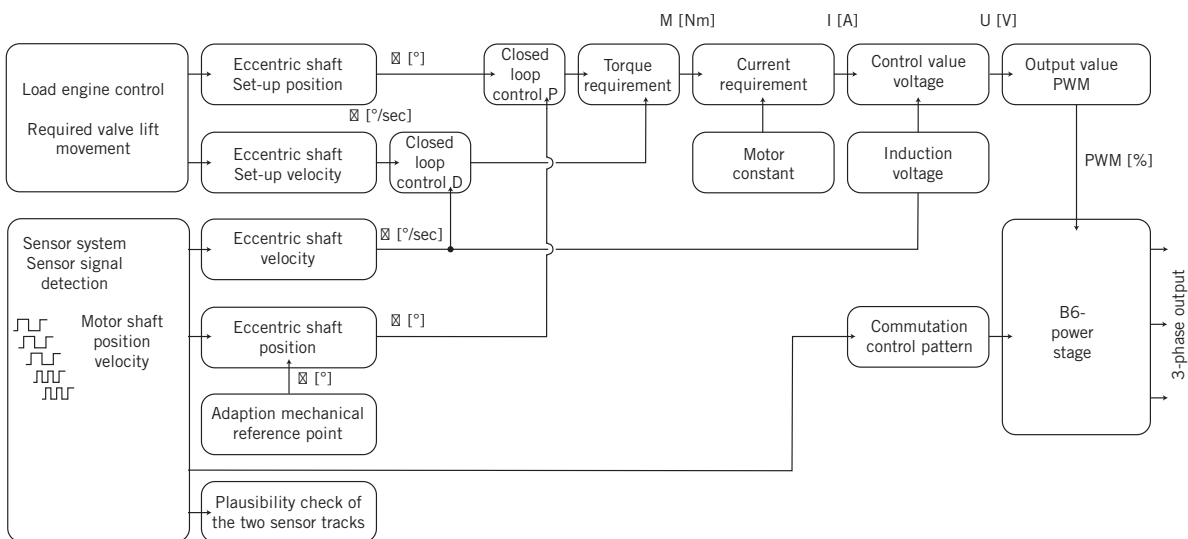
Clear optimisation compared to the Mini's predecessor motor, the 1.6 l TGDI, was achieved through the use of third-generation Valvetronic technology. The final customer can experience this directly. Fuel consumption was reduced again by about 9 % due to the Valvetronic and resulting further optimisation of frictional losses. Responsiveness became more dynamic and, besides a faster torque build-up, more than 40 Nm more torque was provided.

Due to the high development and validation costs, a modular system was of central importance for BMW so it could combine additional applications with standardised hardware, software, control strategy and BLDC-motor building blocks into new scalable systems – all within a short and manageable time frame.

**CONTROL STRATEGY**

The regulator structure for control of the BLDC motor is presented in the block diagram, 7, and has the following special characteristics:

- : The position sensors are divided into two groups. In addition to three commutation sensors, two Hall sensors with their own target wheel are built in. The thereby implemented magnetic encoder has a resolution that is more precise by a factor of 2 than the commutation sensors.
- : Through a worm gear, the servomotor drives an eccentric shaft whose position determines the stroke of the intake valves



7 Control layout

of the combustion engine. To determine this position, the mechanical reference position is driven to at the start of each movement, which defines the reference point. The validity of the sensor signal is constantly monitored by comparing the two sensor groups. As a result, the system fulfils the requirements of the E-gas guideline.

- : The position control is designed so that the motor control determines the optimal valve stroke in connection with the suitable actuator speed for the respective current operating condition. The eccentric angle assigned to the valve stroke is set by a PD control. From the input signals (setpoint, eccentric angle, actual value of eccentric angle and setpoint of actuator speed) and the characteristic system variables (servomotor constants, controlling torque, electrical resistance of the servomotor circuit), the necessary pulse-duty factor is determined in the 1 ms computation raster.
- : To control the VVT3 motor dependent on the current rotor position and the pulse-duty factor specified by the control, a frequency of 16 kHz is applied to the three motor phases via a B6 bridge. If the current rotor position cannot be determined as a result of an error, there is also the possibility of operating the BLDC servomotor in the stepper motor

mode. The three motor phases are controlled in a firmly specified time sequence to generate the stator rotary magnetic field necessary for adjustment.

- : The adjustment characteristics of the control are continuously monitored by a diagnostic function. An error is displayed if control deviations occur or the adjustment speed does not meet the requirements.
- : If one of the above diagnostic functions recognises an error, system demand control of the combustion engine is passed on to the throttle, which avoids impairment of the driving behaviour that the driver experiences.

**QUALITY IN DESIGN**

Tools were also used to achieve the high quality requirements. In close cooperation with BMW, first FTA analyses were performed, followed by D-FMEA. As soon as the first prototypes were available, high accelerated lifetime tests (HALT tests), 8, and other extreme tests, 9, were carried out to uncover weaknesses within just a few days. As a result, initial correction processes were initiated as quickly as possible so the official qualification cycles could be started with a good basis of confidence. Here, too, the time specifications did not permit an iterative development due to the successive elimination of errors.

The assembly concepts were also developed simultaneously. P-FMEA were used as main tool here to systematically verify the concepts. For Sonceboz Automotive, it was the first project in which fully automated assembly immediately followed prototype construction. Previously, the corresponding experience was always gained first on a

manual assembly line. Process stability is monitored using suitable tools. Processes such as glueing and welding can thus be checked for consistency even before a delivery lot is shipped.

**SUMMARY AND OUTLOOK FOR EURO 6**

The TVDI technology, the various measures for CO<sub>2</sub> reduction combined with a simultaneous increase in performance, were optimised towards achieving the coming Euro 6 emission requirements. Experience with VVT1 and VVT2 has been gained with fully variable valve control since 2001. For VVT3, more compact and dynamic actuators can now be used to drive the eccentric shaft, 10. The improved dynamics permit a finer and faster adjustment to the optimal parameters for every condition. The Valvetronic technology, continuously improved over the past ten years, displays a high performance level, is robust and efficient, and is already on the road today.

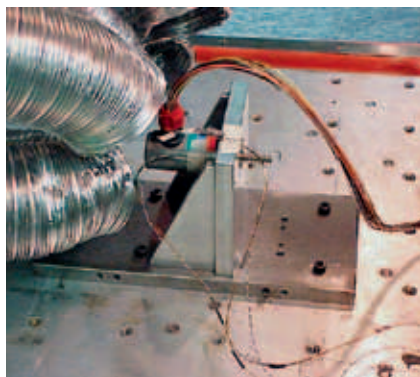
The modular concept permits transferring this technology to other engines in future. The cooperation partner PSA is also using the new Valvetronic technology, which has been available in the RCZ sports car since the beginning of 2010, for example. Additional models will follow. BMW and PSA have already agreed to continue the cooperation and develop this TwinPower Turbo combustion engine further so that it qualifies for Euro 6.

**REFERENCES**

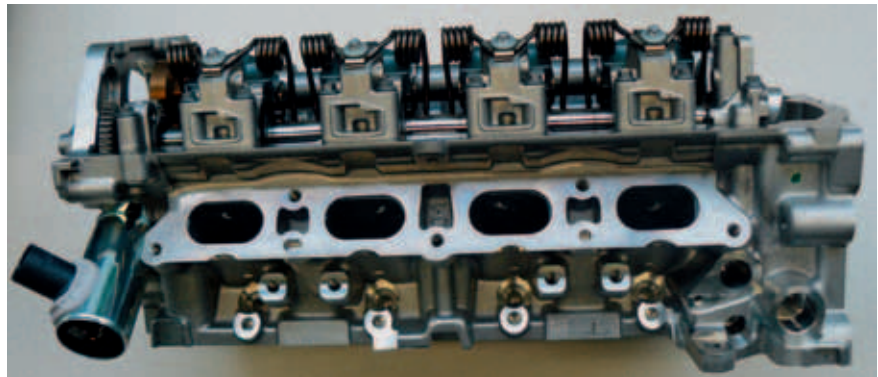
[1] Liebl, J.; Klütting, M.; Poggel, J.; Missy, S.: Der neue BMW Vierzylinder-Ottomotor mit Valvetronic. In: MTZ 62 (2001) Nr. 7/8  
 [2] Unger, H.; Schwarz, C.; Schneider, J.; Koch, K. F.: Die Valvetronic – Erfahrungen aus sieben Jahren Großserie und Ausblick in die Zukunft. In: MTZ 69 (2008) Nr. 7/8

TEST	UNIT
Temperature lower operating limit (LOL)	-70 °C
Temperature upper operating limit (UOL)	+200 °C
Vibration operating limit (VOL)	50G <sub>(RMS)</sub>

8 HALT test conditions



9 BLDC motor in the TÜV test chamber



10 Compact, dynamic and with integrated sensors: BLDC motor

# ATZ live

## OPTIMISED PROCESS CHAIN

Efficiency for the powertrain of tomorrow

## SIMULATION OF THE POWERTRAIN AND ITS COMPONENTS

Reduced fuel consumption and emissions, improved dynamics and driving pleasure

## VIRTUAL PRODUCT DEVELOPMENT

More quality at lower costs



personal buildup for Force Motors Ltd.

# Virtual Powertrain Creation 2010

12th International Conference

30 November and 1 December 2010

Munich | Germany



PROGRAM AND REGISTRATION  
[www.ATZlive.de](http://www.ATZlive.de)

PEER REVIEW ATZ | MTZ

PEER REVIEW PROCESS FOR RESEARCH ARTICLES  
IN ATZ AND MTZ

STEERING COMMITTEE

Prof. Dr.-Ing. Lutz Eckstein	RWTH Aachen	Institut für Kraftfahrzeuge Aachen
Prof. Dipl.-Des. Wolfgang Kraus	HAW Hamburg	Department Fahrzeugtechnik und Flugzeugbau
Prof. Dr.-Ing. Ferit Küçükyay	Technische Universität Braunschweig	Institut für Fahrzeugtechnik
Prof. Dr.-Ing. Stefan Pischinger	RWTH Aachen	Lehrstuhl für Verbrennungskraftmaschinen
Prof. Dr.-Ing. Hans-Christian Reuss	Universität Stuttgart	Institut für Verbrennungsmotoren und Kraftfahrwesen
Prof. Dr.-Ing. Ulrich Spicher	Universität Karlsruhe	Institut für Kolbenmaschinen
Prof. Dr.-Ing. Hans Zellbeck	Technische Universität Dresden	Lehrstuhl für Verbrennungsmotoren

ADVISORY BOARD

Prof. Dr.-Ing. Klaus Augsburg	Dr.-Ing. Markus Lienkamp
Prof. Dr.-Ing. Bernard Bäker	Prof. Dr. rer. nat. habil. Ulrich Maas
Prof. Dr.-Ing. Michael Bargende	Prof. Dr.-Ing. Martin Meywerk
Prof. Dipl.-Ing. Dr. techn. Christian Beidl	Prof. Dr.-Ing. Klaus D. Müller-Glaser
Dr.-Ing. Christoph Bollig	Dr. techn. Reinhard Mundl
Prof. Dr. sc. techn. Konstantinos Boulouchos	Prof. Dr. rer. nat. Cornelius Neumann
Prof. Dr.-Ing. Ralph Bruder	Dr.-Ing. Lothar Patberg
Dr. Gerhard Bruner	Prof. Dr.-Ing. Peter Pelz
Prof. Dr. rer. nat. Heiner Bubb	Prof. Dr. techn. Ernst Pucher
Prof. Dr. rer. nat. habil. Olaf Deutschmann	Dr. Jochen Rauh
Dr. techn. Arno Eichberger	Prof. Dr.-Ing. Konrad Reif
Prof. Dr. techn. Helmut Eichseder	Prof. Dr.-Ing. Stephan Rinderknecht
Dr.-Ing. Gerald Eifler	Dr.-Ing. Swen Schaub
Prof. Dr.-Ing. Wolfgang Eifler	Prof. Dr. sc. nat. Christoph Schierz
Prof. Dr. rer. nat. Frank Gauterin	Prof. Dr. rer.-nat. Christof Schulz
Prof. Dr. techn. Bernhard Geringer	Prof. Dr. rer. nat. Andy Schürr
Prof. Dr.-Ing. Uwe Grebe	Prof. Dr.-Ing. Ulrich Seiffert
Prof. Dr.-Ing. Horst Harndorf	Prof. Dr.-Ing. Hermann J. Stadtfeld
Prof. Dr. techn. Wolfgang Hirschberg	Prof. Dr. techn. Hermann Steffan
Univ.-Doz. Dr. techn. Peter Hofmann	Dr.-Ing. Wolfgang Steiger
Prof. Dr.-Ing. Bernd-Robert Höhn	Prof. Dr.-Ing. Peter Steinberg
Prof. Dr. rer. nat. Peter Holstein	Prof. Dr.-Ing. Christoph Stiller
Prof. Dr.-Ing. habil. Werner Hufenbach	Dr.-Ing. Peter Stommel
Prof. Dr.-Ing. Roland Kasper	Prof. Dr.-Ing. Wolfgang Thiemann
Prof. Dr.-Ing. Tran Quoc Khanh	Prof. Dr.-Ing. Helmut Tschöke
Dr. Philip Köhn	Dr.-Ing. Pim van der Jagt
Prof. Dr.-Ing. Ulrich Konigorski	Prof. Dr.-Ing. Georg Wachtmeister
Dr. Oliver Kröcher	Prof. Dr.-Ing. Jochen Wiedemann
Dr. Christian Krüger	Prof. Dr. techn. Andreas Wimmer
Univ.-Ass. Dr. techn. Thomas Lauer	Prof. Dr. rer. nat. Hermann Winner
Prof. Dr. rer. nat. Uli Lemmer	Prof. Dr. med. habil. Hartmut Witte
Dr. Malte Lewerenz	

Scientific articles of universities in ATZ Automobiltechnische Zeitschrift and MTZ Motortechnische Zeitschrift are subject to a proofing method, the so-called peer review process. Articles accepted by the editors are reviewed by experts from research and industry before publication. For the reader, the peer review process further enhances the quality of the magazines' content on a national and international level. For authors in the institutes, it provides a scientifically recognised publication platform.

In the ATZ | MTZ Peer Review Process, once the editors has received an article, it is reviewed by two experts from the Advisory Board. If these experts do not reach a unanimous agreement, a member of the Steering Committee acts as an arbitrator. Following the experts' recommended corrections and subsequent editing by the author, the article is accepted.

In 2008, the peer review process utilized by ATZ and MTZ was presented by the WKM (Wissenschaftliche Gesellschaft für Kraftfahrzeug- und Motorentechnik e. V. / German Professional Association for Automotive and Motor Engineering) to the DFG (Deutsche Forschungsgemeinschaft / German Research Foundation) for official recognition.



Founded 1939 by Prof. Dr.-Ing. E. h. Heinrich Buschmann and Dr.-Ing. E. h. Prosper L'Orange

Organ of the Fachverband Motoren und Systeme im VDMA, Verband Deutscher Maschinen- und Anlagenbau e.V., Frankfurt/Main, for the areas combustion engines and gas turbines  
 Organ of the Forschungsvereinigung Verbrennungskraftmaschinen e.V. (FVV)  
 Organ of the Wissenschaftliche Gesellschaft für Kraftfahrzeug- und Motorentechnik e.V. (WKM)  
 Organ of the Österreichischer Verein für Kraftfahrzeugtechnik (ÖVK)  
 Cooperation with the STG, Schiffbautechnische Gesellschaft e.V., Hamburg, in the area of ship drives by combustion engine

10 | 2010 – October 2010 – Volume 71

Springer Automotive Media | Springer Fachmedien Wiesbaden GmbH

P. O. Box 15 46 · 65173 Wiesbaden · Germany | Abraham-Lincoln-Straße 46 · 65189 Wiesbaden · Germany  
 Amtsgericht Wiesbaden, HRB 9754, USt-IdNr. DE811148419

**Managing Directors** Dr. Ralf Birkelbach (Chairman), Armin Gross, Albrecht Schirmacher | **Senior Advertising** Armin Gross | **Senior Marketing** Rolf-Günther Hobbeling  
**Senior Production** Christian Staral | **Sales Director** Gabriel Göttlinger

**SCIENTIFIC  
 ADVISORY BOARD**

**Prof. Dr.-Ing. Michael Bargende**  
 Universität Stuttgart

**Prof. Dr. techn. Christian Beidl**  
 TU Darmstadt

**Dr.-Ing. Ulrich Dohle**  
 Tognum AG

**Dipl.-Ing. Wolfgang Dürheimer**  
 Dr. Ing. h. c. F. Porsche AG

**Dr. Klaus Egger**

**Dipl.-Ing. Dietmar Goericke**  
 Forschungsvereinigung  
 Verbrennungskraftmaschinen e.V.

**Prof. Dr.-Ing. Uwe-Dieter Grebe**  
 GM Powertrain

**Dipl.-Ing. Thorsten Herdan**  
 VDMA-Fachverband Motoren  
 und Systeme

**Prof. Dr.-Ing. Heinz K. Junker**  
 Mahle GmbH

**Prof. Dr. Hans Peter Lenz**  
 ÖVK

**Prof. Dr. h. c. Helmut List**  
 AVL List GmbH

**Dipl.-Ing. Wolfgang Maus**  
 Emitec Gesellschaft für  
 Emissionstechnologie mbH

**Prof. Dr.-Ing. Stefan Pischinger**  
 FEV Motorentechnik GmbH

**Prof. Dr. Hans-Peter Schmalz**  
 APC – Advanced Propulsion  
 Concepts Mannheim GmbH

**Prof. Dr.-Ing. Ulrich Seiffert**  
 TU Braunschweig

**Prof. Dr.-Ing. Ulrich Spicher**  
 WKM

**EDITORS-IN-CHARGE**

Dr.-Ing. E. h. Richard van Basshuysen  
 Wolfgang Siebenpeiffer

**EDITORIAL STAFF**

**EDITOR-IN-CHIEF**  
 Johannes Winterhagen (win)  
 phone +49 611 7878-342 · fax +49 611 7878-78462  
 johannes.winterhagen@springer.com

**VICE-EDITOR-IN-CHIEF**  
 Ruben Danisch (rd)  
 phone +49 611 7878-393 · fax +49 611 7878-78462  
 ruben.danisch@springer.com

**CHIEF-ON-DUTY**  
 Kirsten Beckmann M. A. (kb)  
 phone +49 611 7878-343 · fax +49 611 7878-78462  
 kirsten.beckmann@springer.com

**SECTIONS**  
*Electrics, Electronics*  
 Markus Schöttle (scho)  
 phone +49 611 7878-257 · fax +49 611 7878-78462  
 markus.schoettle@springer.com

*Engine*  
 Ruben Danisch (rd)  
 phone +49 611 7878-393 · fax +49 611 7878-78462  
 ruben.danisch@springer.com

*Online*  
 Katrin Pudenz M. A. (pu)  
 phone +49 6172 301-288 · fax +49 6172 301-299  
 redaktion@kpz-publishing.com

*Production, Materials*  
 Stefan Schlott (hlo)  
 phone +49 8191 70845 · fax +49 8191 66002  
 Redaktion\_Schlott@gmx.net

*Research*  
 Dipl.-Ing. (FH) Moritz-York von Hohenthal (mvh)  
 phone +49 611 7878-278 · fax +49 611 7878-78462  
 moritz.von.hohenthal@springer.com

*Service, Event Calendar*  
 Martina Schraad (mas)  
 phone +49 611 7878-276 · fax +49 611 7878-78462  
 martina.schraad@springer.com

*Transmission*  
 Dipl.-Ing. Michael Reichenbach (rei)  
 phone +49 611 7878-341 · fax +49 611 7878-78462  
 michael.reichenbach@springer.com

**PERMANENT CONTRIBUTORS**

Richard Backhaus (rb),  
 Dipl.-Reg.-Wiss. Caroline Behle (beh),  
 Prof. Dr.-Ing. Stefan Breuer (sb),  
 Jürgen Grandel (gl), Ulrich Knorra (kno),  
 Prof. Dr.-Ing. Fred Schäfer (fs),  
 Roland Schedel (rs)

**ENGLISH LANGUAGE CONSULTANT**

Paul Willin (pw)

**ADDRESS**  
 P. O. Box 15 46, 65173 Wiesbaden, Germany  
 redaktion@ATZonline.de

**MARKETING | OFFPRINTS**

**PRODUCT MANAGEMENT  
 AUTOMOTIVE MEDIA**  
 Sabrina Brokopp  
 phone +49 611 7878-192 · fax +49 611 7878-78407  
 sabrina.brokopp@springer.com

**OFFPRINTS**  
 Martin Leopold  
 phone +49 2642 9075-96 · fax +49 2642 9075-97  
 leopold@medien-kontor.de

**ADVERTISING**  
**AD MANAGER**  
 Britta Dolch  
 phone +49 611 7878-323 · fax +49 611 7878-78140  
 britta.dolch@gvw-media.de

**KEY ACCOUNT MANAGEMENT**  
 Elisabeth Maßfeller  
 phone +49 611 7878-399 · fax +49 611 7878-78140  
 elisabeth.massfeller@gvw-media.de

**AD SALES MANAGER**  
 Sabine Röck  
 phone +49 611 7878-269 · fax +49 611 7878-78140  
 sabine.roeck@gvw-media.de

**AD SALES**  
 Frank Nagel  
 phone +49 611 7878-395 · fax +49 611 7878-78140  
 frank.nagel@gvw-media.de

**DISPLAY AD MANAGER**  
 Petra Steffen-Munserg  
 tel +49 611 7878-164 · fax +49 611 7878-443  
 petra.steffen-munserg@gvw-media.de

**AD PRICES**  
 Price List No. 53 (10/2009)

**PRODUCTION | LAYOUT**  
 Heiko Köllner  
 phone +49 611 7878-177 · fax +49 611 7878-78464  
 heiko.koellner@springer.com

**SUBSCRIPTIONS**  
 VVA-Zeitschriftenservice, Abt. D6 F6, MTZ  
 P. O. Box 77 77, 33310 Gütersloh, Germany  
 Renate Vies  
 phone +49 5241 80-1692 · fax +49 5241 80-9620  
 SpringerAutomotive@abo-service.info

**YOUR HOTLINE  
 TO MTZ**

- Editorial Staff
- +49 611 7878-393
- Reader's Service
- +49 611 7878-151
- Advertising
- +49 611 7878-395

**SUBSCRIPTION CONDITIONS**  
 The eMagazine appears 11 times a year at an annual subscription rate of 269 €. Special rate for students on proof of status in the form of current registration certificate 124 €. Special rate for VDI/ÖVK/VKS members on proof of status in the form of current member certificate 208 €. Special rate for studying VDI members on proof of status in the form of current registration and member certificate 89 €. The subscription can be cancelled in written form at any time with effect from the next available issue.

**HINTS FOR AUTHORS**  
 All manuscripts should be sent directly to the editors. By submitting photographs and drawings the sender releases the publishers from claims by third parties. Only works not yet published in Germany or abroad can generally be accepted for publication. The manuscripts must not be offered for publication to other journals simultaneously. In accepting the manuscript the publisher acquires the right to produce royalty-free offprints. The journal and all articles and figures are protected by copyright. Any utilisation beyond the strict limits of the copyright law without permission of the publisher is illegal. This applies particularly to duplications, translations, microfilming and storage and processing in electronic systems.

© Springer Automotive Media /  
 Springer Fachmedien Wiesbaden GmbH,  
 Wiesbaden 2010

Springer Automotive Media is a brand of Springer Fachmedien. Springer Fachmedien is part of the specialist publishing group Springer Science+Business Media.

AUTHORS



**DIPL.-ING. HARALD ECHTLE**  
is Computational Engineer at Group Research & Advanced Engineering Powertrain at Daimler AG in Stuttgart (Germany).



**DR. STEFAN SCHÖFFEL**  
is Computational Engineer at Group Research & Advanced Engineering Powertrain at Daimler AG in Stuttgart (Germany).



**DIPL.-ING. GÜNTER WENNINGER**  
is Manager at Group Research & Advanced Engineering Powertrain at Daimler AG in Stuttgart (Germany).



**DIPL.-PHYS. SIMON FISCHER**  
is Assistant at the Institute for Powertrains and Automotive Technology at TU Wien (Austria).



**DR. THOMAS LAUER**  
is Assistant at the Institute for Powertrains and Automotive Technology at TU Wien (Austria).



**DIPL.-ING. (FH) LUKAS MÖLTNER**  
is Assistant at the Institute for Powertrains and Automotive Technology at TU Wien (Austria).

# OPTIMIZATION OF THE SELECTIVE CATALYTIC REDUCTION BY MEANS OF NUMERICAL METHODS

At present the Selective Catalytic Reduction (SCR) with ammonia as reducing agent is frequently used for Diesel powered vehicles to decrease significantly the nitric oxide ( $\text{NO}_x$ ) emissions. The preparation of ammonia includes numerous sub-processes that need to be understood completely to develop exhaust gas systems efficiently. Within a co-operation project between Daimler AG and the Institute for Powertrains and Automotive Technology (IPA) of the Vienna University of Technology especially the CFD simulation method was employed successfully to solve this task.



personal buildup for Force Motors Ltd.

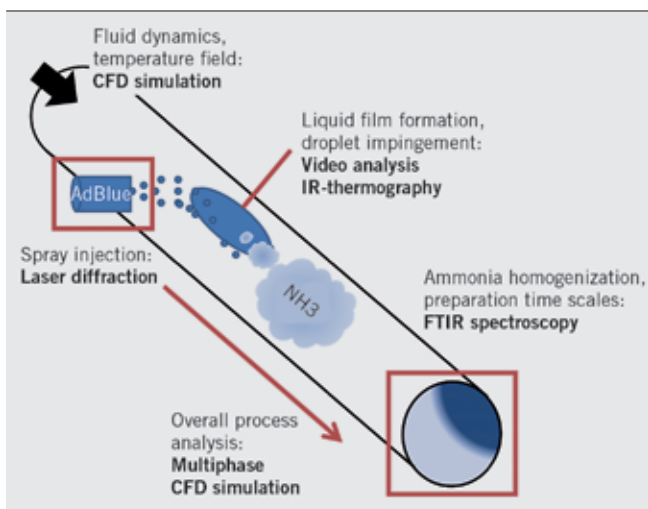
1	INTRODUCTION
2	AMMONIA PREPARATION IN THE EXHAUST SYSTEM
3	APPLICATION OF THE NUMERICAL SIMULATION
4	BASIC INVESTIGATIONS ON AMMONIA PREPARATION
5	APPLICATION TO A CLOSE-TO-PRODUCTION EXHAUST SYSTEM
6	SUMMARY AND OUTLOOK

## 1 INTRODUCTION

Because of the future exhaust gas legislation a significant decrease of nitric oxide ( $\text{NO}_x$ ) emissions will become a development focus for diesel powertrains. Besides a further improvement of the combustion process the efficient exhaust gas treatment with Selective Catalytic Reduction (SCR) is a method on a near- and midterm range that offers a high potential and has already been applied to series production vehicles. In this process a urea-water solution (UWS) is injected in the exhaust gas system that reacts in the following and over numerous sub-processes to gaseous ammonia that finally reduces the nitrogen oxides to elementary nitrogen in a downstream SCR catalyst.

In spite of the successful market launch of this technology there still exists a high potential to optimize the system. To reach an ideal conversion level of the SCR system under all operating conditions and additionally a uniform distribution of ammonia at the SCR catalyst a quick transformation of the urea-water solution to ammonia is necessary. Therefore, a deep understanding of all sub-processes that are included in the formation of gaseous ammonia from the urea-water solution is necessary. This includes the interaction of the liquid urea-water solution with the turbulent exhaust flow and the hot surfaces of the exhaust gas system and the convective and diffusive species transport that affects the uniform distribution of ammonia [1, 2]. There is still a need for research activities to investigate these processes for different engine operating points.

This was done within a co-operation project between Daimler AG and the Institute for Powertrains and Automotive Technology



① Process chain of UWS preparation upstream of the SCR catalyst and analysis methodology

(IPA) of the Vienna University of Technology. Besides basic investigations for model validation the developed methodology was validated on a close-to-production exhaust gas system.

## 2 AMMONIA PREPARATION IN THE EXHAUST SYSTEM

Within the SCR process ammonia is used as a reducing agent for the nitric oxides. The storage of ammonia in the vehicle is realised by means of a carrier substance that consists of a eutectic aqueous solution with a urea mass fraction of 32.5%. This urea-water solution is injected into the exhaust gas system where it is converted by physical and chemical processes to gaseous ammonia. ① gives an overview of these processes.

During the injection aerodynamic forces and heat are transferred from the turbulent exhaust flow to the droplets of the spray. First, this induces an evaporation of the water in the droplets (drying). The remaining urea melts, evaporates and dissociates to ammonia and isocyanic acid (thermolysis) that, on its part, reacts by absorbing water to ammonia and carbon dioxide (hydrolyses):



The droplets impinge on the hot surfaces of the exhaust system in different scenarios that depend on the wall temperature, the fluid properties and the kinetic energy of the droplets and reach from an elastic rebound over a thermal droplet breakup to a wall film formation. In the latter case the urea is stored in a wall film and released via the mentioned reactions in the following.

Each of the described processes has a high influence on the time scales of the ammonia preparation and on the uniform distribution upstream of the SCR catalyst. A purposeful and methodic approach to describe these complex processes is the integration of the numerical simulation method combined with experimental investigations to validate the model.

## 3 APPLICATION OF THE NUMERICAL SIMULATION

For the following investigations the commercially available software code Star-CD from CD-adapco was used.

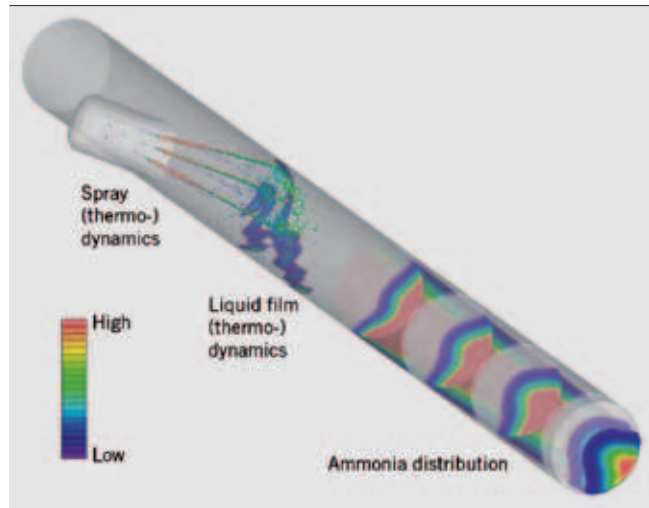
The fluid flow was calculated with the Euler approach combined with a  $k\epsilon$  turbulent model and the liquid phase following Lagrange. The size distribution of the injected droplets and their initial speed were determined empirically with laser optical methods and triggered camera measurements. In the following, the experimental data was implemented as an initial condition to the model [3].

The fluid properties, like viscosity, vapour pressure, heat capacity etc. of the urea-water solution were specified in dependency of the urea concentration [2], the fluid properties of the gaseous components water vapour, ammonia and isocyanic acid were obtained from [4]. The simulation of the droplet evaporation was validated with experimental data of evaporation curves from the literature [5, 6].

Our own experimental investigations showed that the thermolysis takes place instantly and without any time lag. The hydrolysis, on the other hand, could not be observed in the investigated temperature range and without catalytic support, see chapter 4. Thus, a detailed modelling of reaction kinetics could be avoided. The enthalpies of urea melting and evaporation and the enthalpy of reaction of the endothermal thermolysis were obtained from [7].

	OP 1	OP 2	OP 3
MASS FLOW [KG/H]	100	200	350
EXHAUST TEMPERATURE [°C]	250	350	450
UWS INJECTION [G/H]	20	90	90
INJECTION DURATION [MS]	7	10	10
INJECTION INTERVAL [MS]	1000	333	333

② Operation points for the basic analysis



③ Geometry for the basic investigations on the preparation process chain and exemplary results of the CFD simulation

A commonly used time step size in the CFD simulation is  $10^{-5}$  to  $10^{-3}$  seconds, but very often an equilibrium is not reached until numerous injection events have passed. For this reason the stationary flow field without injection of the urea-water solution was solved first and considered as constant in the following, i.e. an influence from the injection does not occur. This assumption is acceptable due to the small amount of injected fluid and the low droplet velocities. For the following transient calculations of the injection events a solving of the transport equations for the velocity components, the turbulence and dissipation was not necessary, what implicated a calculation time acceleration by a factor of up to ten.

4 BASIC INVESTIGATIONS ON AMMONIA PREPARATION

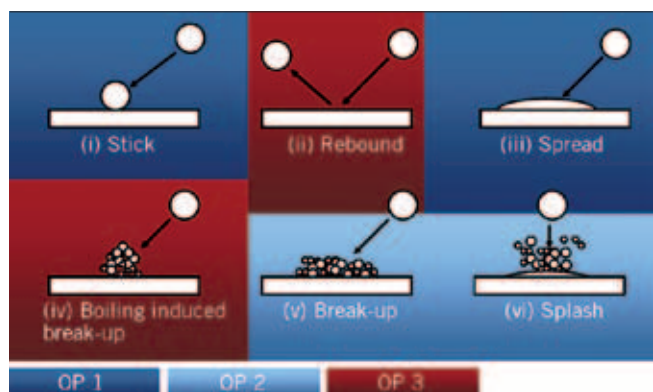
For the model validation three characteristic operating points (OP) were analysed on the engine test bench. They were chosen with the aim to cover all typical effects of the process chain of the ammonia preparation, ②.

The mixing pipe of the exhaust gas system upstream of the SCR catalyst was replaced by a simple straight exhaust pipe. This way, the basic effects of the ammonia preparation could be studied with simple boundary conditions. The urea-water solution was injected in a 45° angle to the flow direction. The distance between the injection position and the end of the mixing pipe was 550 mm, which is approximately a typical distance to the SCR catalyst in a passenger car.

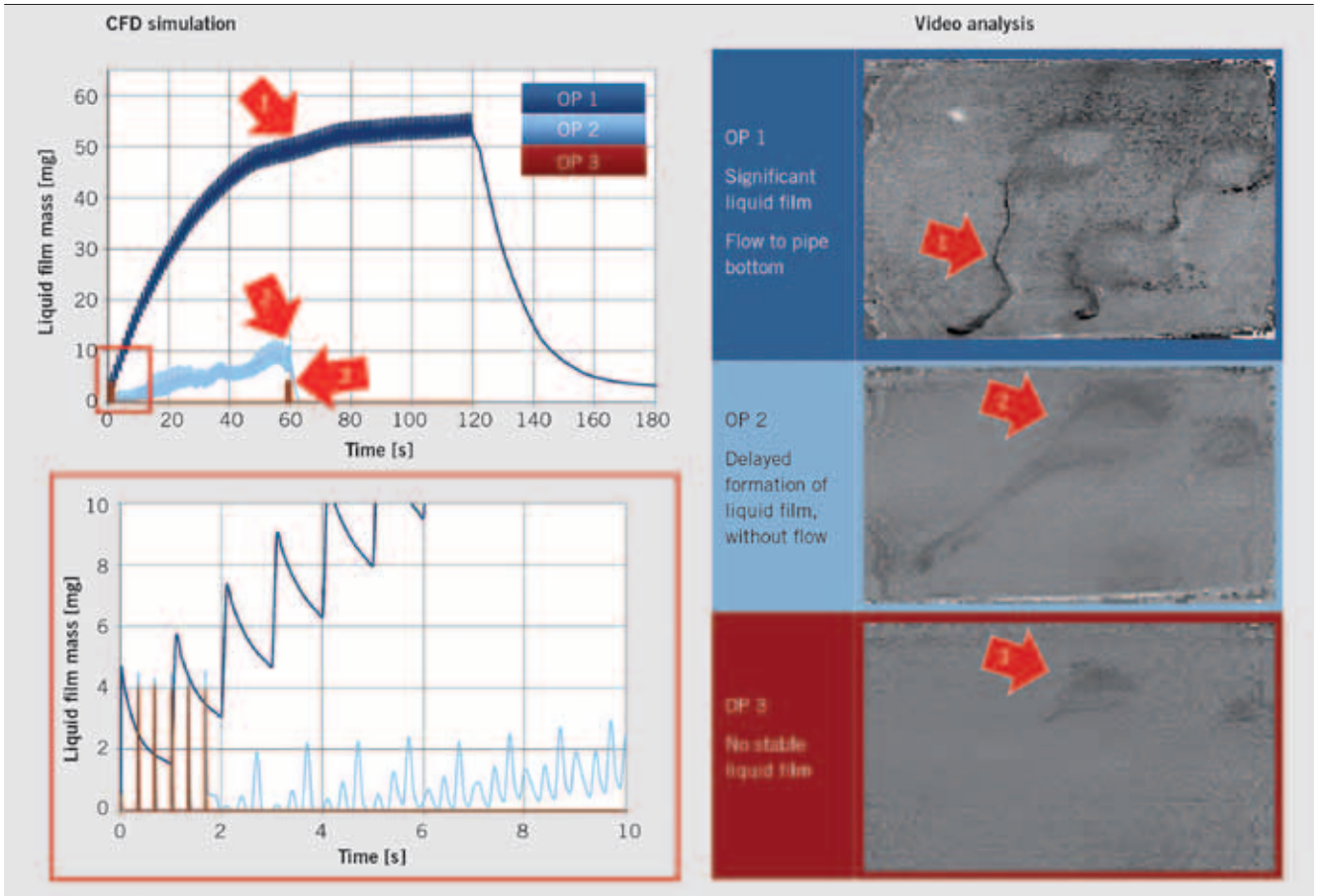
③ shows the geometry and exemplary results from the CFD calculation as well as the typical influencing variables on the uniform distribution. The location of the injection is indicated as well as the spray pattern, which is typical for the investigated injector type, a liquid film formed on the pipe wall and the ammonia concentration in the measuring volume.

First experimental investigations showed that for the mentioned operating points the different interactions of the droplets with the hot surfaces of the exhaust gas system have a significant influence. There exist numerous physical models that describe the behaviour of liquid droplets when impinging on rigid walls [8, 9]. Different regimes are defined that are distinguished by dimensionless indicators of the droplet behaviour, like the Weber and Laplace number or a number for the dimensionless wall temperature. All these indicators have in common that they describe the stability of droplets under the influence of external forces and heat fluxes. However, the application of these models on a multi-component fluid and on surface temperatures beyond the liquid's boiling temperature is a challenge. At the IPA the Bai model has been successfully applied to injection problems of SI engines in the past and was therefore chosen as a starting model for the following investigations. ④ shows different scenarios that are described in the Bai model and the expected regimes for the three investigated operating points, which are marked in different colours. It can already be derived on a theoretical basis that the droplets will behave differently for the three operating points, which will have an impact on the time scales and the uniform distribution.

Experiments were carried out on the mentioned basic geometry to investigate on the behaviour of the droplets and an optionally occurring wall film. Optical measurements with a CCD camera and recordings with an infrared camera were employed to demonstrate the wall cooling at the impact point of the spray jets, as well as the FTIR spectroscopy at different cross sections of the mixing pipe to determine the reducing agent's uniform distribution [3]. For the FTIR spectroscopy, a conditioning device consisting of a pre-filter and a heating/cooling tube was assembled upstream of the actual measuring cell to maintain well-defined inlet conditions. The extraction of the exhaust gas sample stream was carried out with a probe at discrete points of the exhaust system, each of them successively analyzed by repeating a defined injection strategy.



④ Impingement regimes according to the Bai model for the investigated operating points



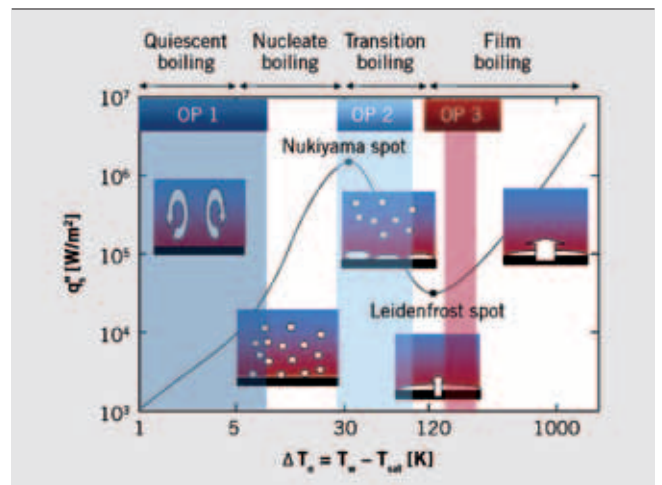
5 Calculated wall film formation (left) and corresponding results of the video analysis (right)

It could be shown for OP 1 that immediately after the start of the injection a massive formation of wall film can be observed. For OP 2 a thin wall film is formed after a certain time period and for OP 3 no wall film formation can be observed. The simulations with the CFD method were in a good qualitative agreement with the observations, 5.

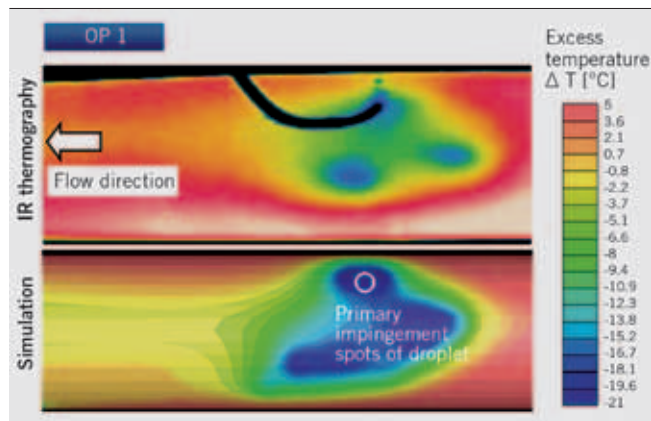
The observed and calculated behaviour can be explained with the Nukiyama characteristics of the fluid. It describes the heat fluxes on a superheated, wetted surface in a quiescent fluid as a function of the difference between wall and boiling temperature. In 6 the characteristic regimes of nucleate, transition and film boiling are shown.

In case of OP 3 the wall temperature is significantly above the Leidenfrost temperature of the water-urea solution  $T \cong 500$  K. Due to the forming of a steam cushion no wall wetting occurs. At the beginning, OP 2 shows the same behaviour. However, the thermal contact causes a slow cooling of the wall and a regime change from the film to the transition regime, i.e. a wall film is formed after some time. Therefore, a correct prediction of the wall film can only be achieved with a correct calculation of the wall temperature. For this reason, solid elements were used in the mentioned numerical model to take into account the heat capacity and heat conductance of the pipe walls. For the OP 1 the regime of quiescent boiling and nucleate boiling prevails, i.e. a wall film can be formed immediately. The following motion of the wall film is determined

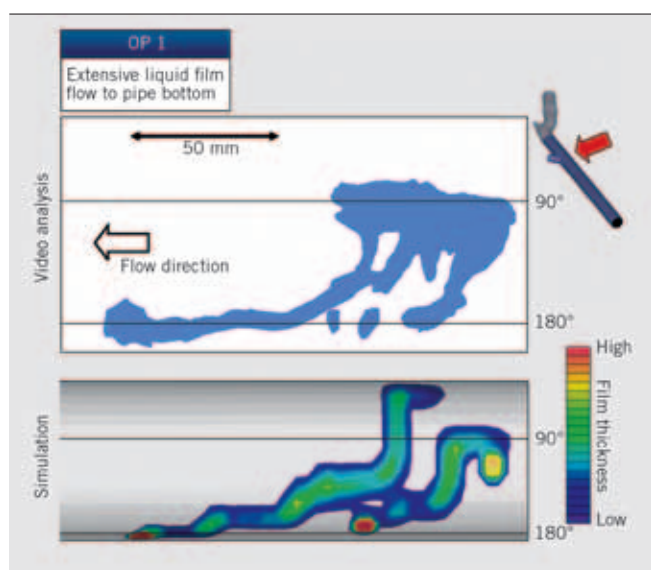
by the shear forces of the flow and gravitation, its evaporation by the mentioned Nukiyama curve. For an experimental validation the wall wetting process was recorded with a CCD camera at an optically accessible part of the pipe wall. 7 shows a comparison of



6 Nukiyama curve: approximation of the heat flux density of a wall film forming fluid as a function of the excess temperature (difference between wall and boiling temperature)



7 Simulated and measured stationary temperature field of the pipe wall in the region of the spray impingement (OP1)



8 Spread of the stationary wall film after 120 s for OP 1

the calculated wall temperature and measurements that were carried out with an infrared camera.

After that, the recordings were visually post-processed. From every single image a “zero image” of the non wetted pipe wall was subtracted. Afterwards, the resulting image was analysed with an appropriate threshold filter to extract the wetted surface. 8 shows exemplarily the stationary spread of the wall film for OP 1 after 120 s of injection time in comparison with the corresponding results of the simulation. Thus, the formation and motion of the wall film were in good agreement with the experiment.

Furthermore, both chemical reactions that are following the physical evaporation had to be determined. For all three operating points it could be shown experimentally with highly time-resolved Fourier transform infrared spectroscopy (FTIR) [3] that the time scales of the thermolysis are so small that the kinetics can be neglected in good approximation. It can be rather assumed that the gaseous urea dissociates immediately. Besides, it could be demonstrated once again with FTIR spectroscopy that for all investigated operating points equimolar concentrations of isocyanic acid

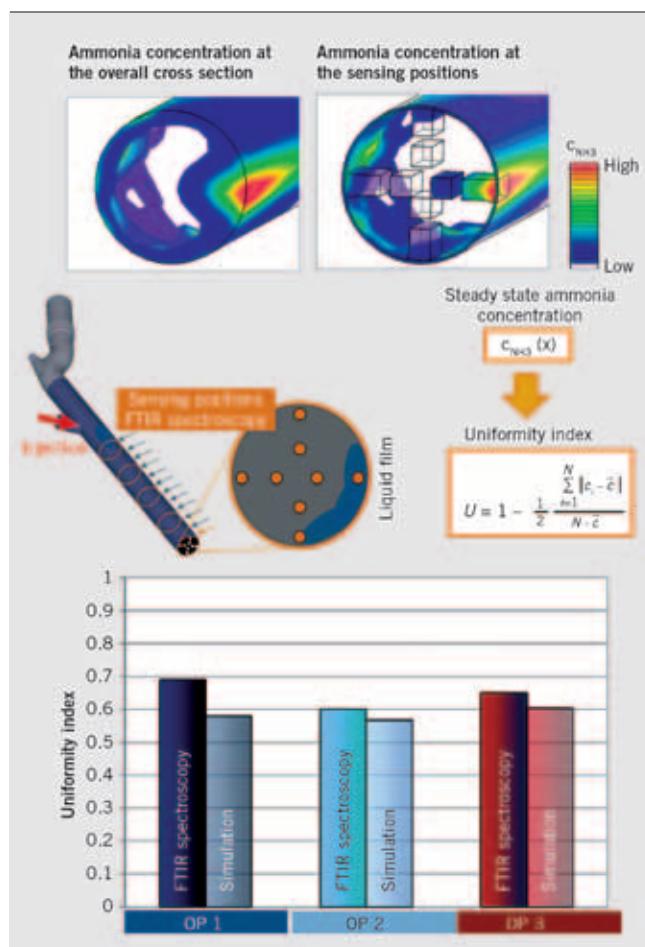
and ammonia can be observed, i.e. no hydrolysis reaction occurs. The time scales of this reaction are only sufficiently small at higher temperature or on the reactive surfaces of the SCR catalyst, respectively.

A calculation of the uniform distribution was carried out at various positions of the mixing pipe and compared with FTIR measurements at eight measuring positions in every cross section. The calculation of the uniformity indices was carried out in analogy to the measurements at the eight measuring positions. Basically, the results showed a good correlation with the measurements. Only the uniform distribution for OP 1 was underestimated, what can be explained with the particularly complex situation of a high amount of urea stored in the wall film, 9.

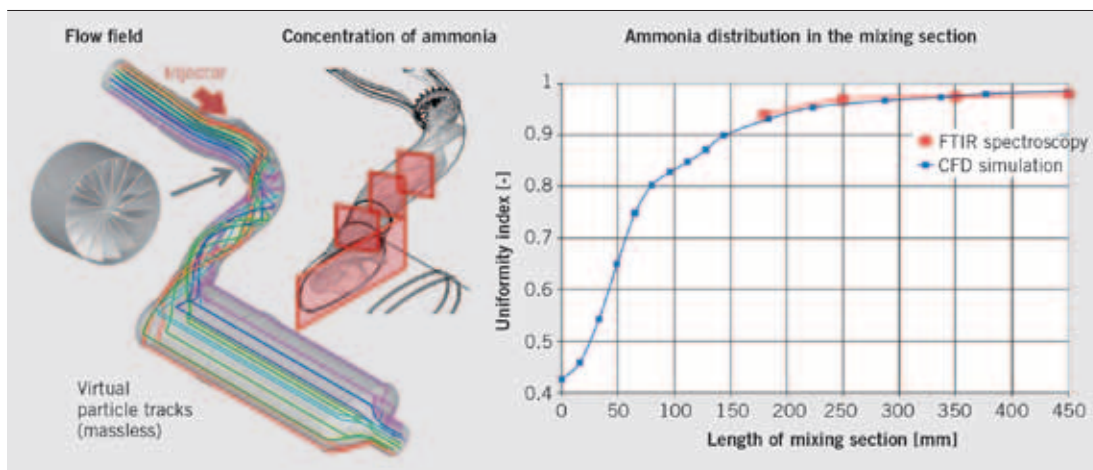
The results that were gained for these basic investigations were applied in the following on the design of the mixing pipe of a close-to-production exhaust system.

### 5 APPLICATION TO A CLOSE-TO-PRODUCTION EXHAUST SYSTEM

10 contains an extract of results that were calculated with the CFD model of a close-to-production exhaust system. In the figure, the comparison of the simulation and measurements is shown for



9 Methodology to determine the ammonia uniform distribution (top) and the uniformity index at the end of the mixing pipe (bottom)



10 Simulation of the flow field and the ammonia distribution for a close-to-production exhaust system with mixing device (left), calculated and measured uniformity index along the mixing pipe (right)

an exhaust system with a mixing device. The mixing device creates an airflow with a high vortex density that causes a better convective mixing of the ammonia vapour (10, left side). A dramatically improved uniform distribution follows from that at the catalyst entry (10, right side). Besides, the mixing device prevents to a high amount wall wetting, what improves the wall film formation and the problems coming along with it.

To validate the simulation results spatially resolved measurements of the ammonia concentration were carried out. The detection of the reducing agent was once again realized with the FTIR methodology at pipe cross sections varying from the beginning to the end of the mixing pipe. The ammonia distribution that was experimentally determined for OP 1 is plotted against the simulation results in 10, right side. An excellent correlation can be observed.

## 6 SUMMARY AND OUTLOOK

The efficient reduction of nitric oxides formed during Diesel combustion with SCR technology will contribute to the compliance of future exhaust legislation. In a co-operation between Daimler AG and the Institute for Powertrains and Automotive Technology (IPA) of the Vienna University of Technology basic investigations on the conversion process of the injected liquid urea-water solution to the gaseous ammonia were carried out. On a simple exhaust pipe geometry the behaviour of the injected droplets on the hot surfaces of the exhaust pipes and the formation of wall film were investigated in particular. Focus of the investigations was the modelling of all processes involved with the CFD simulation method. It could be shown that there is a good correlation between the simulation results and the experiments from the engine test bench concerning uniform distribution of ammonia and wall film formation. In spite of the generally successful application of the CFD

simulation the universal validity of the impingement models at low and high temperatures must be improved. This will be the content of future projects.

The results gained from these investigations were applied successfully to the development of the mixing tube of a close-to-production exhaust system. The uniform distribution of the reducing agent upstream of the SCR catalyst was predicted in good correlation with the experiments.

## REFERENCES

- [1] Grünwald, J.; Sattelmayer, T.; Steinbach, S.: Wirbelmischer für SCR-Verfahren im Pkw. In: MTZ 66 (2005), Nr. 1/2005, S. 44-48
- [2] Birkhold, F.; Meingast, U.; Wassermann, P.; Deutschmann, O.: Analysis of the Injection of Urea-water-solution for automotive SCR DeNO<sub>x</sub>-Systems: Modeling of Two-phase Flow and Spray/Wall-Interaction; SAE Technical paper 2006-01-0643, 2006
- [3] Geringer, B.; Fischer, S.; Hofmann, P.; Lauer, T.; Möltner, L.; Schneeweiss, B.; Teiner, P.: Neue Ansätze und Entwicklungsmethoden zur Minimierung der NO<sub>x</sub>-Emissionen von Dieselmotoren; 31. Wiener Motorensymposium, Fortschritts-Berichte VDI, Reihe 12, Nr.716, Band 2, S. 374-394, 2010
- [4] Verein Deutscher Ingenieure (Hrsg.): VDI-Wärmeatlas, 5. Auflage, Düsseldorf, 1988
- [5] Deutsche Chemische Gesellschaft (Herausgeber): Gmelins Handbuch der anorganischen Chemie, Band C, D, 1. Verlag Chemie, 1971
- [6] Fischer, S.; Lauer, T.: Urea-injection and – preparation in Diesel Applications – Multiphase Multicomponent Modeling using Star-CD; STAR European Conference, London, 2010
- [7] Wang, T.; Baek, S.; Lee, S.: Experimental Investigation on Evaporation of Urea-Water-Solution Droplet for SCR Applications; AIChE Journal, Vol. 55, No. 12 3267, 2009
- [8] Köbel, M.; Strutz, E. O.: Thermal and Hydrolytic Decomposition of Urea for Automotive Selective Catalytic Reduction Systems: Thermochemical and Practical Aspects; Ind. Eng. Chem. Res. 2003, 42, 2093-2100, 2003
- [9] Bai, C.; Gosman, A. D.: Development of Methodology for Spray Impingement Simulation; SAE Paper 950283, 1995
- [10] Kuhnke, D.: Spray/ Wall-Interaction Modelling by Dimensionless Data Analysis. Dissertation Universität Darmstadt, Fachbereich Mathematik; Shaker Verlag, Strömungstechnik, Aachen 2004

AUTHORS



**DIPL.-ING. DOMINIK RETHER** is Research Associate at IVK at the University of Stuttgart and was Employee at the Internal Combustion Engines Section at FKFS in Stuttgart (Germany).



**DIPL.-ING. ANDREAS SCHMID** is Research Associate at IVK at the University of Stuttgart and was Employee at the Internal Combustion Engines Section at FKFS in Stuttgart (Germany).



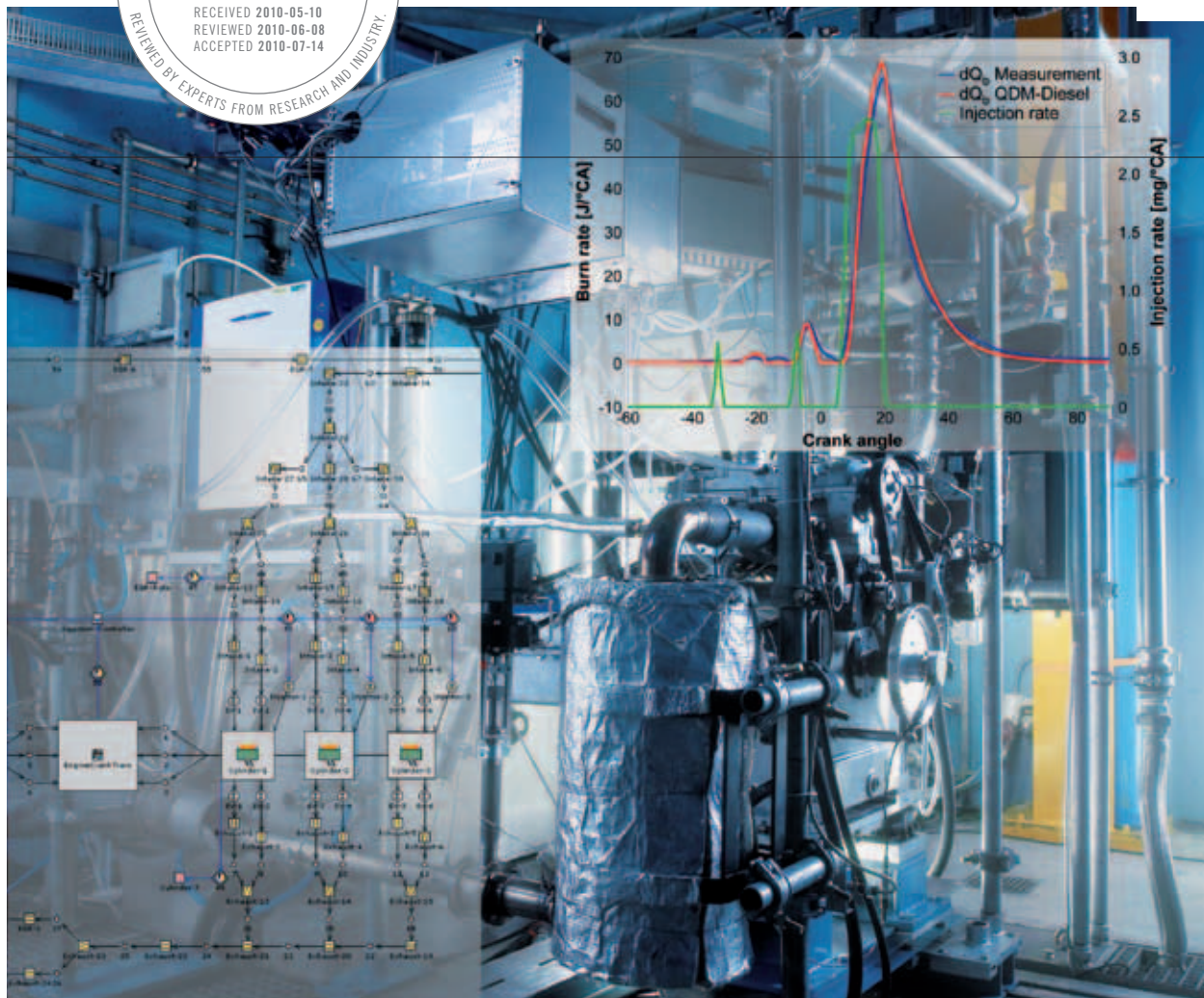
**DR.-ING. MICHAEL GRILL** is Project Manager for Working Process Calculation at the Internal Combustion Engines Section at FKFS in Stuttgart (Germany).



**PROF. DR.-ING. MICHAEL BARGE** is Board Member of FKFS and Professor for Internal Combustion Engines at the Institute for Internal Combustion Engines and Automotive Engineering (IVK) at the University of Stuttgart (Germany).

# QUASIDIMENSIONAL SIMULATION OF CI-COMBUSTION WITH PILOT AND POST INJECTIONS

Diesel engines have become much more complex over the last two decades. By means of simulations the number of test bench investigations can be reduced. The difficulty in modelling the conventional CI-combustion is to reproduce self-ignition, gas mixture and the combustion in such a way that predictive calculations are possible. At FKFS a phenomenological combustion model has been developed, which can simulate operating points with an arbitrary number of pilot and post injections in high quality within short computation times.



personal buildup for Force Motors Ltd.

1	MODEL INTRODUCTION
2	CALCULATION OF IGNITION DELAY
3	MODELLING THE PRE-COMBUSTION
4	MODELLING THE MAIN- AND POST-COMBUSTION
5	VALIDATION
6	SUMMARY

## 1 MODEL INTRODUCTION

The present combustion model has been integrated into the ‘cylinder module’ developed by Grill [1, 2]. Hence all the usual approaches for calculating the calorics and the wall heat transfer can be combined with the new combustion model. The combustion chamber is modelled as one zone, which means all calculations are done using the mass mean temperature. The large influence of injection rate on CI-combustion makes it a necessary input for the model. Furthermore the cylinder geometrics, trapped air mass, EGR rate and in-cylinder pressure at intake valve closing are required like in any other working process calculations. When using the combustion model inside a 1-D flow simulation model, the masses and starting pressures calculated by the flow model are used for the working process calculation.

## 2 CALCULATION OF IGNITION DELAY

In order to simulate the combustion of a CI engine, it is necessary to compute the ignition delay first, based on separate ignition integrals for each pilot, main or post injection. Similarly to Chmela et al. [3] a combined Arrhenius and Magnussen approach has been implemented.

The Arrhenius term Eq. 1 is used to calculate the chemical ignition delay while the Magnussen term Eq. 2 shall reproduce the influence of the injection turbulence on the ignition delay.

<b>EQ. 1</b>	$r_{Arr} = k_{ID1} \cdot k_{Arr} \cdot c_f \cdot c_{ox} \cdot e^{\frac{-k_a \cdot T_{act}}{T + Q_b \cdot k_{ID2}}}$
--------------	---

<b>EQ. 2</b>	$r_{Mag} = k_{ID1} \cdot k_{Mag} \cdot c_{ox} \cdot \frac{\sqrt{k}}{\sqrt[3]{V_{cyl}}}$
--------------	---

To better represent the wide spread of temperature over the whole cycle, the Arrhenius equation has been modified in comparison to previous publications. The enhancements make it possible to calculate the ignition delay of pilot, main and post injections with just one equation.

The additional term in the denominator of the exponent is intended to depict the influence of previous combustions/injections on the ignition delay of subsequent combustions. This was necessary, as the ignition delay calculation is made with the mass mean temperature. With the usually low injection rates, the pre-combus-

tions however mostly result only in a comparatively faint rise in the mass mean temperature. Instead there are clearly hotter areas present during local precombustions giving rise to a correspondingly shorter ignition delay in the subsequent combustions. These local, hot areas are taken into account in the Arrhenius equation by way of the already released combustion energy  $Q_b$  of previous injections.

$k_{ID1}$  is a prefactor with which the reaction rates of the main and post injections are reduced compared with the pilot injections. According to [4] vaporization with increasing injection rates has a greater influence on the local temperature. This effect is considered by the prefactor  $k_{ID1}$ .

Higher injection velocities lead to a higher density of turbulent energy and therefore a higher reaction rate of the Magnussen term.

The characteristic reaction time of a process is proportional to the reciprocal value of its reaction rate.

On the assumption that the characteristic time of the ignition delay is obtained from the sum of the characteristic times for the Arrhenius and Magnussen approaches, one obtains the following equation for the reaction rate of the ignition delay.

<b>EQ. 3</b>	$r_{ID} = \frac{r_{Arr} \cdot r_{Mag}}{r_{Arr} + r_{Mag}}$
--------------	--

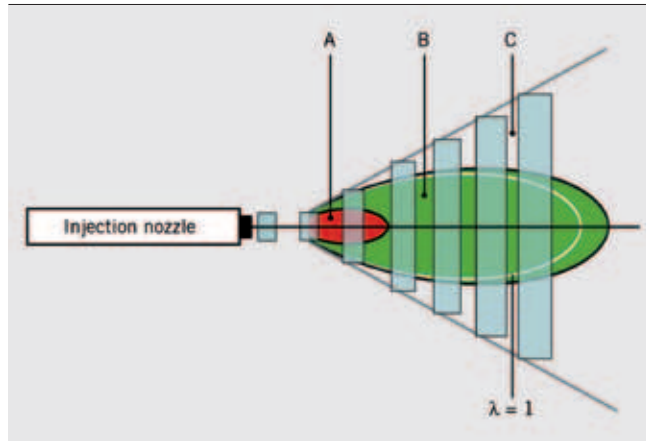
For each individual injection there is a separate integration of this reaction rate against the crank angle, Eq. 4. Combustion begins as soon as the integral value R of the respective injection exceeds an established limit value.

<b>EQ. 4</b>	$R = \int_{t_{SOI}}^{t_{curr}} r_{ID} \cdot dt$
--------------	---

With the aid of the modifications presented the combustion model is able to forecast the ignition delay of pilot, main and if necessary post injections of the whole engine map with just one set of parameters.

## 3 MODELLING THE PRE-COMBUSTION

Pilot injections serve first and foremost to shorten the ignition delay of the main injection. The shorter this is, the smaller the amount premixed in the main combustion will be. In this way the pressure gradients in the combustion chamber get smaller and thus the engine noise emissions and component loads decrease. It is known that small pilot injection rates at operating points at high rotational speed or long ignition delay do not start to burn and are only converted with the main injection. For this reason each pilot injection is modeled as a separate air-fuel mixture cloud whose excess air ratio leans out with time by way of air admixture. Inside this cloud a homogenous mixture is assumed for each timestep. During the injection the mixture cloud is added proportionally to the injected fuel mass combustion air gas. After the end of injection a constant entrainment rate is assumed against the crank angle. If a mixture cloud leans out too dramatically, it is no longer possible for ignition to occur inside the cloud or a combustion already occurring is extinguished.



1 Slice propagation through the combustion chamber

In order to translate the effects of the leaning out of pilot injections on combustion as exactly as possible, the approach of Barba [4] was used to calculate premixed combustions. In this approach the laminar flame velocity is also included in the calculation of the burn rate. The laminar flame velocity can be calculated as a function of the excess air ratio by way of Eq. 5. With the aid of Eq. 8 and using Eq. 6 and Eq. 7 the calculated velocity is adapted as a function of temperature, pressure and residual gas content in the combustion chamber.

EQ. 5 
$$s_{lam,0} = 0,276 \frac{m}{s} - 0,47 \frac{m}{s} \cdot \left( \frac{1}{\lambda_{mc}} - \frac{1}{0,91} \right)^2$$

EQ. 6 
$$\gamma = 2,18 - 0,8 \cdot \left( \frac{1}{\lambda_{mc}} - 1 \right)$$

EQ. 7 
$$\delta = -0,16 + 0,22 \cdot \left( \frac{1}{\lambda_{mc}} - 1 \right)$$

EQ. 8 
$$s_{lam} = s_{lam,0} \cdot \left( \frac{T}{T_0} \right)^\gamma \cdot \left( \frac{p}{p_0} \right)^\delta \cdot (1 - 2,1 \cdot x_{EGR})$$

ENGINE	A	B	C	D	E
STROKE [MM]	88.4	88.4	88.4	130	156
BORE [MM]	88	88	88	102	132
COMPRESSION RATIO	1801	1801	16.71	1801	17.51
DISPLACEMENT PER CYLINDER [LITER]	0.54	0.54	0.54	1.06	2.13
MAX. INJECTION PRESSURE [BAR]	1350	1600	1600	2000	2500
INJECTION SYSTEM	CR	CR	CR	PLN	CR
INVESTIGATED OPERATING POINTS	56	39	50	115	175

Calculation of the turbulent flame velocity follows

EQ. 9 
$$s_{turb} = s_{lam} \cdot \left( 1 - k_{fs} \cdot \left( \frac{C_m}{s_{lam}} \right)^{0,8} \right)$$

In the subsequent characteristic initially a spherical propagation of the combustion from a single ignition point is assumed. The change in the sphere radius corresponds here to the turbulent flame velocity. By disregarding the time-based change in density in the combustion chamber the current flame sphere surface Eq. 10 is determined. Using this it is possible to calculate the current mass flow which flows into the flame sphere caused by flame propagation, Eq. 11. Finally the burning fuel mass of each pilot injection based on the flame propagation can be calculated in each timestep by Eq. 12.

EQ. 10 
$$A_{flm} = 4 \cdot \pi \cdot r_{flm}^2$$

EQ. 11 
$$\frac{dm_{sphere}}{dt} = \rho_{mc} \cdot A_{flm} \cdot s_{turb}$$

EQ. 12 
$$\frac{dm_{b,1}}{dt} = \frac{dm_{sphere}}{dt} \cdot \frac{m_f}{m_f + m_a + m_{f,b} + m_{a,b}}$$

However, it must be assumed from this that ignition occurs not just at one local point of the combustion chamber, especially when combustion is already advanced. Following [4] a second approach to calculating the burn rate was therefore implemented

EQ. 13 
$$\frac{dm_{b,2}}{dt} = k_{comb} \cdot \frac{1}{\Lambda_{mc}^2} \cdot \frac{s_{turb}}{r_{mc}} \cdot m_f$$

The shape irregularity of the mixture cloud  $\Lambda_{mc}$  is defined as follows

EQ. 14 
$$\Lambda_{mc} = \frac{m_a + m_{a,b} + m_{f,b}}{a_{stoech} \cdot m_{inj,PI}}$$

2 Overview of engines used for validation

It puts the current fresh air and residual gas mass of the mixture cloud in proportion to the air mass which would be necessary for a stoichiometric combustion. The shape irregularity thus continues to increase proportionally to the entrainment, and also as combustion advances. The conversion rate of a precombustion is obtained from the smaller value of the two equations Eq. 12 and Eq. 13. If a precombustion cannot burn completely because of leaning out, the unburned fuel contained in it is burned during Premixed-combustion of the main injection.

**4 MODELLING THE MAIN AND POST-COMBUSTION**

Main and post-combustion are calculated independently of each other using the approach described below. A mixture doesn't occur, however a "feedback" by variation by the global values pressure and in-cylinder temperature is given.

During main or post injections, fuel slices are generated isochronously as a function of the injection rate and propagate through the combustion chamber in the direction of injection. During initialization a fixed amount of combustion air gas is mixed with each slice. Before the ignition delay elapses the fuel inside the slices is diffused to two fuel pools. The first is the so-called "premixed pool", while the second is known in the further characteristic as the "diffusion pool". Slices which are created after the ignition delay has elapsed contain only one diffusion pool.

It is assumed that the mixing of fuel and air inside the premixed pool of each slice is almost concluded at the ignition point. The upshot of this is that the fuel of the premixed pools is converted relatively quickly after the start of combustion. The combustion is therefore, along similar lines to [3], modeled by means of an Arrhenius approach Eq. 15.

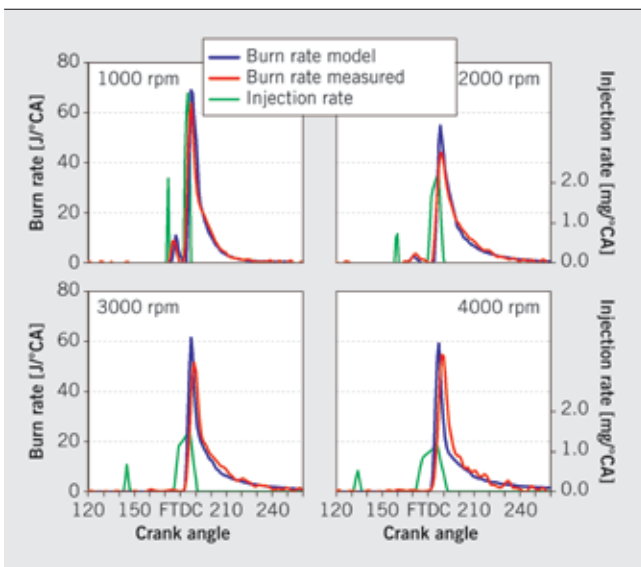
EQ. 15 
$$r_{Pre} = k_{Pre} \cdot c_f \cdot c_{ox} \cdot e^{\frac{-k_i \cdot T_{act}}{T}}$$

The mass conversion rate of the premixed combustion is finally obtained using the following equation

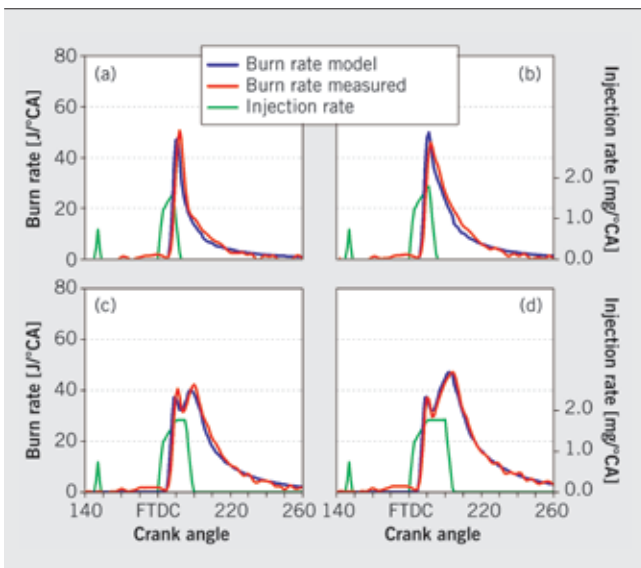
EQ. 17 
$$t_{Breakup} = \frac{k_v \cdot d_{noz,eq}}{u_{inj}}$$

The current axial slice position during the second phase is determined using Eq. 18, the current slice velocity is obtained from Eq. 19.

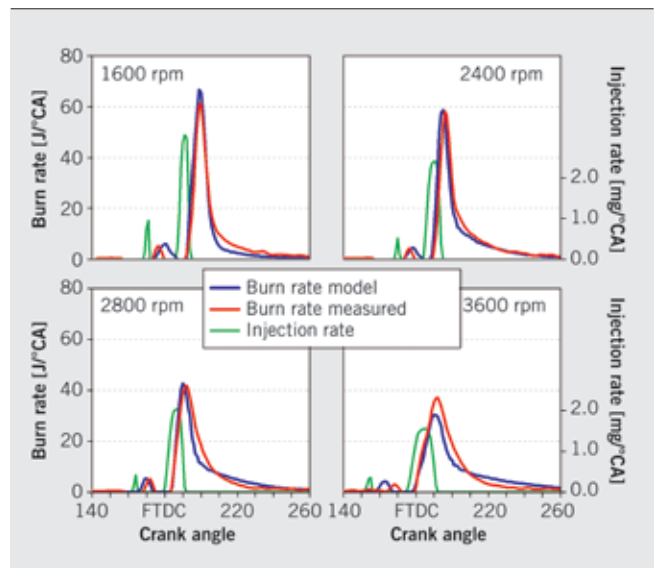
EQ. 18 
$$x_{ax} = \sqrt{\frac{2 \cdot k_v \cdot u_{inj} \cdot d_{noz,eq} \cdot t}{2 \cdot k_v^2 \cdot d_{noz,eq}^2 + k_v \cdot d_{noz,eq}}}$$



3 Engine A, 1000 – 4000 rpm, 6 bar IMEP



4 Engine A, 3200 rpm, 5, 7, 9 and 11.5 bar IMEP



5 Engine B, 1600 – 3600 rpm, 5.5 bar IMEP

EQ. 19

$$u_{ax} = k_v \cdot u_{inj} \cdot \frac{d_{noz,eq}}{x_{ax}}$$

As they propagate the mixture of combustion chamber gas to the slices is described by means of an empirical distribution of the excess air ratio “lambda”. This lambda distribution has a decisive influence on diffusion combustion. As can be seen in ❶, three lambda zones can be delimited. The first zone (A) is extremely rich and is therefore unable to burn. As can be easily identified, it is limited to a certain penetration depth. This is followed by the zone of diffusion combustion I (B), which also contains the stoichiometric excess air ratio ( $\lambda = 1$ ). The third zone is very lean (C). The slow Diffusion combustion II takes place in this zone. The actual slice position is used finally to assign in each slice the unburnt fuel mass of the diffusion pool to one of the three zones (rich, diffusion I, diffusion II).

The mass change rate of diffusion pool I on account of combustion is calculated for each slice using the following equation

EQ. 20

$$\frac{dm_{b,Diff I}}{dt} = \frac{k_{mod,I} \cdot m_{f,I} \cdot k_i^{0.5} \cdot k_t \exp}{I_c}$$

The specific turbulence  $k_i$  of the fuel in diffusion pool I required in Eq. 20 is calculated with the aid of the velocity distribution in the spray. Here, only those parts of the spray which are within the lambda limits of diffusion combustion I are taken into consideration. To calculate the characteristic length, the current combustion chamber volume is used, provided that it is smaller than 2.5 times the compression volume. In this representation the characteristic length cannot be any size, but instead runs to a maximum value. This prevents the combustion from becoming too slow during the burn-out phase.

Slices or partial sections of the slices which are in areas with a local excess air ratio above 1.1, whose fuel is thus assigned to diffusion pool II, are combusted by way of Eq. 21.

EQ. 21

$$\frac{dm_{b,Diff II}}{dt} = \frac{k_{mod,II} \cdot m_{f,II} \cdot k_{II}^{0.5} \cdot k_t \exp}{I_c}$$

The combustion model can be calibrated very quickly and clearly to different engines by means of the factors  $k_{mod,I}$  and  $k_{mod,II}$ . The burn rate of the main injection is finally obtained by adding up the slice conversion rates

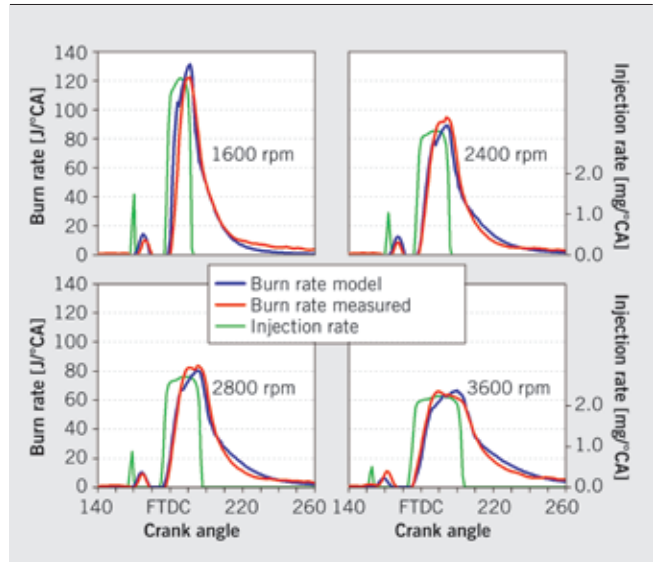
EQ. 22

$$\frac{dQ_{b,MI}}{dt} = H_u \cdot \sum_{n=1}^{n_{max}} \left( \frac{dm_{b,Pre}}{dt} + \frac{dm_{b,Diff I}}{dt} + \frac{dm_{b,Diff II}}{dt} \right)$$

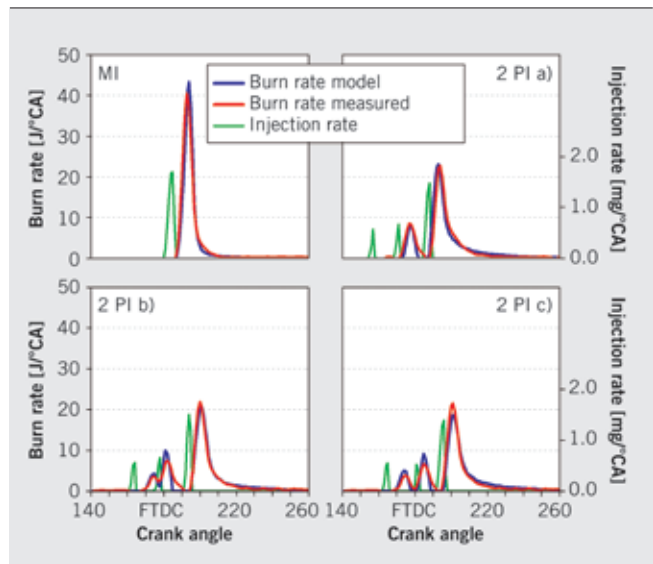
A more detailed description of the model has been published in [5].

5 VALIDATION

Development and validation of the model were conducted with the aid of test bench data of several engines, ❷. The three passenger car engines A, B and C differ primarily in their maximum



❶ Engine B, 1600 - 3600 rpm, 18 bar IMEP

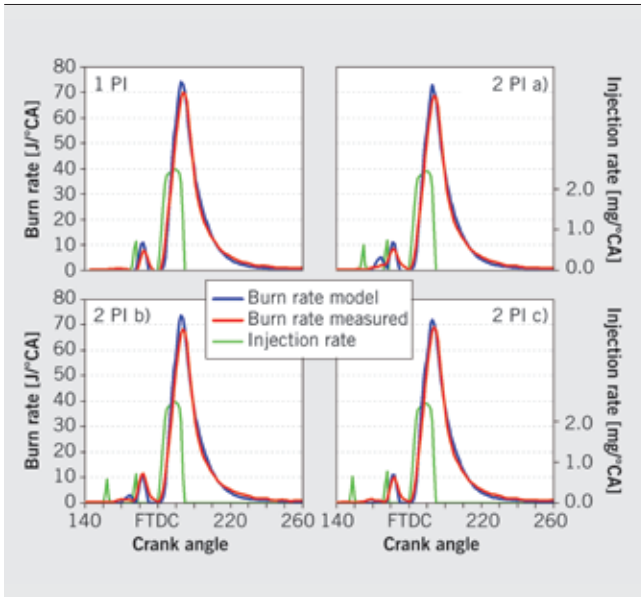


❷ Engine C, 2000 rpm, 2.3 bar IMEP

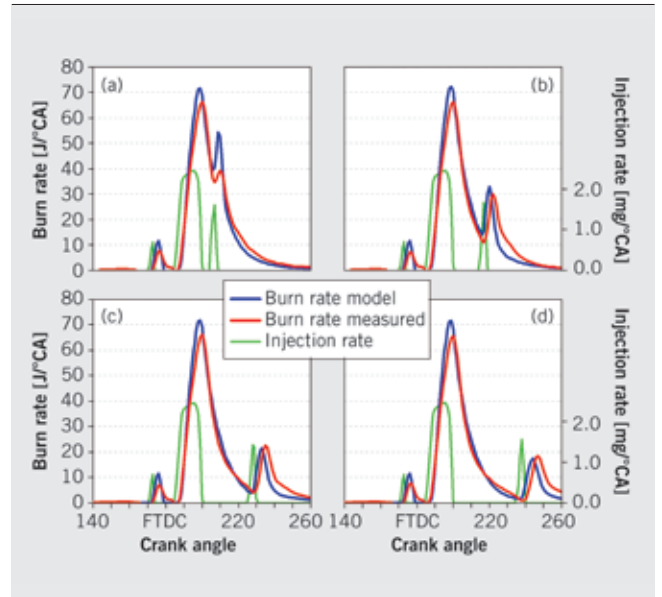
injection pressure and the number of injections. Engine D is an engine for smaller commercial vehicles. It has a unit pump injection system with a maximum injection pressure of 2000 bar. Simulation results of engine E, which is equipped with a pressure boosted Common rail system has been published in [6, 7].

All the simulation results presented in the following were calculated with a common set of parameters for each engine. The test bench data was subjected to a pressure trace analysis, during which the same caloric, wall heat and zone modeling approaches as in the ensuing work process calculation were used.

❸ shows an rpm variation for engine A at low load. It is already possible to discern that at lower rotational speeds the pilot injections burn both during the measurement and in the simulation. At higher rotational speeds no separate precombustions can be discerned.



8 Engine C, 2500 rpm, 10 bar IMEP



9 Engine C, 2500 rpm, 11 bar IMEP

In 4 on engine A, starting out from a standard load point (a), the activation duration of the main injection is successively increased (b, c and d). While in (a) and (b) a large part of the combustion occurs premixed, (c) and (d) have a pronounced diffusion component.

5 shows an rpm variation for engine B at part load. 6 shows the same variation close to full load. As can be easily discerned, the simulation results can correspond very well to the measurement data and this over a high speed and load range.

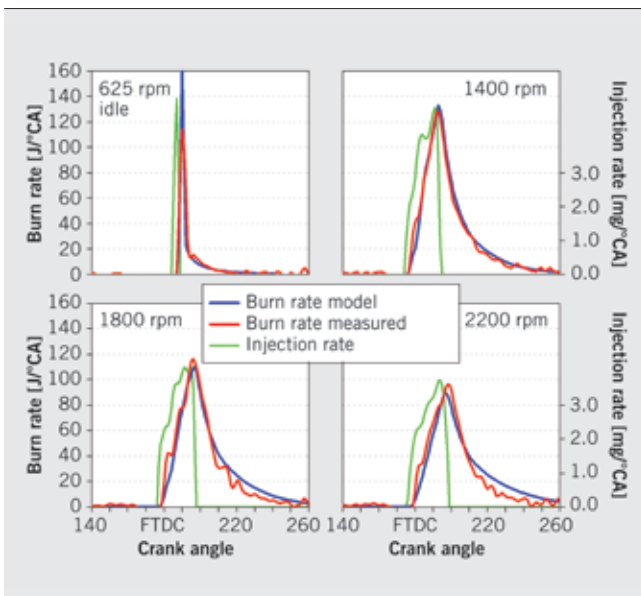
The measurements on engine C were taken specifically to develop the combustion model. 7 shows different injection strategies at one operating point at constant load and speed. Starting

out from a main injection without pilot injections, initially an injection rate was selected in which only the second pilot injection burns (a). After the entire injection rate was retarded, both pilot injections burn (b). By increasing the gap between the two pilot injections, it was finally possible to achieve two separately burning pilot injections (c).

8 shows a further series of measurements with two pilot injections. Starting out from an operating point with one pilot injection, the quantity was initially split between two pilot injections (a) and then the start of injection of the front injection increasingly advanced (b) and (c). In this operation points one sees the leaning out of the first precombustion.

9 shows a post injection variation. In this series of measurements the deviation in percent of the mass mean temperature at exhaust opens between simulation and measurement is max. 2.3%, which is a very good result. This is important in connection with integration in a 1D flow simulation model, as the exhaust gas enthalpy there is an important input variable in the calculations.

Unlike the previous engines, engine D does not have a common rail injection system, but instead a unit pump system. 10 shows an idle point, together with the 50% load point at different rotational speeds.



10 Engine D, 625 - 2200 rpm, idle and 50% load

## 6 SUMMARY

As the simulation results show, the combustion model is able to predict the burn rate of different engines in a wide operation range with one set of calibration parameters. On a standard PC, it generally takes less than 1 s to calculate the high-pressure stage of a working cycle. Due to the very short computing times this combustion model is best suited to supporting the application of standard engines. Even fundamental variant analyses leading up to standard projects can be realized with the aid of this combustion model.

$A_{flm.}$	Flame surface [m <sup>2</sup> ]
$a_{stoech.}$	Stoichiometric fuel rate [-]
$C_f$	Volumetric fuel concentration [kg/m <sup>3</sup> ]
$c_m$	Mean piston speed [m/s]
$C_{ox}$	Volumetric oxygen concentration [kg/m <sup>3</sup> ]
$d_{noz,eq}$	Equivalent nozzle hole diameter [m]
$H_u$	Net calorific value [J/kg]
$k$	Density of turbulent energy [m <sup>2</sup> /s <sup>2</sup> ]
$k_1$	Model constant (4,5) [-]
$k_I$	Density of turbulent energy in fuel-pool I [m <sup>2</sup> /s <sup>2</sup> ]
$k_{II}$	Density of turbulent energy in fuel-pool II [m <sup>2</sup> /s <sup>2</sup> ]
$k_{Arr}$	Calibration parameter [m <sup>3</sup> /(kg·s)]
$k_{comb}$	Calibration parameter precombustion [-]
$k_{Is}$	Calibration parameter precombustion [-]
$k_{ID1}$	Calibration parameter ignition delay [-]
$k_{ID2}$	Calibration parameter ignition delay [-]
$k_{Mag}$	Calibration parameter [-]
$k_{mod,I}$	Calibration parameter diffusion combustion I [-]
$k_{mod,II}$	Calibration parameter diffusion combustion II [-]
$k_{Pre}$	Calibration parameter premixed combustion [m <sup>3</sup> /(kg·s)]
$k_{texp}$	Model constant [-]
$k_v$	Calibration parameter [-]
$k_x$	Calibration parameter [-]
$l_c$	Characteristic length [m]
$m_a$	Unburnt air mass [kg]
$m_{a,b}$	Burnt air mass [kg]
$m_{b,1}$	Burnt fuel mass precombustion term 1 [kg]
$m_{b,2}$	Burnt fuel mass precombustion term 2 [kg]
$m_{b,Diff I}$	Burnt fuel mass diffusion combustion I [kg]
$m_{b,Diff II}$	Burnt fuel mass diffusion combustion II [kg]
$m_{b,Pre}$	Burnt fuel mass premixed combustion [kg]
$m_{f,I}$	Fuel mass in pool I [kg]
$m_{f,II}$	Fuel mass in pool II [kg]
$m_f$	Unburnt fuel mass [kg]
$m_{f,b}$	Burnt fuel mass [kg]

① Formula symbols

REFERENCES

[1] Grill, M. Objektorientierte Prozessrechnung von Verbrennungsmotoren, Dissertation, Universität Stuttgart, 2006, <http://elib.uni-stuttgart.de/opus/volltexte/2006/2725/>

[2] Grill, M.; Bargende, M. The Cylinder Module – New Simulation not only for Combustion Processes. In MTZ worldwide Edition 2009-10, 2009

[3] Chmela, F.; Dimitrov, D.; Pirker, G.; Wimmer, A. A Consistent Simulation Methodology for Combustion in Piston Engines. In MTZ worldwide Edition 2006-06, 2006

[4] Barba, C. Erarbeitung von Verbrennungskennwerten aus Indizierdaten zur verbesserten Prognose und rechnerischen Simulation der Verbrennungs-

$m_{flm.}$	Flame mass [kg]
$m_{inj,PI}$	Total fuel mass of pilot injection [kg]
$n$	Fuel slice [-]
$n_{max}$	Fuel slice count [-]
$p$	Cylinder pressure [Pa]
$p_0$	Reference pressure (0,98-10 <sup>-5</sup> Pa) [Pa]
$Q_b$	Cumulative burn rate [J]
$R$	Integrated reaction rate [kg/m <sup>3</sup> ]
$r_{Arr}$	Reaction rate [kg/(m <sup>3</sup> ·s)]
$r_{flm.}$	Flame radius [m]
$r_{ID}$	Reaction rate of ignition process [kg/(m <sup>3</sup> ·s)]
$r_{Mag}$	Reaction rate [kg/(m <sup>3</sup> ·s)]
$r_{mc}$	Mixture cloud radius [m]
$r_{Pre}$	Reaction rate premixed combustion [kg/(m <sup>3</sup> ·s)]
$s_{lam}$	Laminar flame speed [m/s]
$s_{lam,0}$	Laminar flame speed under reference conditions [m/s]
$s_{turb}$	Tturbulent flame speed [m/s]
$T$	Charge temperature [K]
$T_0$	Rreference charge temperature (298 K) [K]
$T_{Act.}$	Activation temperature (1000 K) [K]
$t$	Current time [s]
$t_{SOC}$	Start of combustion [s]
$t_{Breakup}$	Breakup time [s]
$t_{SOI}$	Start of injection [s]
$u_{inj.}$	Slice speed during injection [m/s]
$u_{ax}$	Slice speed in axial direction [m/s]
$V_{cyl}$	Cylinder volume [m <sup>3</sup> ]
$V_{mix}$	Mixture volume [m <sup>3</sup> ]
$x_{ax}$	Axially distance from nozzle hole [m]
$x_{EGR}$	Mass fraction of residual gas [-]
$\gamma$	Temperature influence exponent [-]
$\delta$	Pressure influence exponent [-]
$\Lambda_{mc.}$	Fissure quantity [-]
$\lambda_{mc.}$	Excess air ratio of the mixture cloud [-]
$\rho_{mc.}$	Density of the mixture cloud [kg/m <sup>3</sup> ]

ablaufes bei PKW-DE-Dieselmotoren mit Common-Rail-Einspritzung. Dissertation, Eidgenössische Technische Hochschule Zürich, 2001

[5] Rether, D.; Grill, M.; Schmid, A.; Bargende, M. Quasi-Dimensional Modeling of CI combustion with Multiple Pilot- and Post Injections, SAE-Paper 2010-01-150, 2010

[6] Grill, M.; Schmid, A.; Rether, D.; Bargende, M. Quasi-dimensional and Empirical Modeling of Compression-Ignition Engine Combustion and Emissions, SAE-Paper 2010-01-151, 2010

[7] Kožuch, P.; Maderthaner, K.; Grill, M.; Schmid, A. Simulation der Verbrennung und Schadstoffbildung bei schweren Nutzfahrzeugmotoren der Daimler AG, 9. Symposium für Verbrennungsdiagnostik, Baden-Baden, 2010